INTRODUCTION

Renal artery stenosis is the narrowing of one or both renal arteries or their branches that can cause hypertension by initiating the release of the enzyme renin from juxtaglomerular cells of the affected kidney. The cross section of the lumen must be decreased by at lest 60% before the occlusion becomes hemodynamically significant. It is the most frequent cause of curable hypertension but it accounts for less than 2% of all cases of hypertension. (***1)***

Renal artery stenosis most commonly caused by fibromuscular dysphasia. However among patients with a significant RAS, only two thirds show improvement of hypertension after revascularization and 27%-80% show improvement or stabilization of renal function. When left untreated, atheromatous RAS tends to worsen, leading to renal artery thrombosis. ***(2)***

Hypertension is a major cause of disability and death throughout the world. Renal artery stenosis is an etiological factor for a small but significant component of this disease with varying estimation of prevalence from l%-10% of patient with hypertension screened ***(3)***

Individuals who develop hypertension between the ages of 30 and 55 are most likely to have primary (essential) hypertension. If the initial diagnosis of hypertension in an adult is made before the age of 30, it is usually the result of fibromuscular dysplasia. Because atherosclerosis occurs in older individuals, it is usually the cause of RAS after the age of 55y. Accelerated or malignant hypertension has also been associated with a very high prevalence of RAS. Resistant hypertension is defined as failure to normalize blood pressure <140/90 mm Hg. ***(4)***

Atherosclerotic renal artery stenosis is the most common primary disease of renal arteries and it is associated with two major clinical syndromes, hypertension and ischemic renal disease. ***(5)***

Atherosclerosis and its related sequelae are leading causes for morbidity and mortality in the western world while hypertension is common in patients with diabetes with nephropathy, occurring in 75% to 85 % of cases. Renovascular hypertension has emerged as the most common reversible cause of secondary hypertension. (***5)***

In addition, medical treatment of renovascular hypertension caused by renal artery stenosis has been proved to be less effective than percutaneous or surgical revascularization Therefore, patients suspected of having RAS should undergo adequate screening. ***(4)***

With the increase in prevalence of renal artery stenosis and ischemic nephropathy clinicians dealing with renovascular disease need noninvasive diagnostic tools and effective therapeutic measures to resolve the problem successfully. ***(6)***

Ultrasonography, Color Doppler Ultrasound, and Magnetic Resonance Angiography (MRA), Spiral Computed Tomography Angiography (CTA), Digital subtraction Angiography (DSA) and Renal scintigraphy can be used in combination to achieve adequate screening of patients. This article describes the roles of these modalities in diagnosis of renal artery stenosis (RAS) and presents an algorithm for their use. ***(7)***

ULTRASONOGRAPHY is ideally suited for imaging kidneys. The renal cortex, medulla, and collecting system have different acoustic properties, and pathological changes are easily discernible and correlate well with histological findings. Furthermore, kidneys are easily visualized and show a limited spectrum of anatomic variation and pathological changes. The safety, simplicity and low cost has made sonography perfect tool in nephrology ***(7).***

Color Doppler ultrasound has emerges as a reliable method helping in the diagnostic work-up of patients with suspected renovascular disease as renal artery stenosis that causes renovascular hypertension ***(8).***

Color Doppler has the advantages of being noninvasive and inexpensive. However, regard to the role. Two approaches are used to detect RAS with Doppler US; direct visualization of the renal arteries and analysis of intrarenal Doppler waveforms ***(9).***

The first approach involves direct scanning of the main renal arteries with color or power Doppler US followed by analysis of renal artery velocity with spectral Doppler US **(10).**

Magnetic resonance angiography (MRA) has a major role in diagnosis of renal artery stenosis in addition, in recent study it has been used to measure the direct pressure in renal artery across the stenotic tract ***(11).***

Renal magnetic resonance (MR) angiography allows accurate evaluation of patients suspected to have renal artery stenosis without the risks associated with nephrotoxic contrast agent, ionizing radiation, or arterial catheterization. Other applications of renal MR angiography are mapping the vascular anatomy for planning renal revascularization planning repair of abdominal aortic aneurysm, assessing renal bypass grafts and

renal transplant anastomosis, and evaluating vascular involvement by renal tumors ***(12).***

Gadolinium-enhanced MRA is now available on high field strength imaging systems with high performance gradients, which are capable of performing breath, hold three-dimensional spoiled gradient echo imaging with short repetition times and echo times ***(13).***

Spiral CT angiography is able to image large columns of tissue very rapidly in a20-30s breath-hold have lead to the development of CT angiography. This produces higher quality axial images with better contrast enhancement than conventional CT and has the added advantages of being able to produce 2D coronal, sagittal, oblique and curved planar reconstructed images as well the 3D maximum intensity projection (MIP) and shaded Surface Display (SSD) reconstructed M images ***(14).***

Renal angiography is the undisputed golden standard in the diagnostic workup for evaluation of renovascular disease ***(15).***

Digital subtraction angiography (DSA) has become a well established modality for visualization of blood vessels in the human body. With this technique, sequence of 2D digital X-ray projection image is acquired to show the passage of a bolus of injected contrast material thought the vessel of interest.

Intra-arterial digital subtraction angiography (**DSA**) allows excellent visualization of all portions of the renal artery and can determine accurately whether the artery is normal, stenotic, or occluded Nevertheless angiography is invasive and costly when compared with other imaging modalities. Angiography is a poor screening test for renal artery stenosis ***(16).***

Renal scintigraphy has an important role in diagnosis of renal artery stenosis and kidney with renovascular hypertension may exhibit impaired function during (**ACEI**), this phenomenon is observed mainly in patients with bilateral RAS or with arterial stenosis in a solitary kidney; it is believed to be caused by disruption of the auto regulation system of the glomerular filtration rate (**GFR**). In patients with unilateral renal artery stenosis, a unilateral change in renal function induced by ACE inhibition can be revealed with scintigraphy. ***(17)***

Baseline and Captopril enhanced 99mTc-mercaptoacetyltriglycine (99mTc-MAG3) Scintigraphy using a 1- day 25-mg Captopril protocol, was recommended by the Working Party Group on Determining the Radionuclide of Choice ***(18).***

AIM OF THE WORK

The aim of this work is to describe recent modalities in imaging of renal artery stenosis, their role in the diagnosis, illustration of the advantages and limitation in each of them.

ANATOMY OF THE KIDNEYS

The kidneys are reddish brown and located on the posterior wall of the abdomen; the kidneys are completely retroperitoneal with their anterior surface covered with parietal peritoneum, and posterior surfaces adjacent to the posterior abdominal wall. The kidneys lie on either side of the vertebral column at vertebral levels T11/12 – L3. The hilum of the kidney is located at the level of the trans pyloric plane, which runs transversely at the level where the pylorus of the stomach begins **(19).**

The kidneys are surrounded by a mass of fat and loose areolar tissue. Their upper extremities are on a level with the upper border of the twelfth (12th) thoracic vertebra, their lower extremities on a level with the third lumbar As a rule the right kidney is situated usually slightly lower than the left, probably on account of the vicinity of the liver .The long axis of each kidney is directed and downward and lateral ward, the transverse axis backward and lateral ward **(20).**

Each kidney is convex, and looks forward and lateral ward. Its normal measurement is about 11.25 cm in length, 5 to 7.5 cm in breadth, and rather more than 2.5 cm in thickness. The left is somewhat longer, and narrower than the right The weight of the kidney in the adult male varies from 115 to 155 gm. the combined weight of the two kidneys in proportion to that of the body is about 1 to 240 **(21).**

Relations: The anterior relations related to the **right kidney** are (fig 1): the second part of duodenum, under surface of liver, hepatic flexure of colon, stomach and small intestine, the suprarenal glands lie along side the upper part of each kidney **(22).**

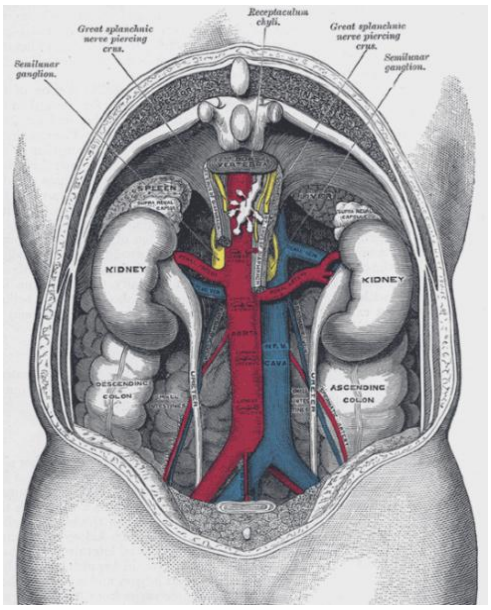

(Figure: 1 - the relations of the viscera and large vessels of the abdomen seen from behind.**) (Quoted from Gray's anatomy)**

Anterior surface of the **left kidney**: A small area along the upper part of the medial border is in relation with the left suprarenal gland, and close to the lateral border is a long strip in contact with the renal impression on the spleen. A somewhat quadrilateral field, about the middle of the anterior surface, marks the site of contact with the body of the pancreas; on the deep surface of which is the lineal vessel above this is a small triangular portion, between the suprarenal and splenic areas in contact with the postero-inferior surface of the stomach. Below the pancreatic area the lateral part is in relation with the left colic flexure, the medial with the small intestine. The areas in contact with the stomach and spleen are covered by the peritoneum of the omental bursa, while that in relation to the small intestine is

covered by the peritoneum of the general cavity; behind the latter are some branches of the left colic vessels. The suprarenal, pancreatic, and colic areas are devoid of peritoneum **(23).**

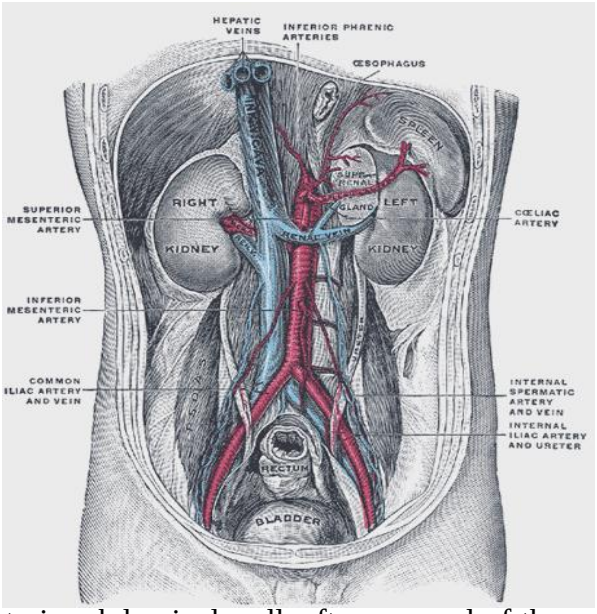

(**Figure: 2 -** posterior abdominal wall, after removal of the peritoneum, showing kidneys, capsules and great vessels) **(Quoted from Gray's anatomy)**

The posterior surface (facies posterior) (Figs 3, 4, 5) the posterior surface of each kidney is directed backward and medialward. It lies upon the diaphragm, the medial and lateral lumbocostal arches the psoas major, the quadratus lumborum, and the tendon of the trasversus abdominus, the subcostal, and one or two of the upper lumbar arteries, and the last thoracic, iliohypogastric and ilioinguinal nerves the right kidney rests upon the twelfth rib, the left usually on the eleventh and twelfth. The diaphragm separates the Kidney from the pleura, which dips down to form the phrenicocostal sinus, but frequently the muscular fibres of the diaphragm are defective or absent over a triangular area immediately above the lateral lumbocostal arch, and when this is the case the perinephric areolar tissue is in contact with the diaphragmatic pleura **(24).**

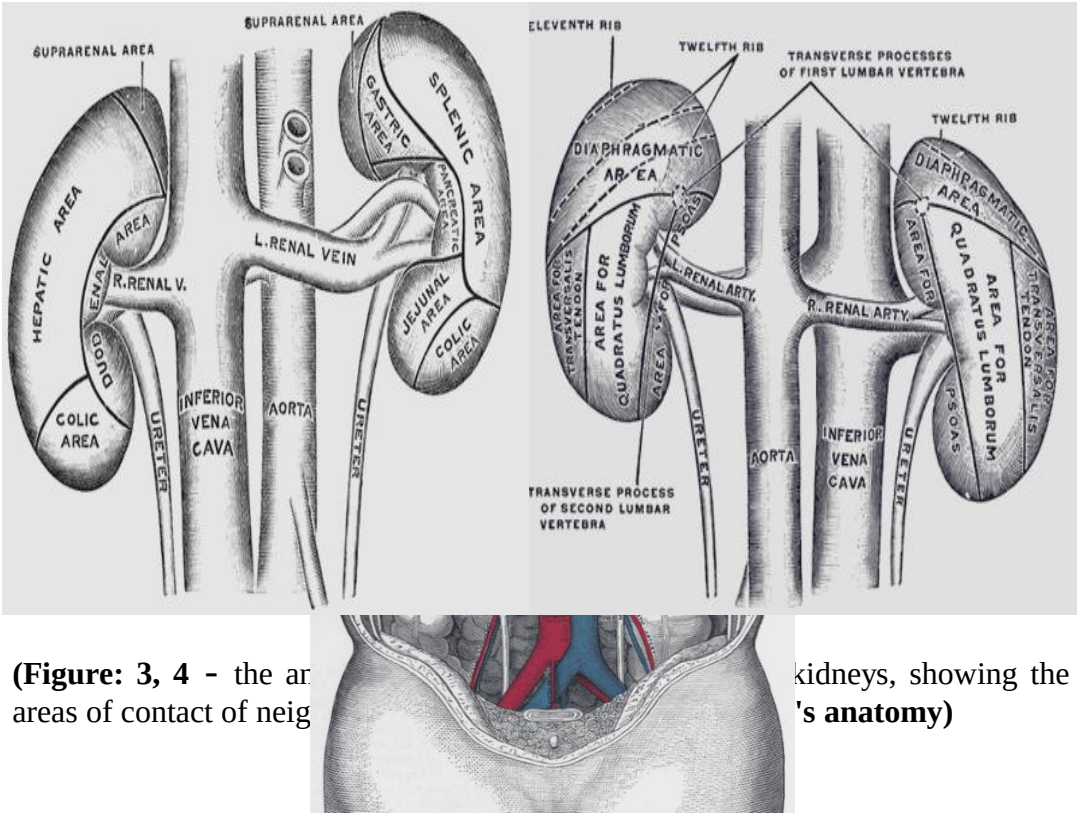

(Figure: 3, 4 - the ar kidneys, showing the areas of contact of neig **'s anatomy)**

(Figure: 5- the relations of the kidneys from behind**)**

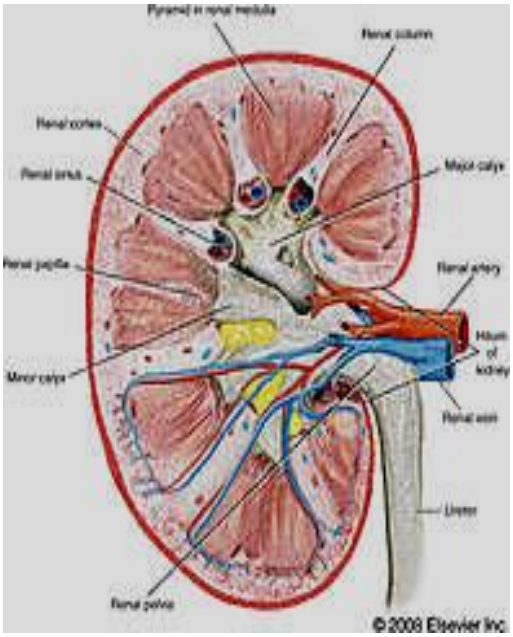

(Figure: 6 - the hilum of kidney, showing vein, artery and ureter**) (Quoted from Snell anatomy)**

Arterial supply:

The kidney is plentifully supplied with blood by the two renal arteries, a large branch of the abdominal aorta just below the superior mesenteric artery, opposite the body of L2 and behind the pancreas and renal vein.

Course and relation;

The renal arteries are two large trunks, which arise from the side of the aorta, immediately below the superior mesenteric artery at the level of the second lumber vertebrae. Each is directed across the crus of the diaphragm, so as to form nearly a right angle with the aorta. The right is longer than the left, on account of the position of the aorta; it passes behind the inferior vena cava, the right renal vein, the head of the pancreas, and the descending part of the duodenum. The left is somewhat higher than the right; it lies behind the left renal vein, the body of the pancreas and the lineal vein, and is crossed by the inferior mesenteric vein **(25).**

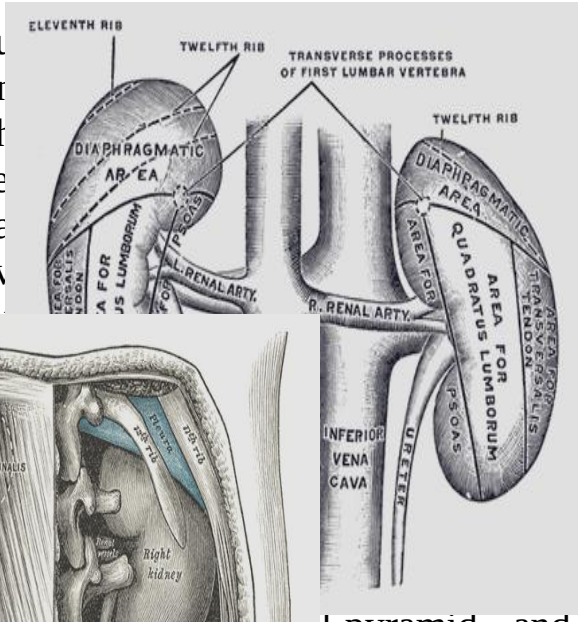

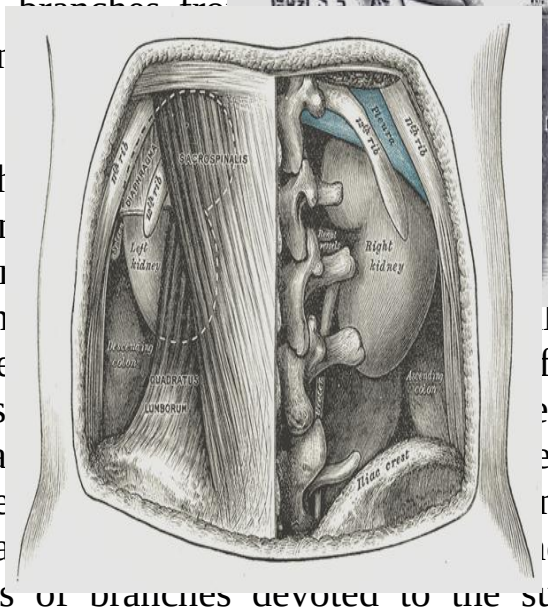

Before reaching the hilu
divides into four or five brar
branch is the posterior branch
renal pelvis to supply a large
The anterior division of the ma
the renal hilum it further div
branches. These
upper, middle, ar

Frequently
given off from th
the lower portion
end as arteriae pr
the renal column
run along its side
the afferent vess
having arrived a
arches or arcade
bases of the pyra
two distinct sets of branches devoted to the supply of the remaining portions of the kidney. **(26)**

l pyramid , and
f in their course
renal columns
ey form arterial
ne between the
d break up into

Branches of Renal arteries

There are five segments Antro superior, Antro inferior, posterior and Apical. Near the renal hilum each artery divides into anterior and posterior division, the anterior division gives branches that supply the apical, superior Antro inferior and inferior segments, the posterior division supplies the posterior segment.

Segmental arteries are;

Apical segmental artery Inferior segmental artery

Posterior segmental artery Antero superior segmental artery

Antero inferior segmental artery **(22)**

Venous drainage:

The renal veins arise from three sources. The veins beneath the fibrous tunic, the plexuses around the convoluted tubules in the cortex, and the plexuses situated at the apices of the renal pyramids. The veins beneath the fibrous tunic are stellate in arrangement, and are derived from the capillary network, into which the terminal branches of the interlobular arteries break up, these join to form the interlobular veins which pass inward between the rays, receive branches from the plexuses around the convoluted tubules and having arrived at the bases of the renal pyramids join with the vena rectae. **(2**1)

Lymphatic

The lymphatic of the kidney drain the Para aortic nodes at the level of the origin of the renal arteries (2nd lumber vertebrae). The surface of the upper pole may drain through the diaphragm into the posterior mediastinum. **(22)**

Nerves of the kidney

The nerves of the kidney, although small are about fifteen in number .They have small ganglia developed upon them and are derived from the renal plexus which is formed by branches from the celiac plexus **(Fig.7)** the lower and outer part of the celiac ganglion and aortic plexus and from the lesser and lowest splanchnic nerves they accompany the renal artery and its branches and are distributed to the blood vessels and to the cells of the urinary tubules. **(21)**

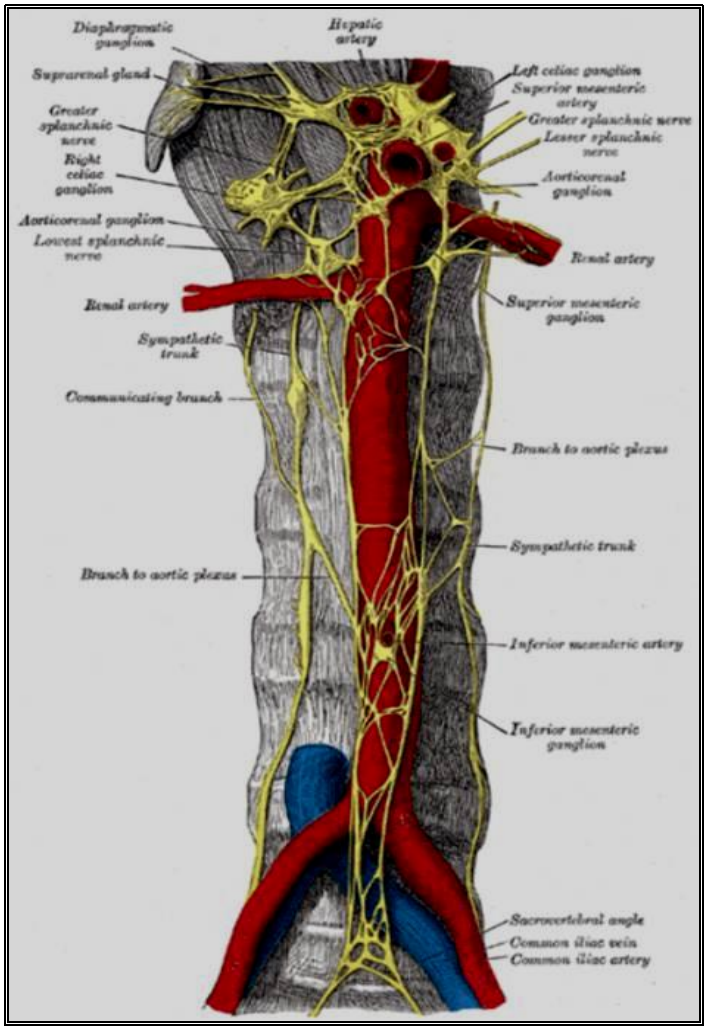

(Figure 7 - innervations of the kidney**) (Quoted from Gray's anatomy)**

Fixation of the kidney:

The kidney and its vessels are imbedded in a mass of fatty tissue termed the adipose capsule, which is thickest at the margins of the kidney and is prolonged through the hilum into the renal sinus. The kidney and adipose capsule are enclosed in a sheath of fibrous tissue continuous with the subperitoneal fascia, and named the renal fascia. The kidney is held in position partly through the attachment of the renal fascia and partly by the apposition of neighboring viscera**. (22)**

Normal variants

I .Accessory Renal Arteries;

Almost one quarter to one third of individuals have variation of the main renal artery. The most common being the occurrence of supernumerary renal arteries, two or more to a single kidney. These usually arise from the lateral aorta and may enter the renal hilum or directly into the parenchyma of one of the poles of the kidney, with the upper pole being the most common. Supernumerary arteries on the right side going to the lower pole tend to cross anterior rather than posterior to the inferior vena cava. Lower pole arteries on both sides must cross anterior to the collecting system and may be the cause of the uretro-pelvic junction obstruction. Supernumerary arteries are more common with the ectopic kidney. In unusual cases these arteries may arise from celiac, superior mesenteric or iliac arteries**. (27)**

It is important to be aware of the possibility of accessory or aberrant renal arteries, which occur in an estimated 30% of patients. Most accessory renal artery originates from the abdominal aorta however rarely an accessory renal arteries arise from a common iliac artery. Accessory renal arteries are especially common in patients with horseshoe kidney**.(27)**

II .Retro-aortic renal vein;

The left renal vein usually passes anterior to aorta just behind the superior mesenteric artery; however, the left renal vein may course behind the aorta, a variant known as a retro aortic renal vein

III .Circumaortic renal vein;

The presence of both a normal left renal vein and a retroaortic vein is known as a Circumaortic renal vein. Duplication of the right renal vein is also common**. (27)**

Developmental Anomalies of the kidney;

Developmental anomalies of the kidney affect one third of all congenital malformation and are responsible for 40 percent of all renal disease**.(28)**

I. Anomalies in number;

a) Agenesis; This may be unilateral agenesis or bilateral agenesis Unilateral agenesis incidence is one in 200 of individuals; bilateral agenesis is a much rarer condition, one in 4000 newborn.

b) Supernumerary; this is where there are more than the usual two kidneys and their number may reach five**.(28)**

II .Anomalies in location;

a- **Ptosed** kidney; this occurs when a normally positioned kidney drops to an abnormally inferior position. It occurs when the perinephric fat cushions are inadequate as in very thin persons who rapidly lose a large amount of weight.

B-**Ectopic kidney**; this is when the kidney is in a position other than its normal position. It can be thoracic (very rare), low abdominal, iliac, or pelvic. When this is found the other side is normal in 80% of cases, but the kidney itself is often abnormal

III-Anomalies in shape;

1-**Horse shoe kidney**: This is shown to be classically due to fusion of the lower poles with an equal amount of renal mass on either side of the midline, with two separate ureters serving each. This represents half of patients with horseshoe kidneys. The other half of patients has

the bulk of the renal mass shifted to one side of the midline, with the ureters not crossing the midline, as it joins the renal pelvis**.(28)**

2-**Crossed, fused renal ectopia**; is another type of abnormality in this case the upper pole of the crossed kidney is fused to the lower pole of the kidney.

3-**Lump** or cake kidney; where the kidneys are completely fused. The kidney is usually in the pelvis and is often drained by single ureters. This is rarely seen**.(28)**

IV-Anomalies in the axis (malrotation);

This is when the kidneys don't follow the normal ascent from their pelvic position and rotate 90 degrees medially to assume their normal anatomical position. It is common in cases of renal ectopy and fusion but rare in otherwise normally positioned kidney. Visualization of malrotated kidney is variable .**(28)**

Structure and Radiological appearance of normal kidney

Intrarenal anatomy: (Fig 8) the cortex forms a rim that envelopes the medulla, which takes the form of regularly spaced pyramids. The pyramids end in papillae that jut into minor calyces that join to form the major calyces. These coalesce into the proximal ureter at the renal pelvis. The blood vessels enter at the hilum, adjacent to the ureter.

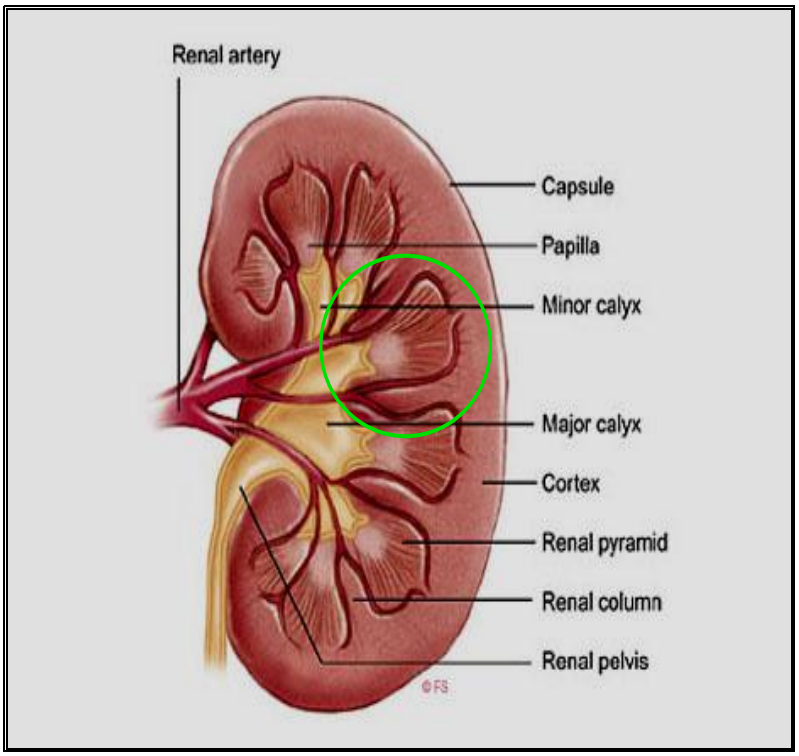

(Figure: 8 - intrarenal anatomy)

Sonographic appearance

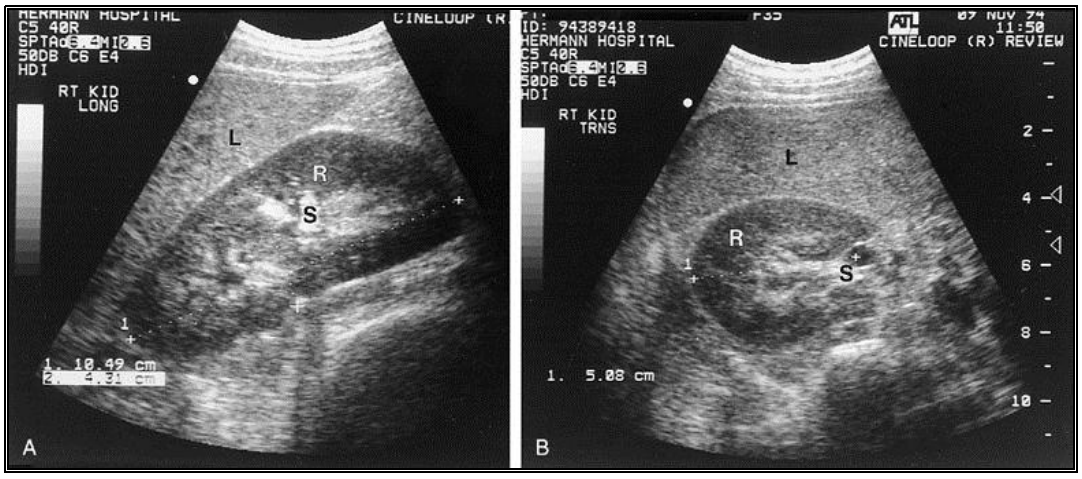

(Figure: 9 - longitudinal scan and Transverse scan of right kidney)

(A) Longitudinal sonogram of right kidney: The renal parenchyma forms a dark rim around the echogenic sinus fat that obscures the calyces and blood vessels. Medullary pyramids appear as regularly spaced areas slightly less echogenic than the cortex, which is less echogenic than the liver.

(B) Transverse scan of right kidney through the lower pole.

(Figure: 10- Intra Venous Pyelogram (IVP**)** or Intra Venous Urogram)

A

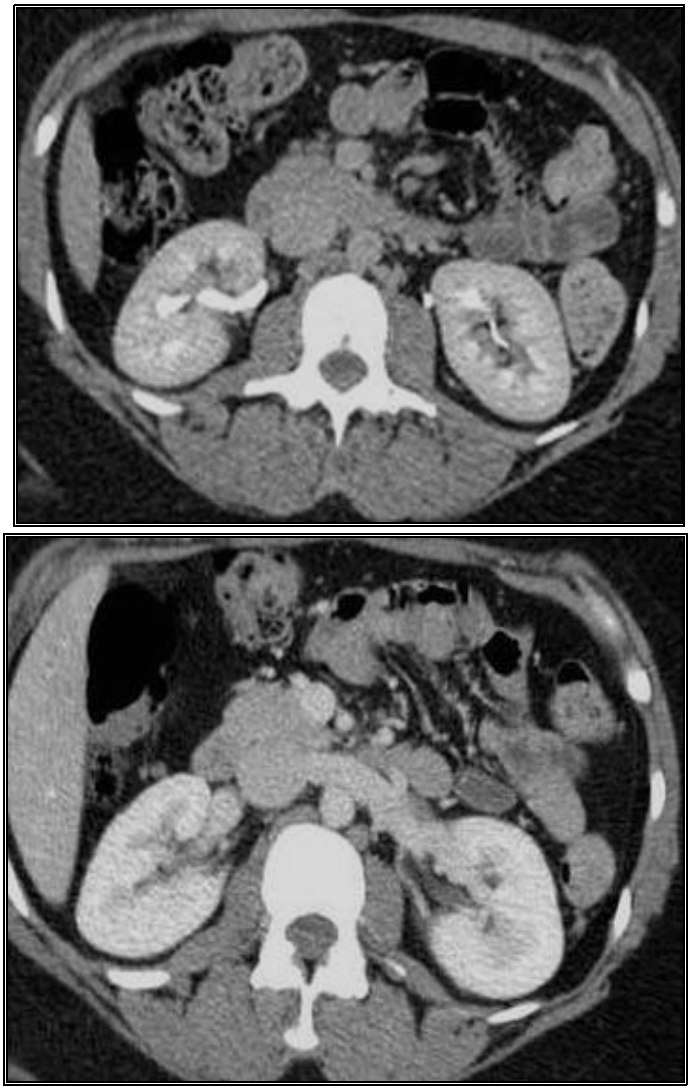

B

(Figure: 11– (A) Contrast enhanced CT scan through the kidneys in nephrogram phase (showing cortico-medullary differentiation). This is approximately 100 seconds following contrast administration and would show renal lesions well – **(B)** in pyelogram phase (showing excretion of contrast into the collecting system). This is approximately 8 minutes following contrast administration and would show urothelial lesions well, such as transitional cell carcinoma, stones, blood clots.)

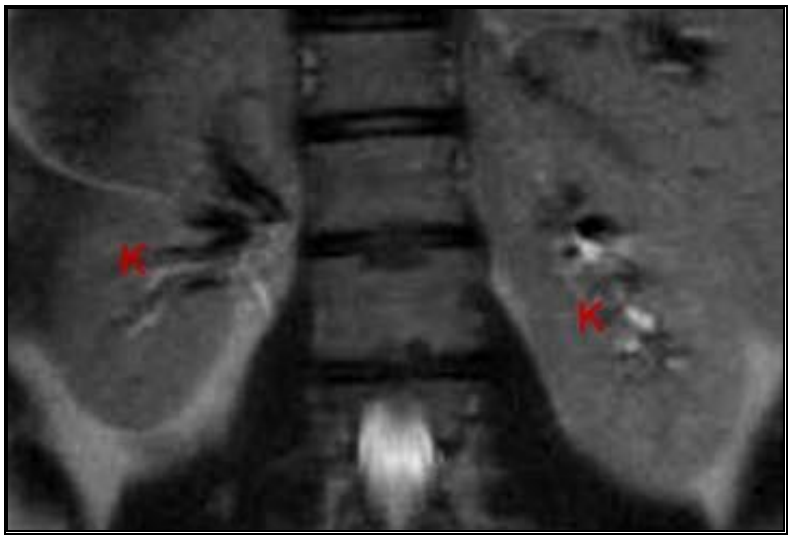

(Figure 11 C-T2 weighted images through the kidneys (K) in the coronal plane

(Figure: 12 -Magnetic resonance imaging demonstrating normal kidney)

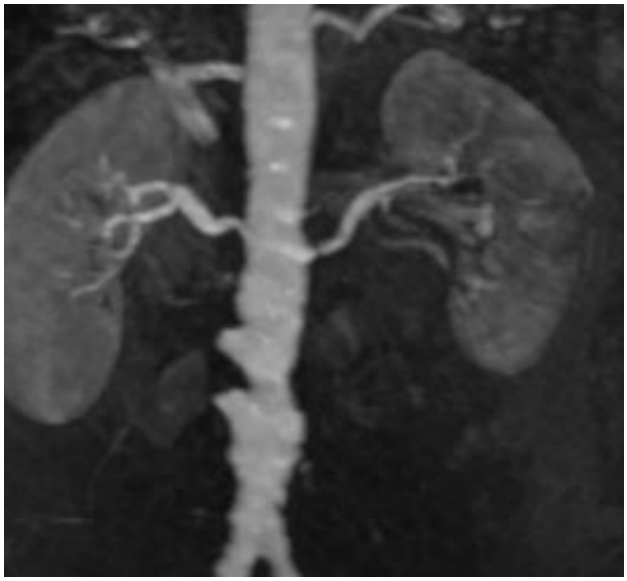

(Figure: 13 - Magnetic resonance angiography demonstrating normal right and left renal artery)

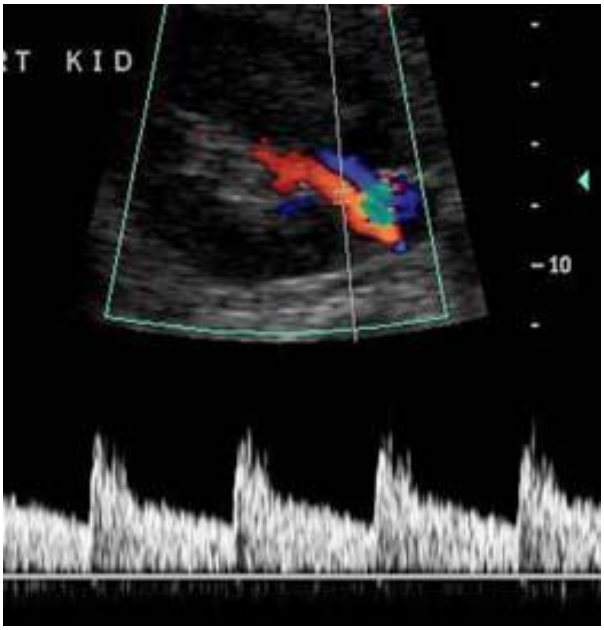

(Figure: 14 (A) **-** Color Doppler Renal Ultrasound. View of normal right renal artery (red) and vein (blue) with spectral analysis (bottom of image) showing normal low resistance wave form in the artery.

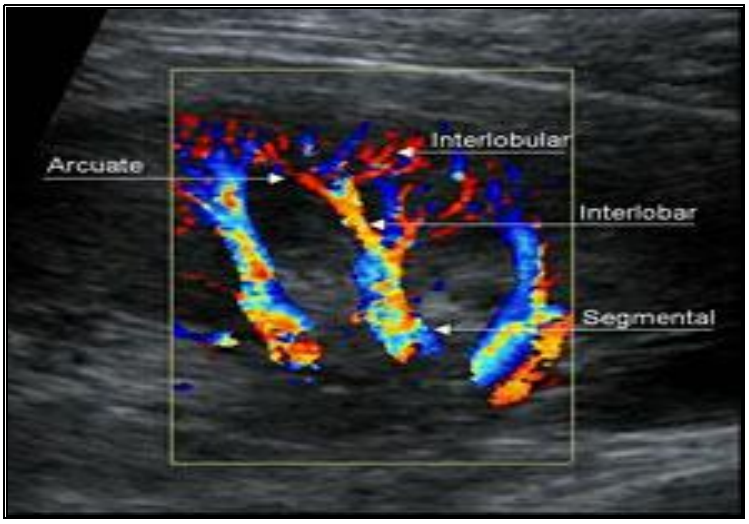

(Figure: 14 (B) - Color Doppler image demonstrating normal intrarenal vasculature. Both arteries and veins are color encoded. The arteries are encoded red, as the flow is coursing toward the probe to the periphery of the kidney. The veins are encoded blue)

Pathology of Renal Artery Stenosis

Renal artery stenosis is the narrowing of both renal arteries and their branches that might results in restriction of blood flow to the kidneys. That can cause hypertension by initiating the release of the enzyme rennin from juxta glomerular cells of affected kidney. The cross section of the lumen must be decreased by at least 60-70 % before the occlusion becomes hemodynamically significant it is the most frequent cause of curable hypertension (RVH) but it accounts for less 2% of all cases of hypertension. **(29)**

RVH occurs when RAS produces a critical narrowing of the artery that supplies one of the kidneys. Critical RAS is defined as at least 70% narrowing of the renal artery, based on angiographic (blood vessel x-ray) evaluation.

When the blood flow through the kidneys decreases ,as incase of renal artery stenosis, the juxta-glomerular cells start to secrete rennin itself is an enzyme that splits the end of one the plasma proteins, called angiotesinogen, to release angiotensin I ,two additional amino- acids are split from angiotensin II This conversion occurs almost entirely in the small vessels Of the lung, catalyzed by an enzyme called converting enzyme. Angiotensin persists in the blood for a minute or so but it is rapidly inactivated by number of blood and tissue enzymes collectively known as angiotensinase to angiotensin III which has some biological activity. Angiotensin II in the blood has several effects that raise the blood pressure, the main effect being vasoconstriction of the both arterioles and to lesser extent the vein which causes an increase in the peripheral resistance and the main circulatory filling pressure. Angiotensin II also affects the body fluid volume causing salt and water retention due to its direct effect on the kidneys and by stimulating the secretion of aldosterone from the adrenal cortex .Angiotensin III main effect is to stimulate aldosterone secretion, causing salt and water retention which in turn leads to an increase in the cardiac output. **(29)**

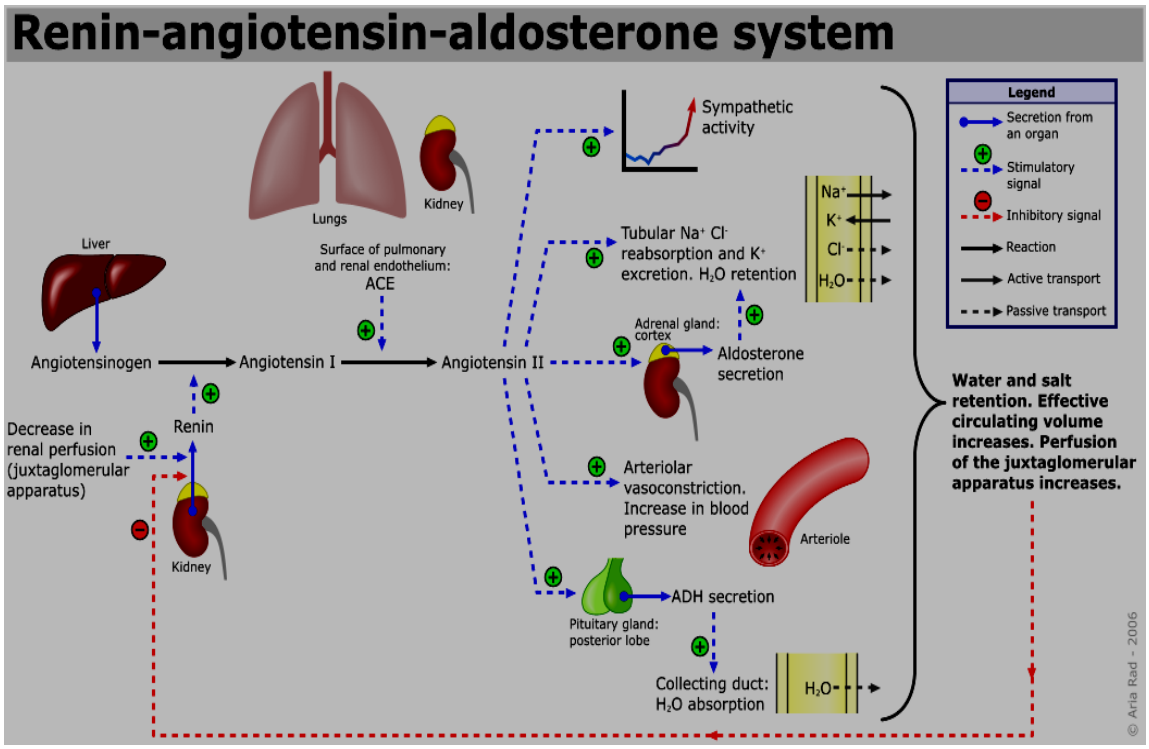

(Figure: 20 – Renin angiotensin- aldosterone system)

Renal artery stenosis has several causes:

1. Atherosclerosis
2. Fibromuscular dysplasia
3. Dissecting aneurysms
4. Takaysu's Disease
5. Other rare causes such as Renovascular diseases, Polyarteritis nodosa, Neurofibromatosis, emboli and traumatic thrombosis. **(30)**

In most cases it is caused by build up of cholesterol and lipid on the lining of arteries (atherosclerosis). This is the same disease that causes heart attack and angina when it affects arteries of the heart. Occasionally other things are responsible:

Risk factors associated with the development of atherosclerotic RAS include the following:

- Carotid artery disease
- Coronary artery disease
- Diabetes mellitus
- Hypertension (high blood pressure)
- Obesity
- Age
- Peripheral vascular disease (vascular disease in the extremities, e.g., the legs)
- Smoking **.(30)**

1- Atherosclerosis

It is the most common cause of renal artery stenosis, representing approximately 70 % of cases **(30).**

It affects individuals over the age of 55y; approximately 90 % of all renovascular lesions are secondary to atherosclerosis. The clinical manifestation of atherosclerotic RAS includes hypertension, renal failure (ischemic nephropathy), congestive heart failure (CHF) and flash pulmonary edema**. (31)**

Atherosclerosis is a disease involving the elastic arteries (such as the Aorta) and large and medium sized muscular arteries (as coronary and renal arteries). The basic lesion is an atheroma,

which consists of a raised focal plaque with a lipid core and covered by fibrous cap within the intima. **(30)**

The pathology of atherosclerosis in details include narrowing of renal artery by eccentric thickening of the intima by fibrous capped plaque .which consists of fibrous thickening under the endothelium and a deeper core of amorphous material .the core is made up of lipid containing macrophage and extra cellular lipid **.(32)**

Atherosclerotic RAS most often occurs at the ostium or the proximal 2 cm of renal artery. Distal arterial or branch involvement is distinctly uncommon renal revascularization. (**33)**

Atheromas increase and advance to cover an entire circumference of an artery leading to intraluminal narrowing of vessel. Small arteries thus become occluded leading to ischemic injury to distal organs and tissues Extensive atheromas are often friable yielding emboli into the distal circulation most commonly noted in the kidneys . (**30)**

2- Fibromuscular Dysplasia:

It is the second most common cause of renal artery stenosis. It is heterogeneous group of lesions characterized by fibrous thickening of different layers of arteries. Normal renal arteries formed of three main layers from inside outwards are tunica intima, tunica media, and tunica adventitia. Tunica intima is formed of three definite layers: Endothelium that lies upon thin basal lamina, a subendothelial layer of delicate collagenous and elastic fibers, and An internal elastic membrane that is prominent and composed of closely interwoven elastic fibers. Tunica media is formed exclusively of circulatory disposed smooth muscle cells with small amount of connective tissue. The adventitia is almost as thick as the media and contains elastic and collagenous fibers. **(34)**

Different layers of the artery may be involved such as the intima; media and adventitia thus sub classifying this disease according to the layer affected. **(30)**

The media type is by far the most common type of the disease. This type of disease is more common in females and tends to occur in younger age groups, in third and fourth decades. The lesion may consist of single well defined constrictions or a series of narrowing of artery, with the media or distal portion affected, this may be bilateral or also involved the segmental branches. **(30)**

The fibrous dysplasia is now classified as intimal fibroplasia; intimal fibroplasias in addition to stenosis may also cause renal artery dissection or aneurismal formation. Medial fibroplasia is characterized by presence of multiple micro-aneurysms that may be associated by large aneurysm.

A concentric segmental stenotic lesion characterizes true Fibromuscular dysplasia. This may be occasionally associated with A concentric segmental stenotic lesion characterizes true fibromuscular dysplasia. This may be occasionally associated with disruption of internal elastic membrane causing dissecting aneurysms the patient with subadventitial fibroplasia usually present with severely stenotic lesion characterized by dense collagen deposition in the outer portion of the media. **(35)**

3- Dissecting aortic aneurysm involving Ostia of the renal artery:

It is a dissecting hematoma in which blood is present within the wall of the vessel and spreads or dissect longitudinally thus creating a cavity by separating the tissue layers. In nearly all instances the dissection is in the media. **(36)**

Dissecting aneurysms occur more often in men, aged between 50 and 70 years. Before the age of 40 there is nearly equal male to female distribution half of all dissection in women

Occurs before the age of 40 and during pregnancy. Other causes include **Marfan's syndrome**, bicuspid aortic valve and coarctation of the Aorta. **(37)**

Morphology; the dissecting column of blood is located primarily between the outer and middle third of aortic media. An intimal tear that continues into the media is presumed to be the origin of the dissecting hematoma. The dissection commonly extends proximally and distally from the tear. This may simply end in the media and adventitia or rupture into adjacent tissue or body cavities or may reenter into the lumen of the aorta or one of its branches. The dissecting process often involves one of the main branches of the aorta such as the renal arteries. **(36)**

4- Takaysu's arteritis:

Takaysu's described a clinical syndrome characterized by ocular disturbance and marked weakening of pulses of upper extremities (pulse less disease) which is related to fibrous thickening of the aortic arch with narrowing or virtual obliteration of the origin of the great vessels arising from the arch. **(30)**

Morphology; although Takaysu's arteritis clinically involves the aortic arch, in one third of cases it also affects the reminder of the aorta and its branches in some patients it is limited to the descending and abdominal aorta.

The gross morphologic changes comprise irregular thickening of the aortic wall with intimal wrinkling. Histological the early changes consist of an adventitial mononuclear infiltrate with perivascular cuffing of the vasa vasorum. Later there may be intense mononuclear inflammation in the media with Langhan's giant cells and central necrosis. **(38)**

5- Neurofibromatosis

Neurofibromatosis is a name given to a group of conditions that have several characteristics in common. "Neuro" refers to nerves, and "fibromatosis" refers to a growth that is fiber-like inside. Thus, a common characteristic of the neurofibromatosis disorders is the growth of round fibrous lumps along the nerves. These tumors are rarely cancerous, but can cause problems if` they push on the nerves or other parts of` the body or it they are visible on the skin. An autosomal dominant gene causes all types neurofibromatosis since all genes come in pairs; a person with neurofibromatosis would have one gene for neurofibromatosis and one "normal" gene.

6- Polyarteritis nodosa

Is a disease of unknown cause that affects arteries, the, blood vessels, which carry, oxygenated blood to organs and tissues. It occurs when certain immune cells attack the affected arteries. The condition affects adults more frequently than children. It damages the tissues supplied by the affected arteries because they don't receive enough oxygen and nourishment without a proper blood supply. In this disease, symptoms result from damage to affected organs, often the skin, heart, kidneys, and nervous system. Generalized symptoms include fever, fatigue, weakness, loss of appetite, and weight loss. Muscle aches (myalgia) and joint aches (arthralgia) are common. The skin may show rashes, swelling, ulcers, and Lumps (nodular lesions). Nerve involvement may cause sensory changes with numbness, pain, burning, and weakness. Central nervous system involvement may cause strokes or seizures. Kidney involvement can produce varying degrees of renal Failure involvement of the arteries of the heart may cause a heart attack (acute myocardial infarction), heart failure, and inflammation of the sack around the heart (pericarditis).**(39)**

Renovascular disease in children:

Renovascular disease constitutes between 4.5% and 11.5% of cases of secondary hypertension in children. The most common abnormality is some from of renal artery stenosis .this may be an isolated abnormality or may be associated with idiopathic hypocalcaemia, Marfan's syndrome, rubella syndrome, Takaysu's disease or neurofibromatosis. Histologically, the commonest lesion is Fibromuscular Dysplasia which may result in areas of arterial narrowing alternating with aneurismal dilatation (string of beads) appearance angiographic ally. Occasionally, intimal proliferation predominates and this is well recognized in neurofibromatosis. **(40)**

Recent Imaging Modalities In Diagnosis of Renal Artery Stenosis

Renovascular hypertension affects l -3 % of the unselected hypertension population and 15 -30 % of patients referred to a subspecialty center because of hypertension. An advance of treatment has renewed interest in developing better diagnosis. For determining which patient has potentially correctable disease. (**41)**

Several different modalities are currently involved in the diagnosis of renal artery stenosis

The most popular are

- Color Doppler ultrasound
- Magnetic resonance angiography (MRA)
- Spiral computer tomography angiography (CTA)
- IV Digital subtraction angiography (DSA)
- Renal scintigraphy

Each method has its advantages and disadvantages. Details will be discussed in this chapter:

I. Ultrasound colored Doppler

Basic Rules: »

Doppler US is used to detect and measure blood flow, and the major reflector is the red blood cell. The Doppler shift is dependent on the isonating frequency, the velocity of moving blood, and the angle between the sound beam and direction of moving blood, as expressed in the Doppler equation. (Fig. **21**) **(42).**

$$DF = 2 F v \cos q / c$$

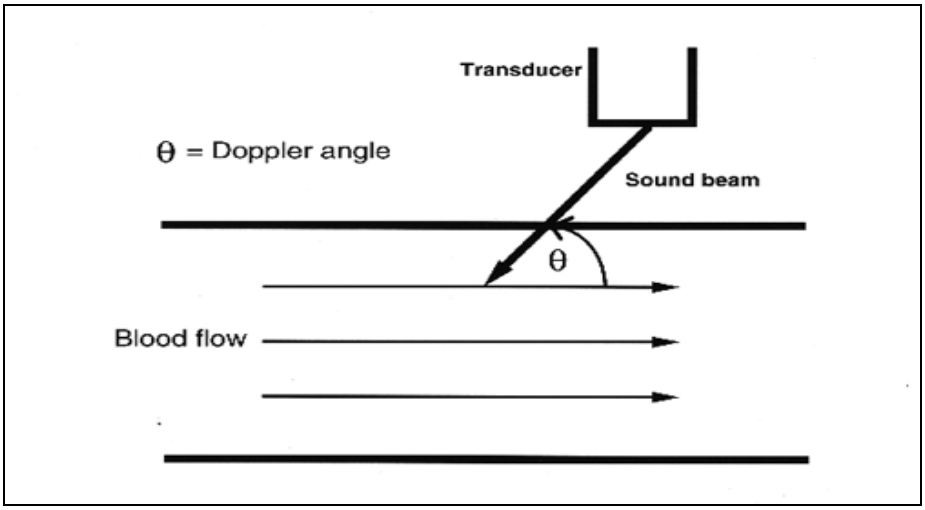

(Figure: 21– Doppler angle**) (Quoted from Olin et al, 1990)**

Doppler angle: The angle of incidence between the ultrasound beam and the estimated flow direction (parallel to the long axis of the vessel) is the Doppler angle: **DF** is the Doppler shift frequency (the difference between transmitted and received frequencies), **F** is the transmitted frequency, **V** is the blood velocity, **C** is the speed of sound, and **q** is the angle between the sound beam and the direction of moving blood. The equation can be rearranged to

solve for blood velocity, and this is the value calculated by the Doppler US machine **(42).**

The angle of insonation should also be less than 60° at all times, since the cosine function has a steeper curve above this angle. And errors in angle correction are therefore magnified.**(43)**

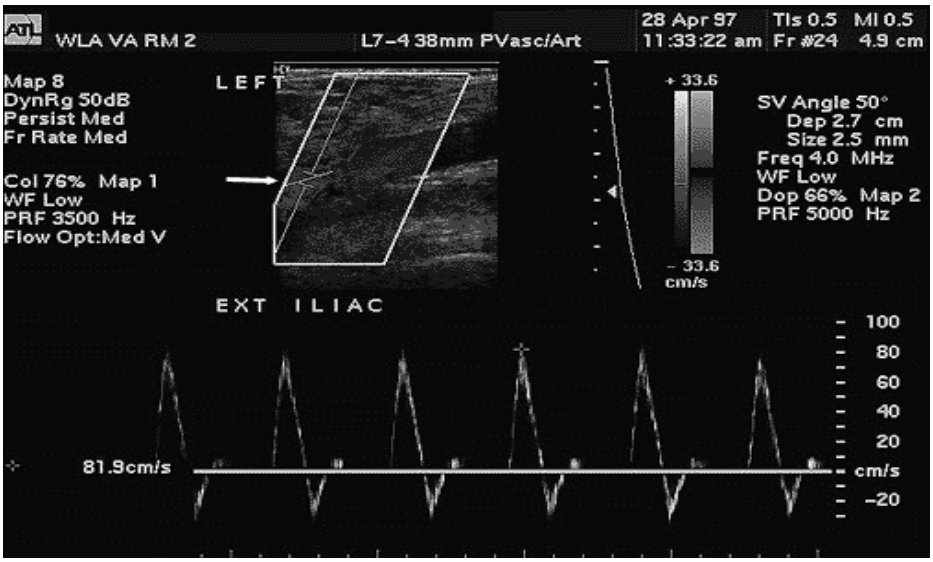

(Figure: 22-Angle Correction, duplex Doppler US. The line (arrow) within the sample gate is used to estimate the Doppler angle. Between the ultrasound beam and the blood flow direction). **(Quoted from Olin et al, 1994)**

TYPES OF THE DOPPLER INSTRUMENTATION

I- Pulsed Doppler

In pulsed Doppler the sound pulse is transmitted and received by a single transducer thus avoiding two or more signal from being superimposed over each other, spatial separation is achieved by an electronic method of selecting the Doppler shifted.

2- Power Doppler

Power Doppler sonography is a Doppler technique that was developed to overcome some of the drawbacks of conventional color Doppler imaging. It displays the integrated power of Doppler signal instead of its mean Doppler frequency shift and extends the dynamic range of the Doppler scale. It is non-angle dependent and can detect fine intraparenehyrnal blood flow **(44).**

Technique;

Examinations are performed using a 3.5-MHZ curvilinear array transducer of` an echo Doppler unit. The patient is in supine position to visualize the origin and proximal course of the main renal arteries and accessory renal arteries (extra renal arteries). Both color Doppler US and power Doppler US (especially in obese patients) have to be employed to detect and correctly evaluate the morphology of the entire course of the renal arteries. **(45)**

Epigastric transverse scans allow the identification of the main renal arteries, which originate laterally (anterolateral, right artery; posterolateral, left artery) in the abdominal aorta at about 1 cm under the anterior emergence of superior mesenteric artery and have a proximal course just posterior to the left renal vein in normal conditions, Color imaging can show the site of stenosis as signs of turbulence in the systolic phase **(45).**

In the first part of the examination, Doppler waveforms should be recorded for the entire course of the renal arteries. With the color Doppler US unit set for high flow velocities (pulse repetition frequency, 4,000 6,000 Hz), to evaluate the peak systolic velocities: The angle correction is essential to obtain the correct measurements **(45).**

A significant arterial stenosis produces an increased peak systolic velocity at or immediately distal to the area of narrowing, have considered peak systolic velocities of 100-200 cm sec as suggestive of mild stenosis (50% narrowing) and those higher than 200 cm/sec as suggestive of severe stenosis (50% -90% narrowing).**(45)**

The second parts of the examination, intrarenal vessels are evaluated. The patient is in the lateral decubitus position, with the same 3.5-MHz curvilinear probe, and with the color Doppler US. Unit set for medium flow velocities (pulse repetition frequency 1,500:2,500 Hz). For more correct evaluation, the blood flow in the intrarenal vessels in the superior third, medium third, and inferior third of each kidney have to be recorded. An acceleration time greater than 0.07 seconds with a tardus-parvus waveform can be considered diagnostic of severe stenosis of the extra renal arteries. **(45)**

Doppler Parameter:

1-cceleration index: it is the slope of the early systolic rise .1t is estimated by dividing the acceleration slope by the transmitted. IF it is less than 3 meters per sec it is suggestive of renal artery stenosis

2-Acceleration time: It is the interval from the onset of systolic flow to the initial peel: systolic velocity (normally 0.07 to 0.1 sec.) .If it is greater than 0.1 sec. This indicates **RAS** greater than 50.

3- There is **increased systolic velocity** through the area of stenosis. The peak systolic velocity required diagnosing renal artery stenosis ranges from 100 to 180 cm/sec .

4- Post stenotic turbulence may be seen in the affected artery.

5- A ratio of PSV at the site of maximum stenosis to that proximal to the stenosis of more than 2 suggests that the stenosis hemodynamically significant.

6- The ratio of end diastolic to systolic velocity obtained from interlobar and arcuate artery waveforms also can be used to evaluate renal vascular resistance and renal parenchyma a ratio under 0.23 is considered abnormal and severe parenchymal vascular disease.

7- Tardus-parvus waveform: Tardus is characterized by delayed early systolic acceleration while parvus is the diminished amplitude and rounding of the systolic peak. That happens distal to the stenosis.

8- Early systolic peak (**ESP**): it usually has an acute angle that in normal artery rises higher than the second part of the systolic Peak. ESP is usually absent distal to the stenosis.

9- Resistive index (**RI**): exceeds 0.70 in renal artery stenosis. **(46)**

Other parameters:

The renal aortic ratio was calculated by dividing the peak systolic velocity in the renal artery by the peak systolic velocity in the aorta. If the renal aortic ratio was 3.5 or more, it indicates 60 % to 99% stenosis of the renal artery.

1-peak systolic velocity is a measure of the maximum velocity of blood flow during systole. Using Doppler principles as an artery narrows the velocity of blood flow increases.

2-The end-diastolic velocity is a measure of the velocity of blood

flow at the end of diastole. In patients with severe degrees of arterial narrowing, the velocity of diastolic flow may be increased. In the study performed by the average time for completion of a renal duplex scan was approximately 1 hour, the common reasons for technical failure were excess bowel gas and obesity. Identification of Accessory renal arteries was sometimes difficult **(46).**

Patient classification;

1- A renal artery ratio of less than 3.5 and a peak systolic velocity of less than 200 cm/s identified patients with 0% to 59% renal artery stenosis.

2- A renal-aortic ratio of 3.5 or more or a peak systolic velocity of more than 200 cm/s (or both) identified patients with 60% to 99% renal artery stenosis.

3- Occlusion of the renal artery was diagnosed by the absence of a flow signal in the renal artery and by a low-amplitude parenchymal signal **(47).**

Other Applications of Duplex and Color Doppler of the Kidneys:

1-The resistive index (RI) has been used to evaluate renal parenchymal disease. Past studies have shown that a resistive - index of > or equal to 0.70 is suggestive of tubulo-interstitial disease or a vasculitis. Patients with a purely glomerular disease often had a resistive index that is < 0.70. The same authors snowed that RI is useful in differentiating the more common causes of acute renal failure such as acute tubular necrosis and pre-renal failure. Patients with acute tubular necrosis (excluding hepato-renal syndrome) often had a resistive index

of > or equal to 0.75 whereas those with pre-renal failure (excluding patients with, severe, prolonged pre-renal failure which can lead to acute tubular necrosis), had a value of <0.75- However, there limitations to the clinical application of these values. **(48)**

When a dilated collecting system is observed with sonography, it is important to differentiate obstructive from non- obstructive dilatation. Prior studies have suggested that intrarenal Doppler analysis (RI) can be used to distinguish obstructive from non obstructive dilatation. It has been shown that in the setting of obstructive dilatation, renal vascular resistance increases due to the presence of a potent renal vasoconstrictor thromboxane A

2. The RI which measures arterial vascular resistance, is elevated > 0.70) in the setting of obstructive dilatation. In mixed population of patients, this value was shown to have a specifity of 88% and a sensitivity of 92%. Other authors have not been able to reproduce these findings and have shown a sensitivity (using RI threshold of`> 0.70) of only- 30% to 47% in a setting of complete or high-grade obstruction. However, an elevated RI in the proper clinical setting was highly specific for obstruction **(48).**

3- Renal vein thrombosis has many different etiologies for its development in adults including nephrotic syndrome, membranous glomemlonepltritis, systemic lupus erythematosis, pyelonephritis, neoplasm, a hypercoagulable state or trauma. It may also be caused by extrinsic compression of the renal vein from acute pancreatitis, retroperitoneal fibrosis, hemorrhage or neoplasm. Patients frequently present with flank pain and hematuria if the renal vein thrombosis is acute but may be asymptomatic if the thrombosis is chronic. At sonography, the kidney is enlarged and hypoechoic with poor cortico-medullary differentiation. There may be patchy areas of increased echogenicity due to hemorrhage at color Doppler sonography, a color void will be noted within the renal vein in an acute setting, a Doppler signal may not be obtained from the renal vein. However, if the thrombosis is chronic, collateral vessels will be present.

It is therefore important to search the entire renal vein for evidence of thrombus including the inferior vena cava The renal artery in a transplanted kidney will often show diastolic flow reversal in the setting of renal vein thrombosis, whereas in the native kidney, a normal arterial waveform is usually observed due to the development of venous collaterals within 24 hours of the thrombosis in the vein **(48).**

4- Renal arteriovenous (AV) fistulae usually occur in the setting of a prior renal biopsy whether in a native or transplanted kidney. The fistulae are usually asymptomatic and self-limiting, but occasionally will cause hypertension, and rarely, high output congestive heart failure. On duplex and color Doppler sonography, there is increased arterial flow with high peak systolic and end diastolic velocities and a decreased resistive index as well as arterialization of the venous waveform and perivascular tissue vibration**(48)**

The contrast-enhanced Doppler ultrasound with perflurocarbon exposed sonicated albumin (PESDL)

Over the past few years, there has been extensive research for a reliable, noninvasive, and nonionizing imaging method renal artery stenosis (RAS). **(49)**

Recently, the use of micro bubble echo-enhancing agents in combination with harmonic Doppler imaging has been proposed to improve Doppler signal intensity in multiple vascular sites **(50).**

In addition, contrast-enhanced harmonic Doppler US can currently provide objective functional assessment of RAS through analysis of time-intensity renal enhancement curve. **(51)**

Using micro bubble levovst® echo-enhancing ultrasonography in

hypertensive with renal stenosis. They demonstrated a sensitivity of 85% and specificity of 79% without contrast and a sensitivity of 94% and a specificity of 88% with contrast, besides an important reduction in the time of procedure **(52).**

The echo-enhancing agent **PESDA** (per fluorocarbon exposit solicited albumin) is a second agent, containing high molecular weight gas, whose use results in higher stability and better reflections of Doppler signs**(53).**

Although the technique of renal arterial US scanning has been well established for years, a lot of difficulties in reliably identifying main and accessory renal arteries remain **(54).**

Most of these difficulties are related to the patient obesity, the presence of bowel gas, excessive respiratory movement, and the depth and tortuosity of the renal arteries. The time expended in the examination can be too long as almost 60 minutes **(55).**

Using Levovst as the US contrast, the infusion increased in by 20 the number of patients in whom renal arteries could be evaluated, % including difficult cases such as those involving patients who are obese and patients with impaired renal function. However, some centers participating of the study also presented a feasibility of l00% and the Levovst infusion did not interfere in the results **(56).**

Infusion of PESDA contrast seems not to improve the accuracy, despite a reduction in the exanimation duration and an increase in specificity based on one Doppler criterion. Also, the feasibility of US is dependent of the quality of the machine, and the infusion of contrast does not add advantages if the performance, US machine is excellent. However it remains unknown if the PESDA infusion can improve feasibility if the machine does not have a good imaging quality. So, there is a need for establishing a consensus opinion regarding Doppler useful criteria and thresholds for renal arterial stenosis regardless of

the US equipment used or infusion of ultrasonographic contrast **(57)**

II. Magnetic resonance angiography (MRA)

Renal Magnetic resonance (**MRA)** angiography allows accurate evaluation of patients suspected to have renal artery stenosis without the risks associated with nephrotoxic contrast agents, ionizing radiation, or arterial catheterization. Other applications of renal MR angiography are mapping the vascular anatomy for planning renal revascularization, planning repair of abdominal aortic aneurysms, assessing renal bypass grafts and renal transplant anastomosis, and evaluating vascular involvement by renal tumors. A variety of pulse sequences provide complementary information about kidney morphology, arterial anatomy, blood flow, and renal function and excretion. Three-dimensional gadolinium-enhanced MR angiography can be combined with several other sequences to produce a comprehensive approach to renal MR angiography. This comprehensive approach is designed to allow hemodynamic characterization of renal artery stenosis with a single MR imaging examination that can be easily completed in 1 hour. Three-dimensional gadolinium-enhanced MR angiography demonstrates the renal arteries along with the abdominal aorta, iliac arteries, and mesenteric arteries in a 20–30-second acquisition that can be performed during breath holding. Numerous projections are reconstructed from a single three-dimensional volume of data acquired with a single injection of contrast material to obtain perpendicular and optimized views of each renal artery. **(58)**

Various MRI techniques are used to diagnose renovascular disease. (58)

I. Non contrast techniques:

A. Time of flight angiography (TOF):

I- 2D TOF MR Angiography:

II- 3D TOF MR Angiography.

1- No TONE conventional techniques.
2-TONE series (TONE = tilted optimized non saturating excitations).
3- SIR-RAGE series (SIR-RAGE = selective inversion recovery rapid gradient echo).

B. Phase contrast MR Angiography:

A) D phase contrast MR Angiography
B) Breathe hold technique.
C) Cardiac gated technique.

Il. Contrast enhanced techniques.

A. Gadolinium enhanced MR Angiography:

l- Dynamic gadolinium 3D spoiled gradient echo MR Angiography
2- Breath holds ultrafast 3D MR Angiography.

B. MR Renograms : 1 - Conventional Renogram.
2- Captopril sensitized MRI Renogram.

Technique:

Patient selection

Initially, patients referred for renal MR angiography usually have contraindications to conventional angiography Such as renal insufficiency (serum creatinine level >2.0 mg/dl) and allergy to iodinated contrast material, according to. **(59)**

However MR angiography has become the preferred primary technique for imaging the renal arteries, all patients suspected to have renal artery stenosis undergo renal angiography routinely;

conventional arteriography is performed only as part of an interventional procedure or in young patient suspected to have fibromuscular dysphasia when results of MR angiography are inadequate **(31).**

Proper technique

Several flow-based MR angiography techniques have been used to directly image the renal arteries and veins. However, there are limitations to these techniques, including turbulence-induced signal loss at stenosis in-plane saturation, non visualization of small-caliber vessels such as distal renal arteries and accessory renal arteries; and poor quality due to slow flow in patients with cardiac disease or aortic aneurysm or older patients. Accordingly Contrast-enhanced MR arteriography performed with a high dose of gadolinium contrast material and a high-resolution 3D spoiled gradient-echo pulse sequence is preferred. **(59)**

Gadolinium contrast material can be used safely, even at high doses; in patients with renal failure .Three-dimensional gadolinium-enhanced MR angiography demonstrates the renal arteries along with the entire abdominal aorta, iliac arteries, and mesenteric arteries in a 20-30-second acquisition that can be performed during breath holding. The renal vein and inferior vena cava can be evaluated by repeating the examination during the venous and equilibrium phases. **(60)**

However, morphologic assessment of the arterial lumen with 3D gadolinium-enhanced MR angiography is not sufficient for complete assessment in patients suspected to have renal artery stenosis. It is necessary to evaluate the hemodynamic significance of any stenosis identified to determine if the patient will benefit from a revascularization procedure. **(30)**

Many MR imaging- based techniques have been proposed for evaluating the haemodynamic significance of renal artery stenosis, Including:

(a) Measurement of renal blood flow with 2D cine C imaging;

(b) Identification of the turbulence–induced spine dephasing at hemodynamically significant stenosis with 3D PC imaging

(c) Examination of the temporal enhancement pattern

(d) Identification of differential excretion of gadolinium

(e) Evaluation of the effect of angiotensin-converting enzyme inhibition on .flow measurement with MR imaging or gadolinium clearance rates. Many of` these approaches are difficult to implement because of` the challenge of reliable electrocardiographic gating and the post processing required. However, 3D PC MR Angiography is substantially improved after administration of a high dose of gadolinium contrast material. The qualities make 3D MR angiography a highly complementary sequence performance after 3D gadolinium-enhanced MR angiography. **(30)**

Imaging protocol.

Comprehensive imaging approach is designed to provide contrast-enhance arteriogram and allow haemodynamic characterization of renal artery stenosis with a single MR imaging examination that cane easily completed in a 1-hour time slot by using a l.5-T imaging System with high performance gradients. Although the data are acquired by the technologist without monitoring, the radiologist performs the post processing. In about 50% of patients, the images obtained with one pulse sequence are of poor quality However; The Complementary information provided by this combination of sequences allows diagnostic results are to be obtained in 95% of patients. **(30)**

Patient Preparation:

Administration of oxygen helps patients who are short of Breath to suspend breathing during entire 3D gadolinium enhanced MR angiography acquisition. **(61)**

It is acceptable and easiest to use a body coil because it provides a large field of view with homogeneous signal. Torso or body phased-array coils allow a higher signal-to-noise ratio to be achieved in thinner patients, although the bright, near-field artifact from tissue close to the coil can be a problem. A landmark is placed on the lower margin of the rib cage along the axillary line to center imaging on the kidneys. **(61)**

- **Sagittal Localization:**

A Tl-weighted spin-echo technique preferably performed and an echo time of approxrimate1y 15-20 seconds, provides, a "black blood" effect for locating arteries (**Fig: 30a**). Alternatively, spoiled gradient-echo imaging can be used with one or two breath holds. Single-shot fast spin-echo imaging can be used without breath holding, although breath holding is preferred (**Fig: 30 b**). **(31)**

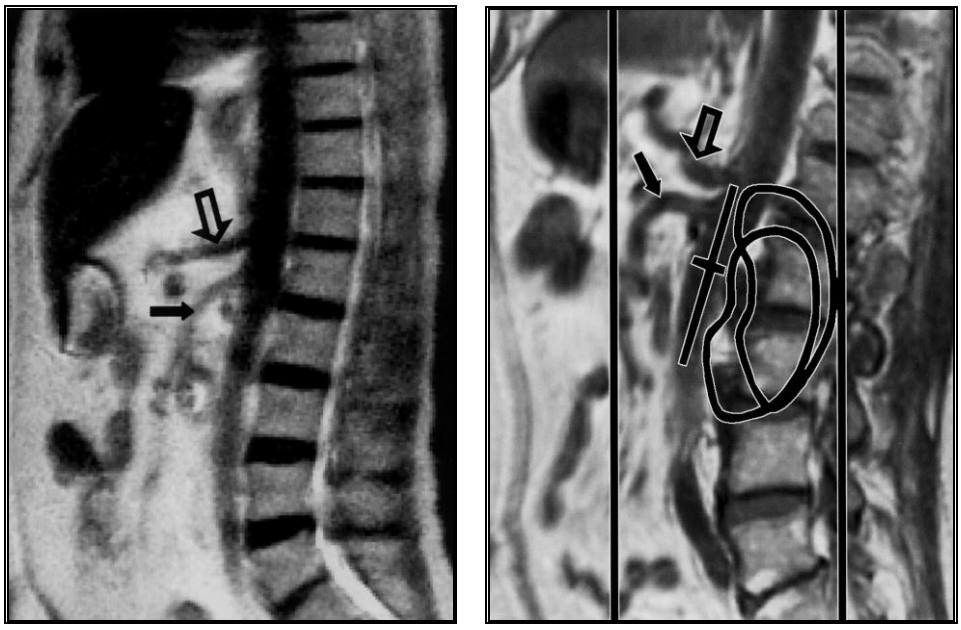

a b

(Figure 30 -Sagittal T I weighted spin-echo **(a)** and single-shot fast spin-echo **(b)** MR images obtained for localization show the abdominal aorta and the origins of the celiac artery (open arrow)and superior mesenteric artery (solid arrow). The angiography is ◌position of` the three-D volume for gadolinium-enhanced MR represented by the rectangular black outline in which includes the abdominal aorta and most of` the kidneys (curved black outlines). The tracker for automatic triggering is placed on the aorta at the level of the superior mesenteric artery**) (Quoted from Dong et al)**

Axial 2D.T2-weighted Imaging;

Axial T2-weighted images obtained with fat saturation are useful for characterizing any masses that are present. On T2- Weighted images, simple renal cysts can distinguished from more complex lesions that are suspicious for malignancy. The entire length of the kidneys is covered in this sequence. By using a sufficient number of signals and repetition time to make this Sequence at least 4-5 minutes long, there will be sufficient time to Set up the following more complex 3D gadolinium-enhanced MR Angiography sequence. **(61)**

Three-dimensional Gadolinium-enhanced MR Angiography;

A 3D spoiled gradient-echo volume that includes the entire abdominal aorta, renal arteries, and iliac arteries are used. In selecting the specific parameters for the 3D spoiled gradient-echo Sequence, one can take advantage of several interesting aspects of` MR physics to obtain the highest-quality images. In general, faster is better for data acquisition with 3D gadolinium-enhanced MR angiography. Faster data acquisitions allow the same dose of` Gadolinium contrast material to be injected over a shorter data Acquisition time with a faster injection rate to produce a higher Arterial gadolinium concentration. This higher arterial gadolinium Concentration may then make up for the reduced time for Tl relaxation and signal averaging. **(62)**

Fast data acquisitions also result in less motion artifact and make it easier for patients to suspend breathing. To make the data acquisition fast, use the shortest possible repetition time, a short echo time, and the smallest number of sections sufficient to cover the arterial anatomy with adequate resolution. However, avoid using too wide of a bandwidth. Widening the bandwidth makes the data acquisition faster but at a substantial sacrifice in signal-to-noise ratio. Also take into consideration that the timing of bolus injection is difficult with data acquisitions of 30 seconds or shorter but relatively easy with data acquisitions of 40 seconds or longer.**(62).**

It is important to make the echo time less than 3 msec to avoid excessive spin dephasing, especially from the swirling jet flow distal to stenosis. Selecting an echo time at which fat and water are out of phase (2–2.5 msec) will help suppress fat. Fat suppression is important because fat is the brightest background tissue. The signal of background tissue can also be reduced by obtaining a 3D data set before contrast material administration to use for digital subtraction **(61).**

In theory, the flip angle should be tuned for optimum T1 contrast on the basis of the repetition time and expected blood gadolinium concentration. However, we have found that a flip angle of 45° works well in nearly all cases. The flip angle could be larger for higher doses of contrast material and longer repetition time or smaller for lower doses of contrast material and shorter repetition time.**(61)**

Correctly estimating the breath-hold capacity of the patient is essential because breath holding is required during image acquisition. Usually, older patients, patients who smoke, and patients with cardiopulmonary disease can suspend breathing for only 20-25 seconds or less. Younger, nonsmoking patients without cardiopulmonary disease can easily hold their breath for 30–40 seconds or longer. The section thickness, number of sections, and number of phase-encoding steps should be adjusted to ensure that the acquisition time is short enough for the patient to suspend breathing for the entire data acquisition. **(60)**

When prescribing the 3D spoiled gradient-echo image volume, one should first estimate how long the patient can suspend breathing. Then, adjust the coverage, section thickness, and number of phase-encoding steps so that the data acquisition covers the aorta and renal arteries and can still be completed within the patient's breath-hold capacity. Prescribe the image volume from anterior to the abdominal aorta to posterior to the mid kidney by using 2–3-mm-thick sections **(Fig: 30a).** Zero padding or zero filling by a factor of 2 in the section direction is useful because it doubles the number of sections without increasing imaging time. Set the top of the imaging volume 2–3 cm above the celiac artery. Use a field of view that is about as large as the patient is wide to avoid wraparound artifact. Typically, 30–36 cm is sufficient and will also ensure that the iliac arteries are included inferiorly. It is also essential to elevate the arms with cushions, exclude them with Faraday shields, or elevate them over the chest or head to prevent wraparound of the arms into the imaging volume **(63).**

The dose of gadolinium contrast material is one of the most important determinants of image quality. A dose of 40 mL is given in most cases to simplify a standard pattern of manual injection with an injection rate of 2mL/sec. It is necessary to flush the contrast material through the intravenous tubing and veins with at least 20 mL of normal saline solution to ensure delivery of the entire dose and rapid venous return. It is helpful to use standardized intravenous tubing set with an automatic mechanism for switching between contrast material infusion and flushing with no delay **(64).**

For further characterization of renal function, the rate of contrast material transit in the kidney should be assessed. Such assessment can be accomplished by obtaining repeat data sets during the arterial, venous, and equilibrium phases with three separate breath holds. Alternatively, several 3D data sets can be acquired in a single breath hold with fast multiphase 3D gadolinium-enhanced MR angiography (38). With this technique, the acquisition time for a single 3D data set is reduced to just a few seconds, thus allowing demonstration of minor changes in the temporal evolution of renal enhancement.(**Fig:31**).

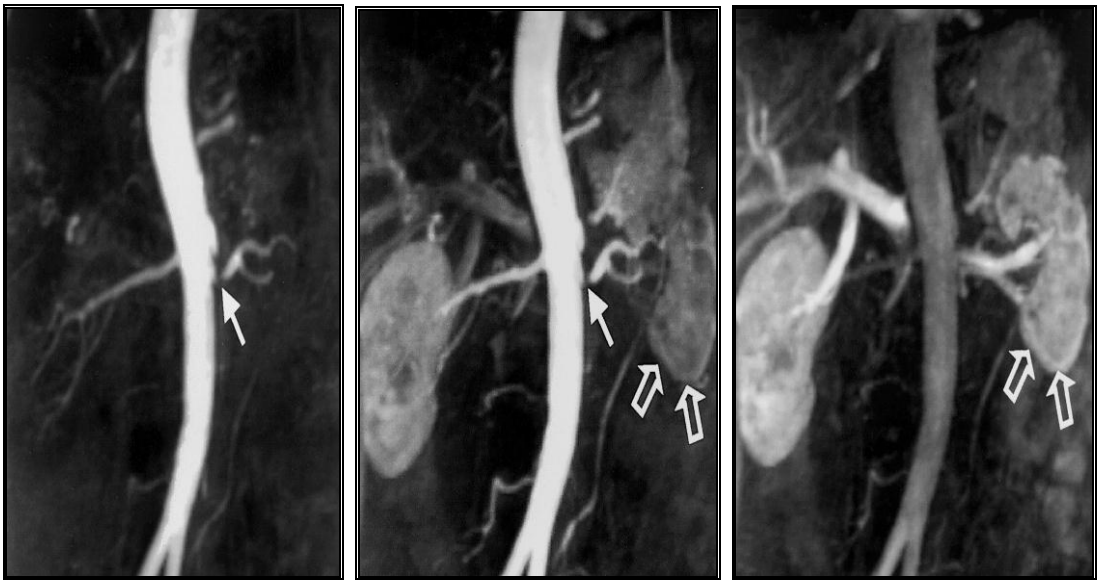

a b c

(Figure: 31– Coronal images obtained with multiphase 3D gadolinium-enhanced MR angiography (repetition time msec/echo time msec = 3.2/1.1, field of view = 27 × 36 cm, slab thickness = 8 cm, number of reconstructed sections = 44, acquisition time per phase = 6.3 seconds) show the evolution of renal enhancement. **(a)** Early arterial-phase image shows that the renal arteries are completely enhanced. There is a proximal high-grade stenosis of the left renal artery (arrow) and a normal right renal artery. No parenchymal enhancement is present. (b) Late arterial-phase image shows the stenosis (solid arrow) and delayed enhancement of the shrunken left kidney (open arrows**). (c)** Early venous-phase image shows that the enhancement of the left kidney (arrows) is equal to that of the right kidney**).**

Three-dimensional PC Imaging:

Finally, axial 3D PC images can be acquired immediately after the dynamic gadolinium-enhanced acquisition to further characterize the functional significance of renal artery stenosis and to improve evaluation of the distal renal artery. The velocity encoding should be set at 50 cm/sec for patients with normal renal blood flow. It can be reduced to 30 cm/sec for patients with heart failure, renal failure (creatinine level >2.0 mg/dL (177 μmol/L), or aortic aneurysm or those aged 70 years or older. Young (<30 years of age) or athletic patients may require a velocity encoding of 60 cm/sec. Precise quantification of renal blood flow can be performed with an electrocardiographically gated 2D cine PC flow measurement technique. With this technique, multiple 2D images are obtained at a single location perpendicular to the long axis of the renal artery to show the cross-sectional renal blood flow at high temporal resolution over the cardiac cycle **(Fig 32). (65)**

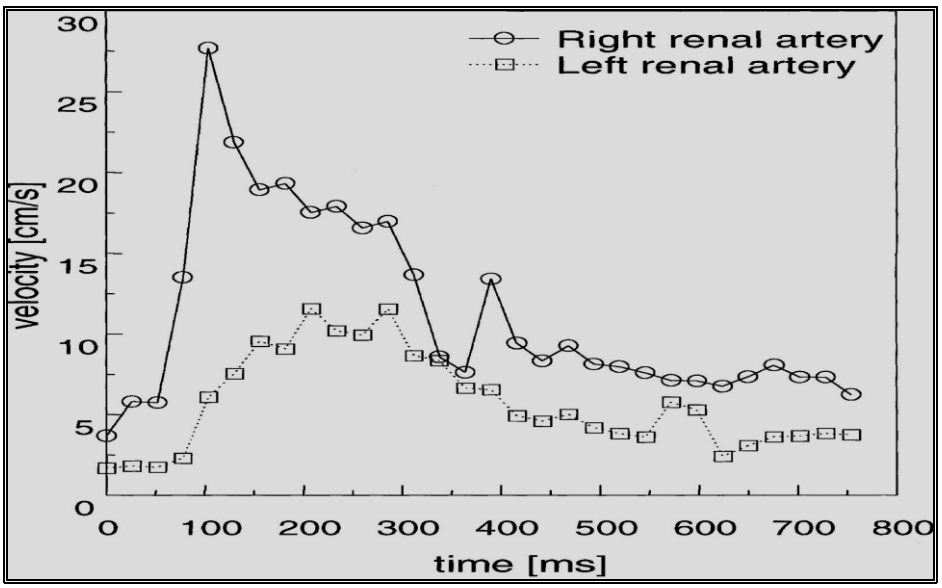

(Figure: 32- Diagram shows renal blood flow measurements obtained with cine PC MR imaging (repetition time/echo time = 26/6) performed bilaterally perpendicular to the vessel axis. The right renal artery has a normal flow profile with an early systolic peak. The mean flow rate is 310 mL/min. The left renal artery has a flattened flow profile with loss of the systolic velocity components. The mean flow rate is only 93 mL/min. The diagnosis of a hemodynamically and functionally significant stenosis of the left renal artery was made).**(Quoted from Dong et al., 1999)**

Image Analysis

Measurement of the Kidney Length and Parenchymal thickness. Kidney length and parenchymal thickness can be measured and cortico-medullary differentiation can be demonstrated on the sagittal localization images **(Fig 33a).** Alternatively, 3D gadolinium-enhanced MR angiograms can be used, especially if the renal axis is unusual (fig 33 b, c). Kidney length and parenchymal thickness are reduced in patients with long-standing renal artery stenosis.

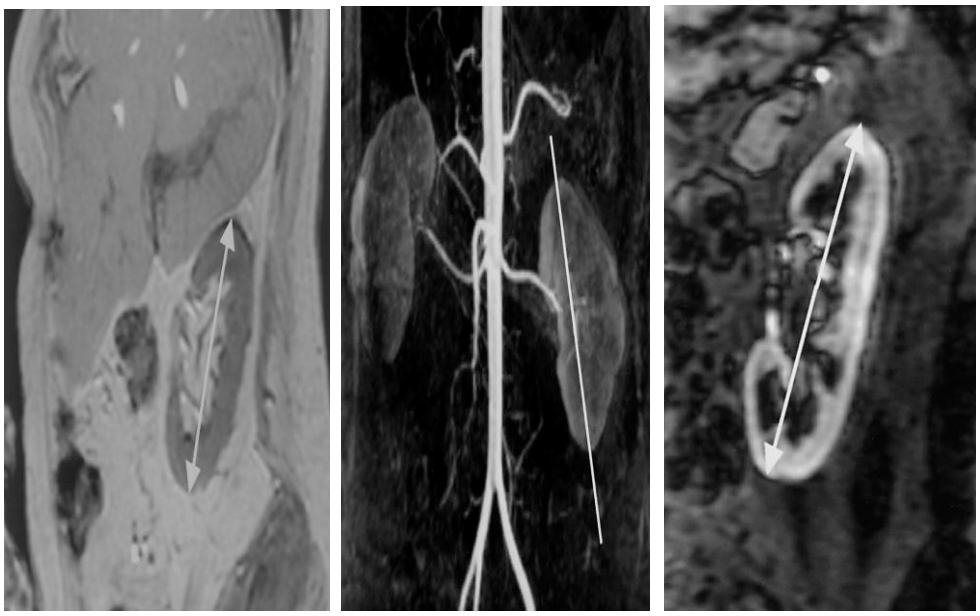

a b c

(Figure: 33- (a) Sagittal T1-weighted spin-echo MR image shows a right kidney of normal length and parenchymal thickness**. (b, c)** Oblique reformation images from arterial-phase 3D gadolinium-enhanced MR angiography show measurement of kidney length**).(Quoted from Dong et al., 1999)**

Characterization of Renal Masses:

The axial T2-weighted images allow evaluation and characterization of any renal masses or other abdominal pathologic conditions. Any suspicious lesion can also be evaluated by examining the 3D gadolinium-enhanced MR angiography source images, which are somewhat analogous to contrast-enhanced CT scans. Do not analyze masses on maximum-intensity projection (MIP) images because important details and sometimes the entire mass may be obscured **(62).**

Reconstruction and Reformatting:

After acquisition of the 3D MR angiographic data, post processing is performed, which requires an additional 10–20 minutes of work on a computer workstation (Advantage Windows; GE Medical Systems) to obtain **MIP** and reformation images of the abdominal aorta, each renal artery, the celiac and superior mesenteric arteries (**Fig . 34 a, b**), and the common iliac arteries. Sub volume MIP images encompassing each renal artery in coronal oblique and axial oblique planes are produced so that each renal artery origin is evaluated with perpendicular views to help identify eccentric atherosclerotic plaque. (Fig. **34 c, d, e**). **(62)**

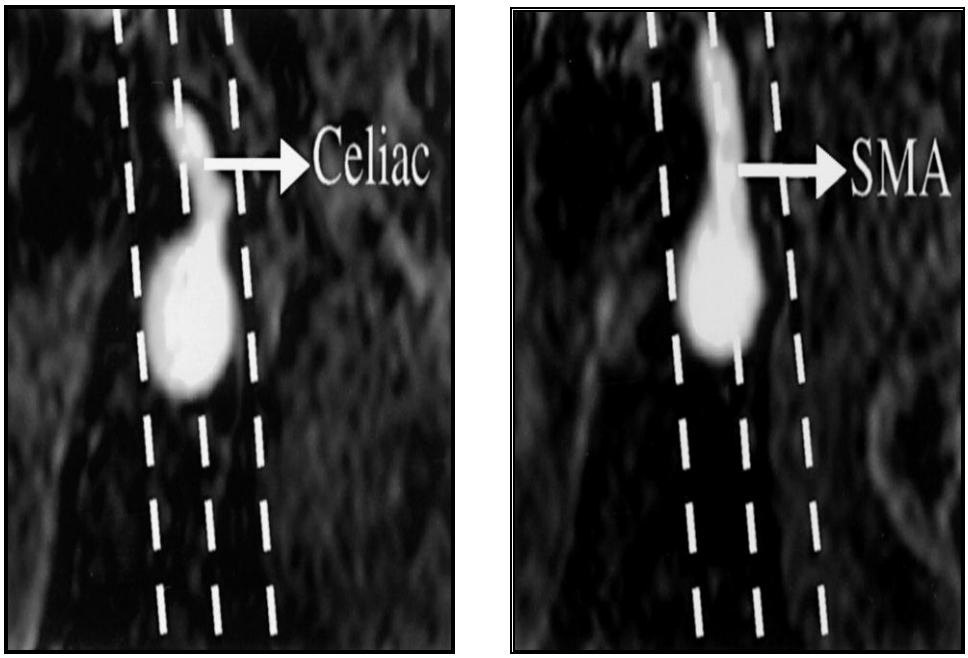

a b

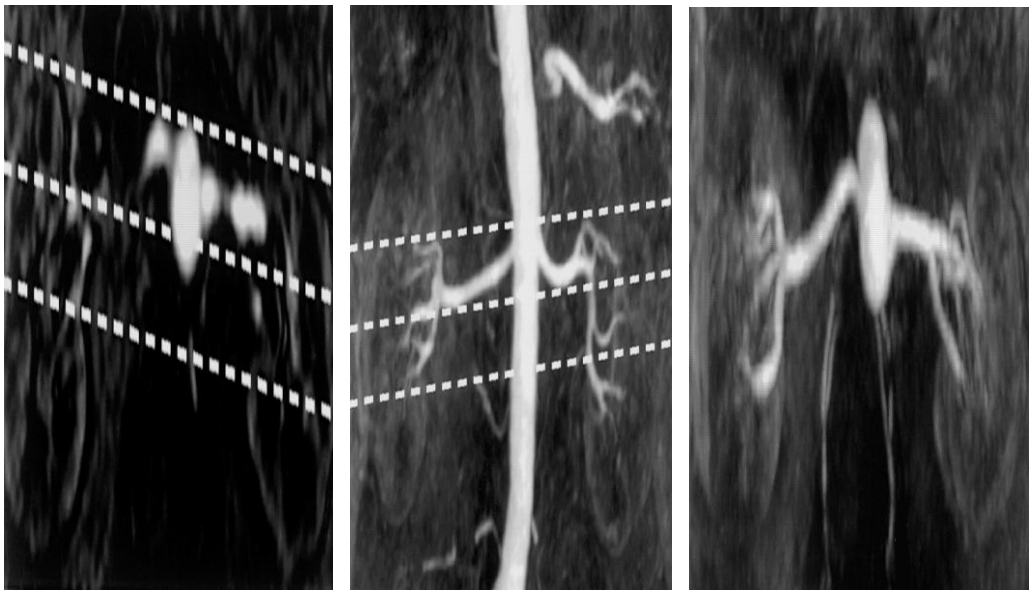

C d e

(Figure: 34 – (**a, b)** Axial reformation images show the origins of the celiac artery (a) and superior mesenteric artery **(b).(c)** Axial reformation image shows the renal arteries. **(d)** Coronal oblique subvolume MIP image reconstructed from axial reformation images shows the renal arteries. **(e)** Axial oblique subvolume MIP image reconstructed from a coronal oblique subvolume MIP shows the entire renal arteries). **(Quoted from Dong et al., 1999)**

Assessing the Severity of Renal Artery Stenosis:

Initial grading of any renal artery stenosis can be performed by evaluating 3D gadolinium-enhanced MR angiograms and 3D PC images for spin dephasing **(Fig: 35).** The determination of hemodynamic significance can be further refined by considering additional factors. Post stenotic dilatation is also associated with hemodynamically significant stenosis. Semi quantitative assessment of the hemodynamic significance can be accomplished by looking at changes in the flow profile produced with cine PC imaging, particularly for delay or loss of the early systolic peak. **(59)**

In addition, functional changes in the renal parenchyma can be appreciated by looking for loss of cortico-medullary differentiation, delayed renal enhancement, and asymmetric concentration of gadolinium in the collecting systems as well as reduced kidney length and parenchymal thickness.

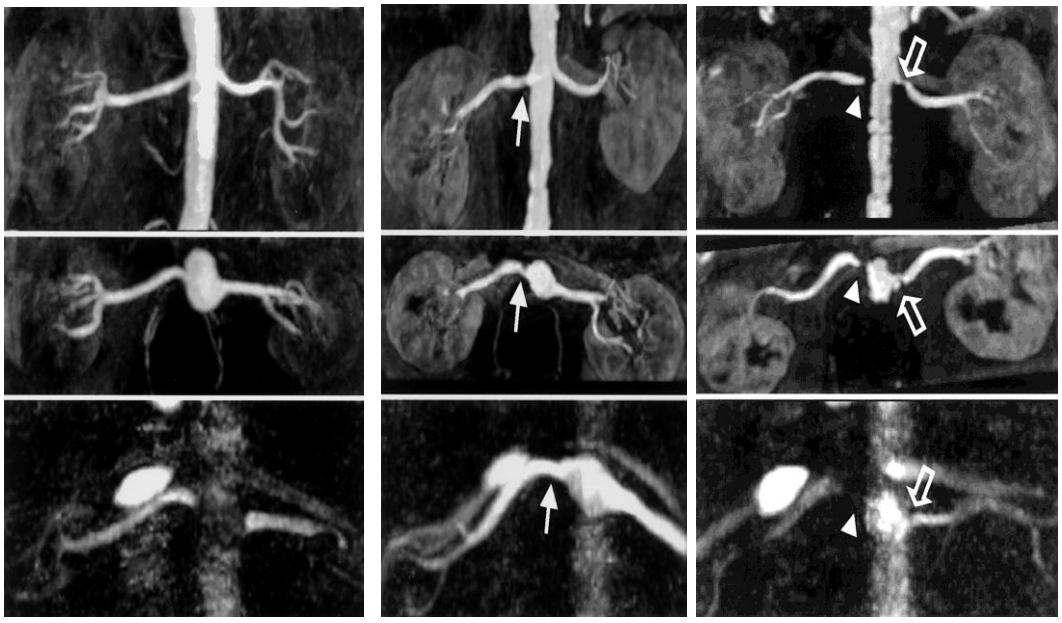

a b c

(Figure 35 - Coronal (top) and axial (middle) 3D gadolinium-enhanced MR angiograms and axial 3D PC MR images (bottom) show normal renal arteries **(a)**, mild right renal artery stenosis (<50%) **(b)**, and moderate left renal artery stenosis and severe right renal artery stenosis **(c)**. The 3D PC image shows a normal artery when there is only mild stenosis (solid arrow) but shows spin dephasing in the region of the severe stenosis (arrowhead). Therefore, in mild stenosis, lesion severity is underestimated with 3D PC imaging and the artery appears normal. In severe stenosis, lesion severity is overestimated with 3D PC imaging, which shows focal occlusion. In moderate stenosis (open arrow), the 3D gadolinium-enhanced MR angiograms and 3D PC images have a similar appearance**)**

(Quoted from Dong et al., 1999)

Evaluation of the two techniques:

In patient with normal function, 3D PC imaging demonstrates intense cortical enhancement with cortico-medullary differentiation and bright arteries .With the combination of 3D PC imaging and 3D gadolinium-enhanced MR angiography, the entire renal artery up to the first level of branching in the renal hilum can be evaluated (fig 35 a) when 3D PC imaging or 3D gadolinium-enhanced MR angiography shows a normal renal artery, it s considered to be normal **(66).**

- **Pitfall in the technique:**

1. Poor quality images:

This is the most common pitfall that caused by:

a- Failure to suspend breathing

b- Poor timing of bolus injection

c- Inadequate dose of Gadolinium contrast material.(66).

2. Limitation of 3D PC imaging :

I - Patient with slow flow or renal failure

II- When the velocity encoding does not closely match the renal flow velocity

III - 3D PC imaging commonly demonstrates artificial spin dephasing at the renal artery .One should also watch out for surgical clip and stent artifacts, which may be identified on source images as an area of signal drop out adjacent to an extremely bright spot related mismapping of signal .**(66)**

3. Pitfalls associated with image reconstruction:

1-Eccentric disease may be identified on only one view; thus it is important to look at renal arteries on multiple views **(66).**

2- When the renal artery overlaps the enhancing cortex or renal vein on an MIP image, there may be an artifactual appearance of stenosis if the MIP is too thin, artifactual stenosis or occlusion may be caused by the artery being outside the MIP volume **(66).**

3- Ringing artifact from bolus timing errors, which can mimic dissection. **(66)**

Stenosis of transplanted renal artery:

Whenever the serum creatinine level rises in renal transplant recipient, the possibility of stenosis of transplanted renal artery must be considered typically stenosis occurs at the surgical anastomosis connecting the transplanted artery to the iliac artery. There may be atherosclerotic narrowing of the iliac artery proximal to the transplant arterial anastomosis (**Fig36**)**. (31)**

Sometimes narrowing occurs at the site where a surgical clamp was placed on the iliac artery at time of transplantation. If the transplanted renal artery is widely patent but there is minimal renal enhancement and no excretion of Gadolinium, then the kidney has probably been rejected. **(31)**

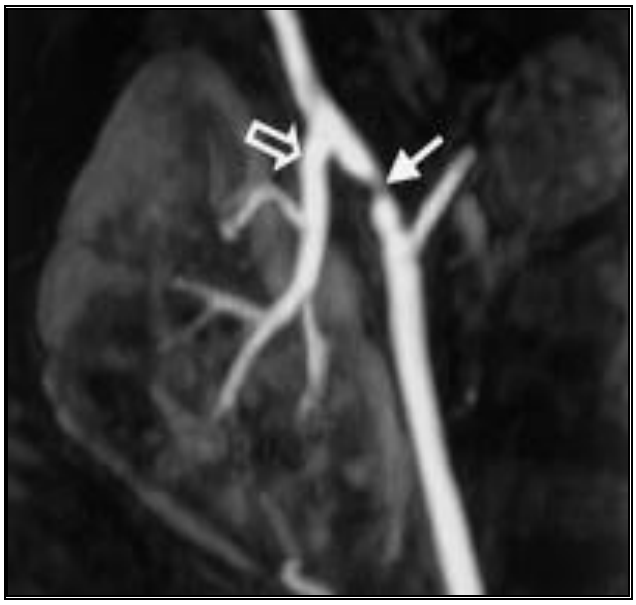

(Figure 36– Coronal subvolume MIP image from 3D gadolinium-enhanced MR angiography shows a stenosis of the left external iliac artery (solid arrow) and a normal transplanted renal artery (open arrow). The stenosis compromised flow to the transplanted kidney, resulting in hypertension and elevation of serum creatinine level, which improved after balloon angioplasty**)**.

New technical developments: high resolution renal MRA and extended anatomic coverage

Compared with digital subtraction angiography (DSA), the spatial resolution of 3D gadolinium MRA used to be substantially lower, by a factor of 3–5 therefore, 3D gadolinium MRA was notorious for over. Therefore, 3D gadolinium MRA was notorious for over- and underestimating the exact degree of stenosis when compared with DSA. The recent introduction of parallel acquisition techniques allows the spatial resolution to be doubled in the same scan time.**(67)**

Thus, at present, using multiplanar reformats, the exact morphology of the stenosis can be viewed in any plane, thereby substantially reducing misinterpretation of the degree of stenosis(**Figures 37- 38**).Preliminary results show improved

agreement with DSA. However, it must be pointed out that DSA by itself has limitations in cases of eccentric stenosis or tortuous vessels in which assessment of the exact morphology of the stenosis requires a high level of operator experience as well as multiple views at various angles to image the stenosis in-plane. This results in a high level of operator dependency. On the contrary, in 3D gadolinium MRA, the most diagnostic imaging plane can be reformatted after the study on a work station (**Figure 37).**For accessory renal arteries, good results have been reported for the evaluation of kidney donors prior to transplantation with regard to the correct identification of the absolute number and location of supernummery vessels.**(68)**

Regard to the correct identification of the absolute number and location of supernummery vessels. **(68)**

So far, however, no large study is available with respect to grading of accessory renal artery stenosis. While hypertension can result from the stenosis of an accessory renal artery, the therapeutic impact of the correct identification of such a lesion remains unclear, as this stenosis cannot be easily addressed by vascular interventions. The high-resolution MRA techniques can be combined with Automatic table movement in the MR scanner, thereby allowing assessment of not only the renal artery but also the peripheral arterial vascular tree in high resolution alters single Contrast media injection. **(69)**

It is well documented that patients with severe peripheral arterial disease reveal renal artery stenosis in a large percentage of cases. **(52)**

Thus, these patients can not be assessed effectively for both the peripheral arteries and the presence of a renal artery stenosis in a single non-invasive study without putting the patients at risk for nephrotoxic contrast agents. In additional this assessrnent of the major vascular territories can be easily combined with an evaluation of cardiac function and perfusion (**Fig 37**) several studies have shown that renal artery stenosis is an independent risk factor for death secondary to myocardial hypertrophy and coronary artery disease.**(70)**

Magnetic resonance imaging offers a unique possibility to add absolute measurements of cardiac functional parameters such as ejection fraction, end-diastolic and end-systolic volume , as well as measurements of regional cardiac tissue perfusion to angiographic studies of the renal arteries**(Fig 37**)while the coronary arteries themselves can still not be imaged reliably by 3d gadolinium MRA ,the assessment of cardiac perfusion under pharmacological stress provides valuable information for the detection of significant coronary artery disease.**(71)**

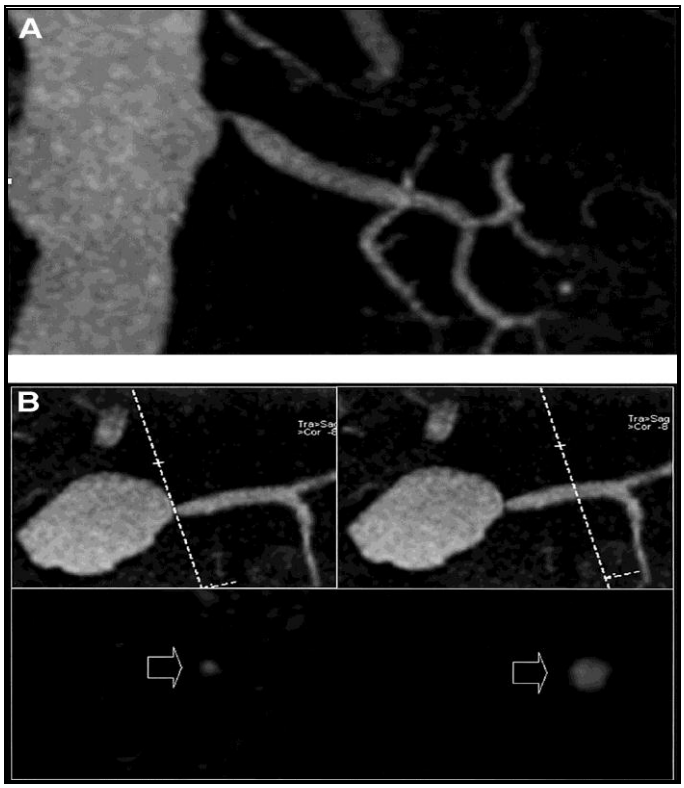

(Figure: 37 a - High-resolution 3D gadolinium MRA of the renal arteries using integrated parallel acquisition techniques (iPAT). Within 23 s, a data set with a voxel size of 0.8x0.8x0.9 mm spatial resolution was acquired on a high performance imaging system Plane view**(A)**as well as in orthogonal cuts of the vessel cross-section(**B**).This three-dimensional multiplanar assessment allows a reduction in the overall misinterpretation of the degree of stenosis) (**Quoted from Aumann et al., 2003).**

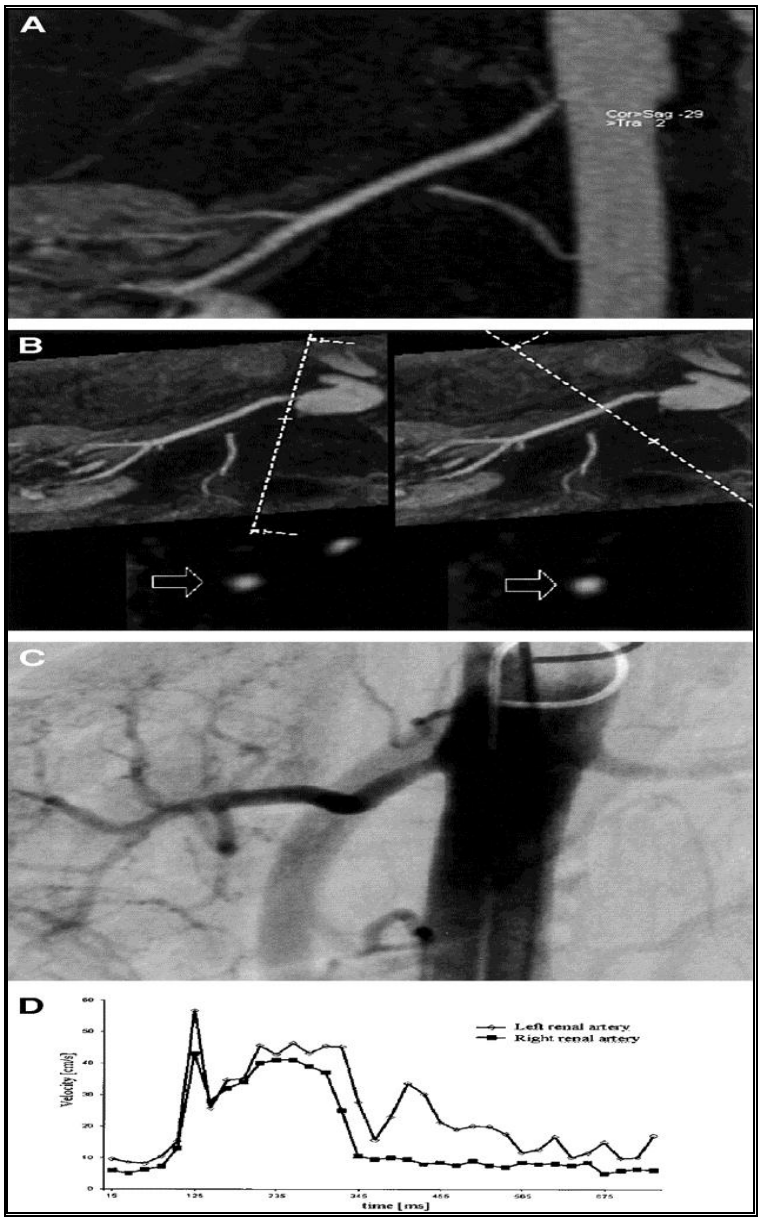

(**Figure: 37 b -** High-resolution 3D gadolinium and flow measurements of a 43-year-old female patient with suspected renal artery stenosis on the right. Standard maximum intensity projection reveals a moderate stenosis on the right **(A**). Multiplanar reformats of the renal artery in the cross-sectional view show that this finding in fact there is almost no stenosis present**(B)**. This is confirmed by which reveal only a partial loss of the early systolic peak(**D**). the renal artery was without the presence of a significant stenosis **(c)** a minor narrowing at the ostium of the renal artery(**Aumann et al., 2003**)

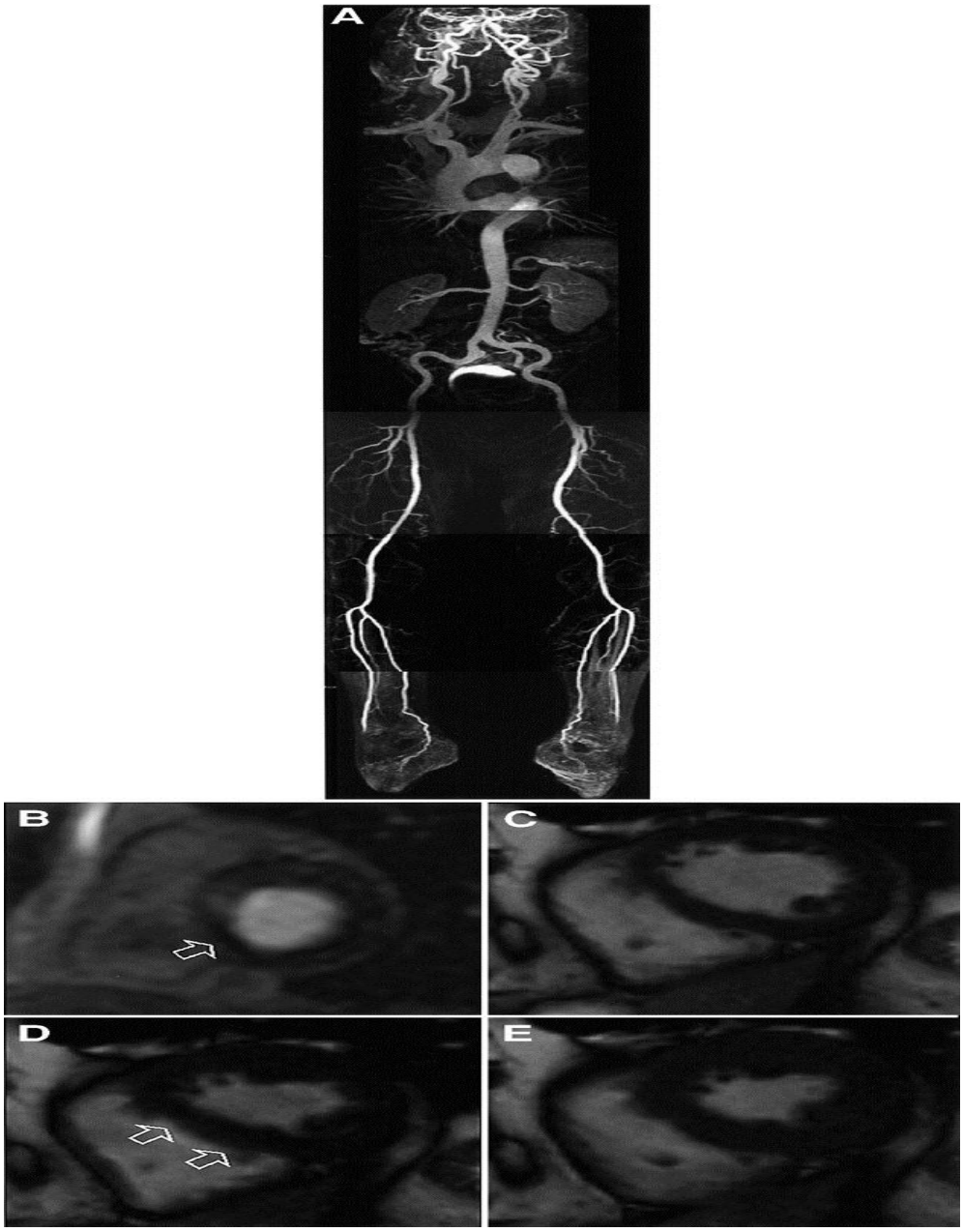

(Figure 37C –High-resolution 3D gadolinium MRA of the entire body with the moving table technique **(A)** reveals normal renal arteries with an accessory renal artery on the left as well as a complete normal assessment of the peripheral arterial vessels and carotid arteries.)

Feasibility of a comprehensive morphological and functional evaluation:Experience of 5 years :

More than 5 years ago, a comprehensive morphological and functional MR imaging protocol for detection and grading of renal artery stenosis was introduced using time-resolved 3D gadolinium MRA as well as cardiac-gated phase contrast flow measurements. **(72)**

This approach allows not only a grading of the morphological degree of stenosis but also an assessment of the haemodynamic significance of the stenosis by means of time-resolved velocity curves in the renal artery. Agreement between the morphological degree of stenosis and changes in the pattern of the flow profile has been well documented in both animal and human studies. **(72)**

In particular, the loss of the so called early systolic peak has been established as a sensitive indicator of the loss of the auto regulatory capacity and onset of significant mean flow reduction. In addition to the assessment of haemodynamic significance, the flow measurement technique provides a functional grading of the degree of stenosis independent of the accurate assessment of stenosis morphology **(Figure 38)**. Thus, the two techniques of flow and MRA can be used for a combined interpretation of renal artery stenosis. A multi center trial has shown that this combined approach allows a significant reduction in inter observer variability and an improvement of overall accuracy compared with DSA, with sensitivities and specificities exceeding 95%. The comprehensive protocol of MRA and flow was shown to reduce inter observer variability significantly. **(72)**

Another advantage of the MR flow measurement technique is the fact that it can still be applied after stent placement in the renal artery, while grading of the morphological degree of stenosis on the 3D gadolinium MRA images is not possible due to artifacts and signal void from the metal stent. A recent report in the New England Journal

of Medicine has again highlighted the fact that renal artery stenosis comprises only a small entity in a large complex of overlapping diseases ranging from essential hypertension to primary parenchymal disease of the kidney. **(73)**

There is increasing evidence that MR techniques based on the assessment of renal perfusion allow renal function to be assessed independent of the presence of renal artery stenosis. **(64)**

Changes of these quantitative parameters have been found in patients with primary parenchymal disease in whom no underlying renal artery stenosis was present. Thus, these techniques appear to be promising for the separation of renovascular disease from parenchymal causes. So far, absolute quantification of parenchymal blood flow has only been possible with the use of intravascular contrast agents. With the use of (both gadolinium chelate-based and iron oxide-based compounds) currently are being evaluated in phase 2 and phase 3 trials, none of them has as yet been approved for clinical use outside control trials. With the use of Faster MR techniques such as saturation recovery perfusion imaging semi-quantitative assessment of renal parenchymal perfusion has now become feasible **(Fig 38)(85)**

The role of the prediction of outcome after interventional or operative revascularization has not been fully established yet for MR imaging. The potential to differentiate patients with predominant renovascular or reno-parenchymal disease based on single comprehensive MR examination could lead to an important role for this technique in the near future (**75).**

Currently, comparative studies using both ultrasound and MR imaging prior to and after revascularization are ongoing. In summary, the high diagnostic accuracy of the technique, the assessment of both haemodynamic and functional changes and large anatomic coverage make MR imaging highly attractive method for the detection grading and differentiation of renovascular diseases. **(73)**

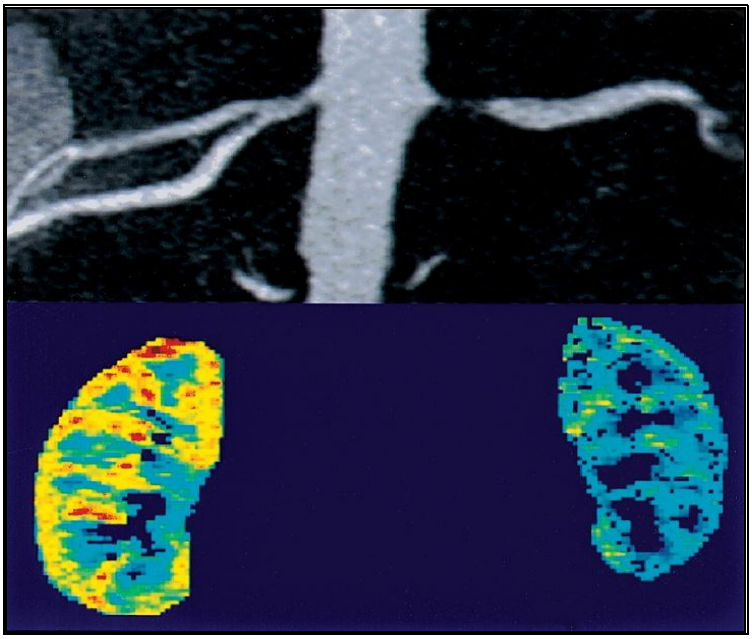

(FIGURE: 38 - High-resolution 3D gadolinium MRA (top) .shows bilateral high-grade stenosis exceeding 80% reduction of vessel diameter. Color-coded semi-quantitative maps (bottom) from dynamic gadolinium perfusion imaging show the right kidney still adequately perfused, while there is a substantial decrease of the perfusion on the left, confirming the presence of unilateral ischemic kidney disease).

III spiral CT angiography

Projection (**MIP**) and shaded surface display (**SSD**) reconstructed. The introduction of spiral or helical CT with its capability of imaging large columns of tissue very rapidly in a (20-30) breath-hold has led to the development of CT angiography. This produces higher quality axial images with better contrast enhancement than conventional CT and has added advantages of being able to produce 2D coronal, sagittal, oblique and curved planar reconstructed

images as well as the 3D maximum intensity images. **(15)**

Basic Physics:

There has been introduction of multislice CT (MSCT) scanners. Since the RSNA l998, as a new technology it was introduced by several manufacturers representing an obvious quantum leap in clinical performance. **(86)**

Currently capable of acquiring four channels of` helical data simultaneously. MSCT scanners have achieved the greatest incremental gain in scan speed since the development of` helical CT and have profound implications for clinical CT scanning, Fundamental advantages of MSCT include substantially shorter acquisition times, retrospective creation of thinner or thicker sections from the same raw data, and improved three dimensional rendering, with diminished helical artifacts.**(86)**

For example, the volume Zoom with a 500 ms rotation time and the simultaneous acquisition of` 4 slices offers an 8-fold increase of` performance compared to previous 1s, single-slice scanning. Obviously, such a quantum leap opens up a new area in spiral CT-affecting all existing applications- and allowing the realization of new clinical applications;. The key issue is correspondingly increased volume coverage per unit time at high axial resolution and a correspondingly improved temporal resolution. **(86)**

In general terms, the capabilities of spiral CT can be expanded in various ways: to scan anatomical volumes with standard techniques at significantly reduced scan times; or to scan larger volumes previously not accessible in practical scan times or to scan anatomical volumes with high axial resolution (narrow collimation) to closely approach the isotropic voxel of` high- quality data sets for excellent 3-dimensional post processing and diagnosis. **(86)**

With spiral CT, multiple overlapping images can be generated

from seen data acquired in a single breath hold. High quality two or three-dimensional reformations can be generated from these images. CT angiography is one of` the new applications involving Multi-dimensional imaging has been made possible by spiral CT **(87)**.

The X ray moves as a helix around the patient surface resulting in a helix of raw projection data from which planar images are generated. Each rotating generates data that is specific to an angled plane of section. For a true trans axial image, points above and below the desired plane of section must be interpolated to estimate the data value in the trans axial plane **(86).**

Design Considerations for MSCT:

It is easy to design a multi-slice scanner for a fixed slice collimation the challenge is to design the detector in such a way as to meet the clinical requirement of different slice collimations adjustable to the diagnostic needs. There are basically two Different approaches, the matrix detector with elements of a fixed size or the adaptive array principle, both principles will be briefly described and compared. An example of a matrix detector is sketched **(Fig 39)** in axial direction the detector is divided into l6 small elements each providing a l mm thick slice at the center of rotation **(88).**

The outer detector rows cannot be used individually. In the example of (**Fig 39)**. The l mm slice is smeared over about 6 mm. The only way out is to sum the signals of the outer rows to generate thick slices. However, the unnecessary mechanical cuts and optical separations between the small elements correspondingly reduce the geometrical efficiency and therefore the dose efficiency of the system. in summary, the matrix detector is well suited to scan at 4 x 1 mm collimations but not more than Wider collimations 4 x 2 mm, etc. can be realized by signal combination during read out but at the expense of dead zones and a corresponding, waste of dose. These arguments lead to the development of the Adaptive Array Detector **(86).**

Narrow detector elements are close to the center; the width of the detector rows increases with distance from the center. Unnecessary dead spaces are avoided and with the corresponding pre patient collimator and the proper read-out schemes the following combinations of collimation can be achieved: 2 x 0.5 mm, 4x1 mm, 4 x 2.5 mm, 4x 5 mm, 2 x 8 mm and 2 x I0 mm.

These combinations represent the collimation of the x-ray beam at center: e. g. a 4 x 5 mm collimation means an X-ray beam width at center of`20 mm. Consequently with sequential imaging four 5 mm slices would be generated during one rotation.

In spiral Imaging, the variety of axial sampling patterns as a function of pitch allows both; obtaining slice widths independent of pitch and reconstructing multiplicity of slice widths from a scan with collimation narrower. Another design criterion should he emphasized: spiral scanning at large pitch, e. g. large table velocity, implies a more severe inconsistency between direct projection and the complementary projections, taken half-a rotation later with a quarter detector offset. The reason is changing anatomy in axial direction, which is particularly pronounced for large pitch applications, i.e. rapid table movement. Consequently, image quality at high spatial resolution· and large pitch is becoming more dependent on the flying spot technology which provides a quasi-instant doubling of the in plane sampling rate **(88).**

In conclusion

Image quality in multi-slice spiral scanning must be optimized with respect to several factors:

1. The narrowest collimation, consistent with the coverage of a certain volume and with a certain scan time, to minimize partial volume effects and to optimize image quality.

2- Fastest rotation time to maximize z-coverage and to minimize motion blurring.

3- Pitch greater than 4 to preserve temporal resolution and to minimize motion blurring.

4-The exploitation of flying focal spot technology to avoid artifacts at high spatial resolution. To measure section profiles of multi- spiral scanning a thin gold plate (thickness 50 um) in air has been aligned orthogonal to the scanner axis and has been scanned in spiral mode **(88).**

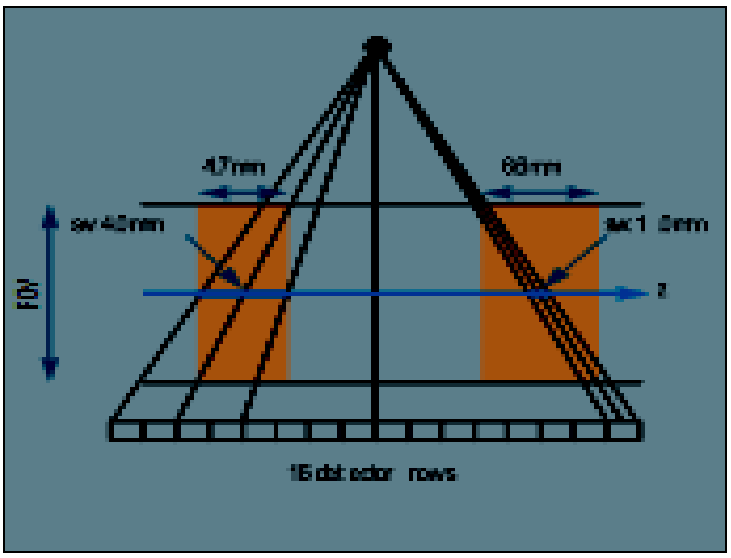

(Figure: 39 -Fixed Array Detector. The slice width is compared to the smearing of the slice caused by the cone-angle; it is shown that for the example of a l6-row detector, the outermost slice of` nominal thickness 1.0 mm is broadened to 6.6 nun by smearing (right half of figure). The problem can he overcomes by combining several slices to a wider slice (left half of figure). Then, however,

separators between the slices are not needed for the outer slices) **(Quoted from Foley et al, 2000)**

CT Protocol;

CT angiography is performed using spiral CT scanning at1 to 2mm images intervals after the administration of a bolus of intravenous contrast. The acquired images can he reformatted using several techniques to produce two or three dimensional reconstructions that allow accurate evaluation of the renal arteries. Depending on the technique used, the sensitivity for diagnosing RAS angiography is 59% to 92% and the specificity is82% to 98% **(89).**

Thin section multislice CT required using 140 kV, 200 mas/slice, a collimation of 4x1.0 mm, increment 0.6, and a pitch of 1.25 with appropriate z axis coverage. Contrast enhancement may require 100 ml of iodinated contrast like (**iopromide**) via an18 gauge antecubital vein catheter at 3 ml/sec- triggered using bolus tracking. Images are then transferred to a workstation For evaluation, using axial data, maximum intensity projections,(MIP) and three dimensional reconstruction manipulated with volume rendering (VR) techniques**.(90)**

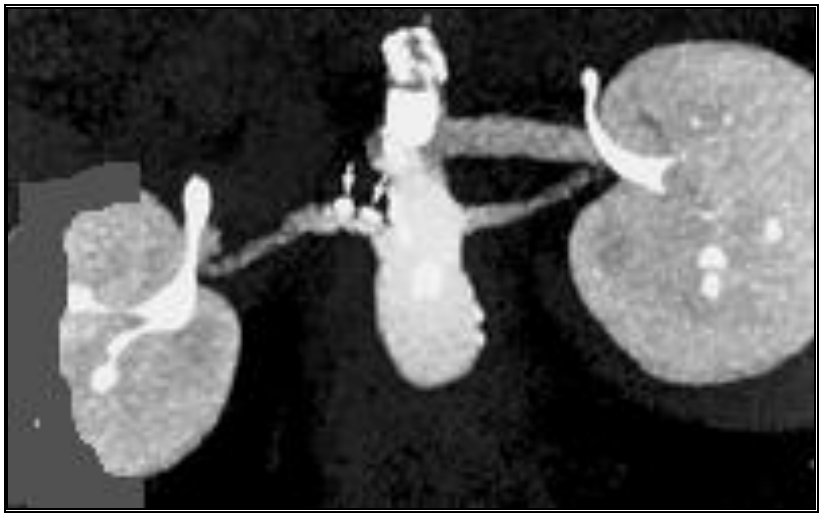

(Figure: 40 - Three dimensional reconstructions of a thin section, multislice CT renal angiography, and the right kidney is reduced in size**)** (**Quoted from Morgan,et al:2003)**

CT Technique:

4 hours fasting is required and a venous access should be obtained using an l8-20 G lntra-cather in the antecubital vein or a large vein in the forearm. Patients should be trained to hold their breath with special attention to avoid diaphragmatic motion .On a frontal scout view, unenhanced helical CT scan is performed using; 10 mm section thickness, pitch of 2, 120 kV, 100 to 130 mA, 0.8 s scan time, and image reconstruction at 5-mm intervals from diaphragm to mid pelvis during a single breath-hold. Using These images, the scanning range has to be determined from the celiac axis to aortic bifurcation, including the entire' kidneys bilaterally; The delay between the initiation of the injection and the scan must be calculated using the (Smart Prep) option, with a test injection of 10 ml of contrast. It may range between 10 and 28sec **(91).**

According to Chapman and Nakielny, 1997:

Non-ionic contrast **(**Iohexol or Iversol, 130-150 ml, 300 mg iodine/ml**)** has to be injected at a rate of 4 ml/s with a power injector. Helical CT scans performed at 2-mm slices; pitch 1.5- 2.0, scans time 0.8 s, 120 kVl50-180 mA, during suspended inspiration. The scan time ranged from 26 to 35 s. The contrast volume reduced to 80-100 ml, and the injection rate to 3 ml/s in the subjects who weighed less than 50 kg. The images could be reconstructed at 1-mm intervals with segmented interpolation and a small field of view of l8 -22 mm yielding 180--270 images, which were sent to the workstation on the network. After 5-7 min. a frontal scoot view can be taken to excess the collecting system and the ureters, to be repeated after 5 min delay if the opacification was incomplete. **(92)**

CT interpretation and 3D processing

Interpretation must be performed on a workstation the unenhanced as well as the contrast-enhanced axial images should be first viewed using cine paging to identity the arterial and venous anatomical variants, the parenchymal abnormalities calcifications. The data have to be then loaded for 3-D processing surface shaded Display and Maximum Intensity projection images are then generated. The vascular anatomy can further be displayed using Curved Multiplanar reconstruction (**MPR**) (**Fig**. **24**). **(93)**

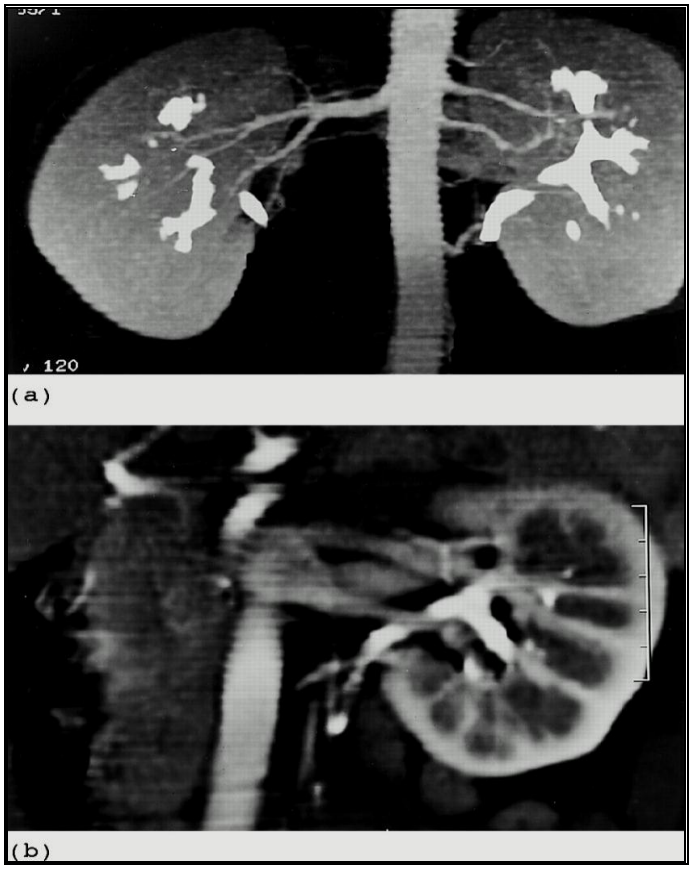

(Figure 41- (a) CT angiogram; frontal maximum intensity projection (MP) image showing five renal arteries on the left side and three on the right **(b)** Same Patient curved Multiplanar reformatting (MPR) image showing three veins forming a distal confluence).(**Quoted from Uday et al., 2001)**

IV- DIGITAI SUBT`RACTION ANGIOGRAPHY (DSA)

Over the past decades, DSA has become a well-established modality for the visualization of blood vessels in the human body. With this technique, a sequence of 2D digital X-ray projection images is acquired to show the passage of a bolus of injected contrast material through the vessels of interest. In the images that show pacified vessels (often referred to as contrast images or live images), background structures are largely removed by subtracting an image acquired prior to injection (usually called the mask image). **(16)**

According to Chapman and Nakielny, 1997:

- There is;

➢ **Intravenous DSA:**

Veins are used as the site of catheter introduction. Dye is injected when the catheter is within the right atrium, Superior vena cava or inferior vena cava.

➢ **Intra-arterial DSA:**

The site of entry of the catheter is via the arterial system. It can be subdivided as follows:

1- Non-selective

This is when-the catheter inside the aorta to produce a mid-stream or flush aortogram. This is of special value when the kidney is supplied by more than one renal artery or when the stenosis is at the origin of the artery. This then may be followed by selective Opacification of the renal vasculature.

2- Selective:

This involves placing the tip of the catheter within the lumen of the main renal artery. As the contrast medium passes through the renovascular system.

Three phases can be identified:

l- Arteriogram where the abdominal aorta (Non selective only), the renal artery with extra renal branches, segmental branches and interlobar arteries are visualized.

2- Nephrogram in which the arcuate arteries, interlobular arteries, afferent arterioles, afferent arterioles, efferent venules, interlobular and medullary veins, arcuate veins interlobular veins are seen.

3- Venous phase where the main renal veins are visualized. All the phases should be included in-order to yield a diagnostic an angiograrn.

Technique:

According to (Chapman & Nakielny, 1997): _

- **Patient Preparation**

The patient is admitted to the hospital, Blood pressure and peripheral pulses have to be measured. There are slight differences in technique depending on which procedure is performed.

- **Intra-venous DSA:**

The basilic vein is most common site of introduction but the femoral vein can also be used. A pigtail catheter is used and

placed within the right atrium, superior vena cava or inferior vena cava **(92).**

- **Intra -arterial DSA:**

- Non selective procedure:

The site of introduction of the catheter may be;

- **A. Percutaneous nonselective catheterization.**

The catheter is within the aorta, at the level above the orifice of the renal artery. The site of entry is most commonly the femoral artery but the brachial artery may also be used. A pig tail catheter is the catheter of choice.

- **B. Translumbar approach.**

In this approach the puncture is at Tl2-Ll level using a catheter. The Tran lumbar approach is not commonly used for several reasons, including the patient must be prone Procedure and surrounding structures such as spinal cord, thoracic duct or cysterna chyli may be damaged. **(92)**

2. Selective procedure:

The site of introduction is via percutaneous catheterization using most commonly the femoral artery but other sites may be used. The preferred catheter is the cobra head. **(92)**

Catheter insertion or Seldenger technique;

The technique is basically the same for intra-arterial or intravenous DSA differing only in the site of` introduction and placement of the catheter. The patient is placed supine on the X

ray table .The femoral arteries are palpated and the one with the stronger pulse is used or the right artery if they are equal for intra-arterial imaging**. (92)**

For intra-venous imaging the patient is placed supine on the table and his antecubital fossa is inspected for a suitable basilic vein. Using aseptic technique, the site of insertion is infiltrated with local anesthetic. A transverse incision is made over the artery and the puncture is made at the apex of the arch with the needle directed 45 degree to the skin surface and slightly medially after immobilization of the vessel. Both walls are punctured with a stab. The stilett is removed and the needle hub is depressed so that is runs parallel to the skin. It is then withdrawn until pulsatile blood flow indicates is a satisfactory puncture. The guide wire. (Usually hydrophilic) is inserted through the needle and is advanced under screen. In the descending aorta the needle is withdrawn while firm pressure is kept on the puncture site. The guide-wire is clean and then the catheter is threaded over it and advanced up in the descending aorta under fluoroscopy control. When it is in a proper position the guide-wire is withdrawn. The catheter is connected via a 2 way tap to a syringe containing heparin zed saline (2500 unite / 500 ml of 0.9 %saline) and trashed. Flushing is done regularly throughout the procedure**. (92)**

A water soluble contrast agent is used either ionic or nonionic, ionic agents are of lower cost hut they are more toxic to the kidney and are more likely to produce allergic reaction. In high risk individuals (those with renal impairment or in patients with previous allergic reaction to the contrast agent), non-ionic agents are used. The amount ranges from 6- to 8 ml in selective techniques to 25 - 30 ml in non selective technique**.(92)**

The contrast agent may be hand injected or by an automatic injector in trans lumbar approach. With catheter techniques injection is done automatically with an electrocardiograph triggering device permits injection to be made immediately

Before the diastole. This permits the contrast agent to maintain a satisfactory level of concentration, requiring less time to be used. **(92)**

With Intravenous technique contrast is injected with each separate projection at a rate of 35 ml at 20 ml\sec. Filming sequence is 2 /second for 3 seconds and then 1\second for 4 seconds. AP and oblique (for origin of artery) views are taken**.(92)**

Renal Scintigraphy:

During the last decades, several noninvasive imaging modalities have been evaluated for their ability to detect renal artery stenosis like renal Scintigraphy**. (18)**

Baseline and Captopril-enhanced 99 mTc- mercaptoacetyltriglycine (99mTc-MAG3) Scintigraphy using a 1- day, 25-mg Captopril protocol, was recommended by the Working Party Group on Determining the Radionuclide of choice. **(18)**

99mTc-MAG3 is a protein-bound radiopharmaceutical tracer, and its clearance is almost exclusively through tubular secretion. 99rnTc-MAG3 is preferred to other tracers because of the high extraction efficiencies, its image quality, and its

favorable dosimetry. Patients must be well hydrated before the examination. Because chronic administration of angiotensin-converting enzyme inhibitors may reduce the sensitivity of Scintigraphy, this medication has to be withheld from all patients for 2-5 days before the examination and replaced by other drugs when indicated.(18)

A large-field-of-view gamma camera interfaced with a computer is positioned beneath the patient to obtain standard posterior views of the kidneys. Images stored in a 64 x 64 word mode pixel matrix.

l-Time- activity curves are generated from data obtained for a minimum of 30 min.

2-After the baseline study, an oral dose of 25 mg of captopril is administered, and the patient instructed to drink 300-500 ml of water.

3-The patient is then placed in the supine position and blood pressure has to be monitored at frequent intervals.

4-The (captopril-enhanced study is then initiated 60 min after captopril administration. Results are then interpreted according to the guidelines of the Society of Nuclear Medicine. **(18)**

The most important criterion for detecting renal artery stenosis in the study performed by was unilateral parenchymal retention of the radiopharmaceutical after captopril administration **(94).(**Fig 42)

Patients with abnormal baseline findings indicative of reduced renal function that. Were not modified alter captopril administration were considered to have an intermediate probability of renal artery stenosis. (**94)**

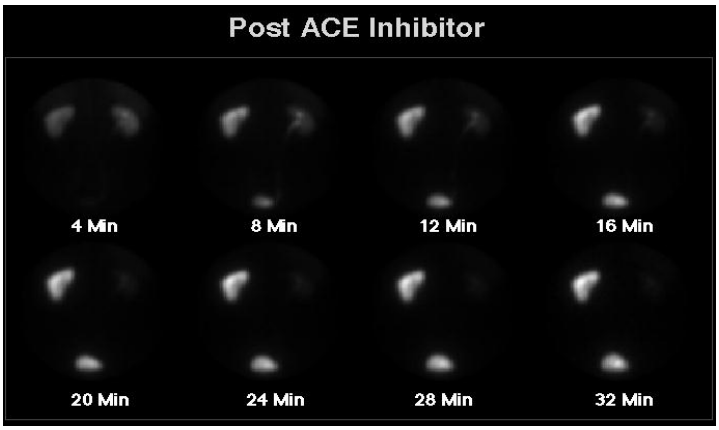

Figure: 42 A

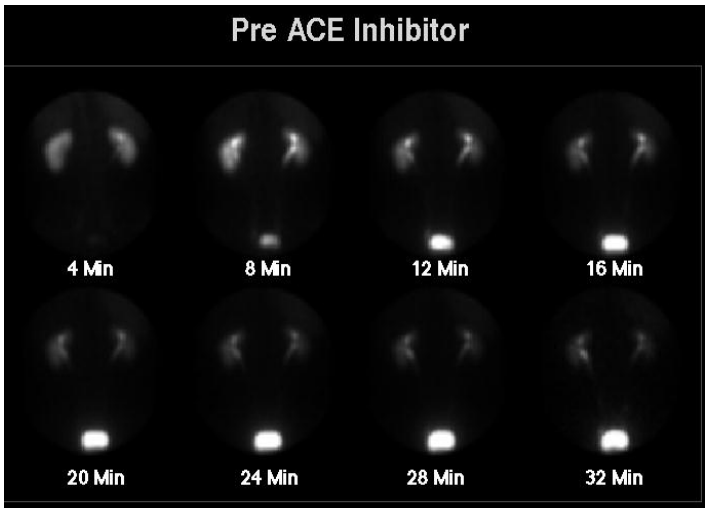

Figure: 42 B

(Figure: 42 A, B -For the first study the patient was given 2.5 mg enalapril intravenously over a five minute period followed by administration of Tc-99m MAG3. There is marked asymmetry in function, with normal uptake and excretion by the right kidney (on the viewer's right), but significant retention of radiopharmaceutical by the left kidney with little or no excretion. Based on initial uptake of tracer, relative split function was equal, with 49% on the right and 51% on the left. The second study, performed without administration of enalapril, shows dramatically improved left renal function. Uptake and excretion are only minimally delayed on the left.)

Discussion:

Renal scintigraphy with angiotensin converting enzyme inhibitors is a sensitive and specific way to screen patients with suspected renovascular hypertension. Either the rapid-onset intravenous ACE inhibitor enalapril or the slower-acting oral captopril agent may be used. Enalapril is probably preferable because of its faster and more reproducible effect. If the initial study performed with the ACE inhibitor is normal, some practitioners will not do the baseline study. If the initial study is abnormal, as in the present case, it is essential that the baseline examination be performed to evaluate the possibility of unilateral, non-renovascular renal disease.

Diagnostic Value of Different Technique

Doppler US

Doppler US has the advantages of being noninvasive and inexpensive However, considerable controversy exists with regard to the role of Doppler US in screening for RAS. Two approaches are used to detect RAS with Doppler US: direct visualization of the renal arteries and analysis of intrarenal Doppler waveforms.

Many studies have been published about the use of intrarenal Doppler US to detect renal artery stenosis. Results have been variable with a sensitivity of up to 92% and speechify of up A to 95% for detection of severe renal artery stenosis, (greater than 70%). Generally, it was found that moderate renal artery narrowing (50-70 %) did not produce convincing Doppler waveform changes in the intra-renal vessels. It was also found that complete occlusion could not always be reliably distinguished from severe stenosis. (**95)**

The technique is time consuming and operator dependent. Inability to fully demonstrate the vessel has been reported in up to 40% of studies. **(96)**

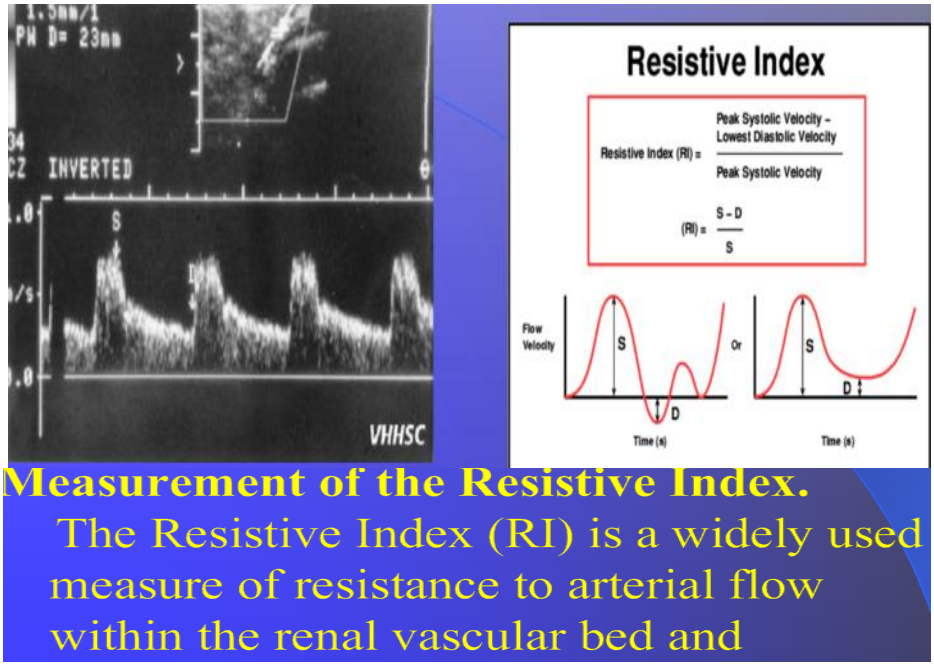

(**Figure 43** – Normal Resistive index of renal artery blood flow)

(Figure: 44–Normal duplex US imaging. A normal resistive index (**0.6**) in this case is associated with a normal systolic arterial waveform (white right arrow) and a normal diastolic flow pattern (yellow left arrow).

Other factors that interfere with quality of images are patient obesity, respiratory motion, transmitted cardiac or aortic pulsation or to overlying bowel gas. If the vessel follows tortuous course there may be difficulty in demonstrating its entire length .There is further doubt in the ability of Doppler US to demonstrate accessory renal arteries. Accessory renal arteries present by angiography in 14-24 % of kidneys and only 0-4% of these were shown with Doppler Us. (**Fig 45**). **(96)**

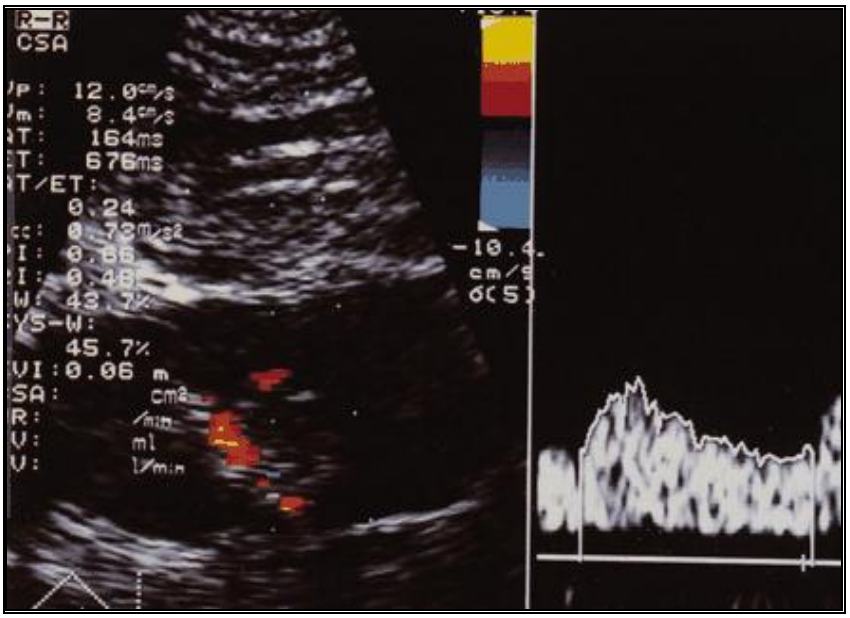

(**Figure 45** - Transverse intrarenal duplex us image shows an acceleration time (AT) of 164 m/sec with atypical tardus-parvus waveform)
(Quoted from Aitchinson et al., 1999)

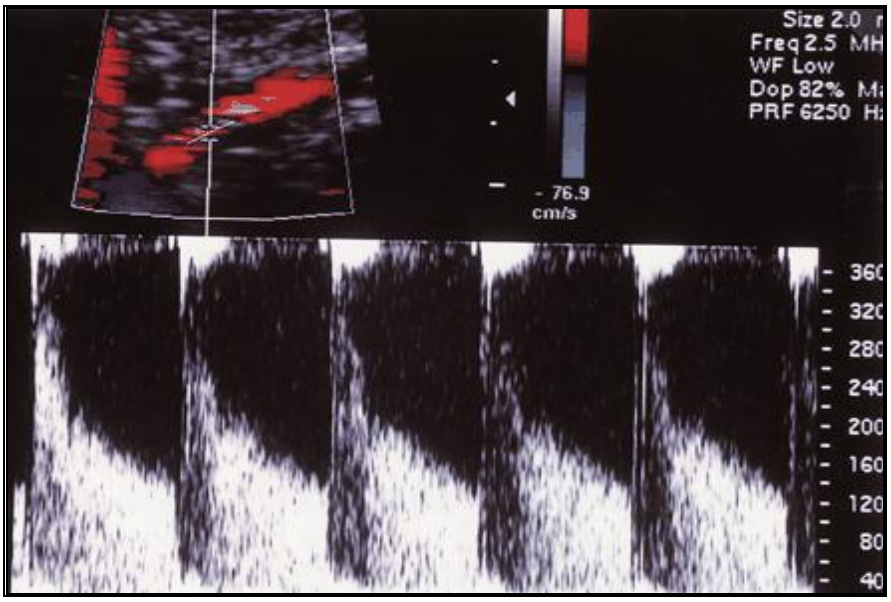

(Figure 46 - Transverse color duplex US image depicts the significant stenosis. The peak systolic velocity in the region of turbulent flow is greater than 200 cm/sec, so the stenosis is considered to be severe).

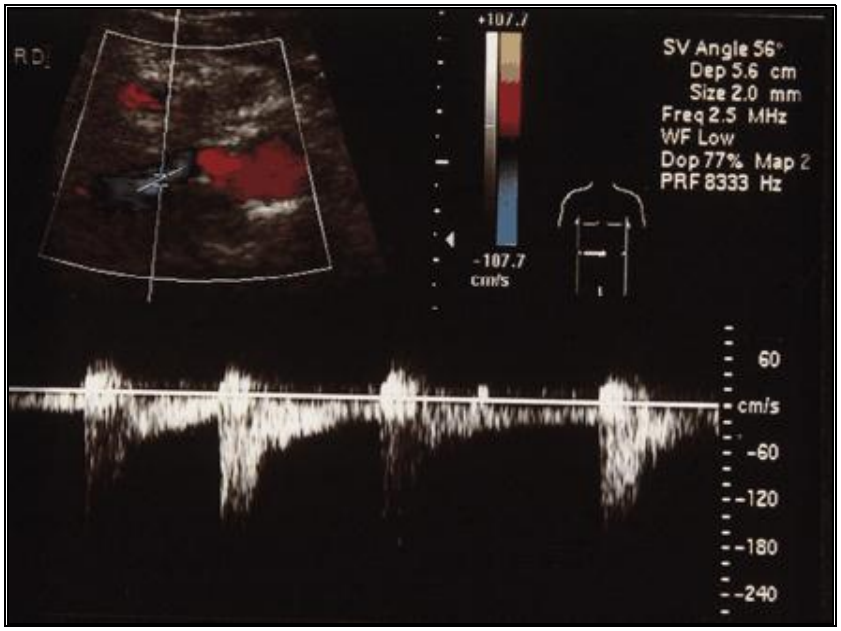

(**Figure 47** - Transverse color duplex US image. The peak systolic velocity immediately distal to the stenosis is 100-200 cm/sec; the stenosis is correctly classified as mild) **(Quoted from Aitchinson et al., 1999)**

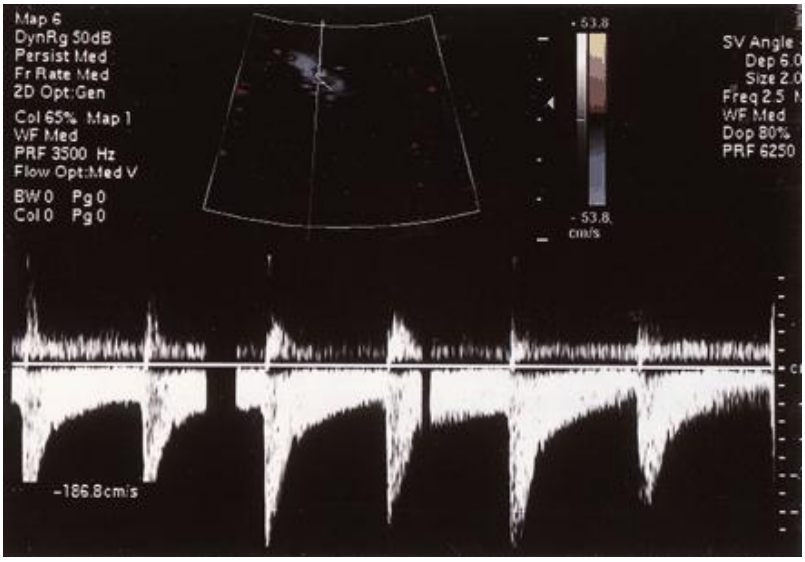

(**Figure 48** - Transverse color duplex US image indicates the peak systolic velocity at the same location as the stenosis was 186 cm/sec. The stenosis was incorrectly classified as mild; this was considered a false-negative color duplex US finding). (**Quoted from Aitchison et al., 1999**)

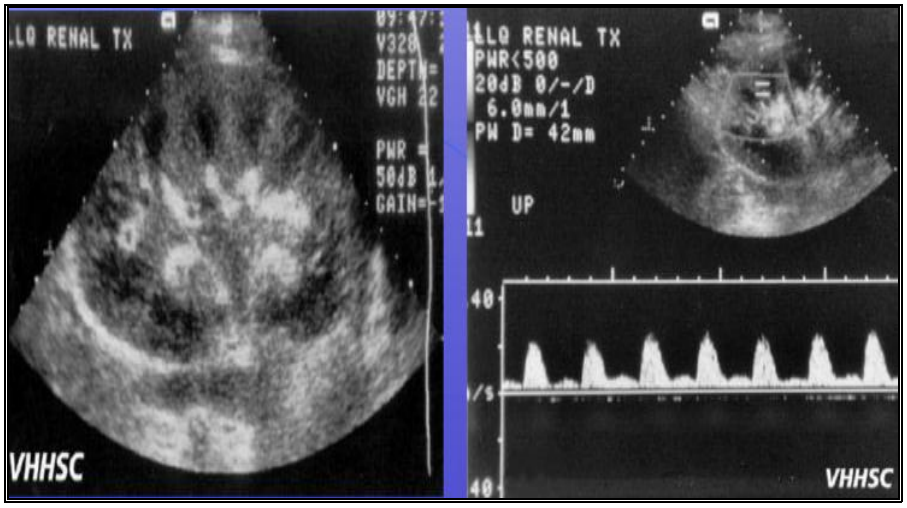

A **B**

(Figure 49 A, B- Acute tubular necrosis .Renal pyramids are clearly visualized and cortico-medullary differentiation is preserved. Debris is present in the collecting system. The Resistive index was moderately elevated, measuring 0.88) **(Quoted from Aitchison et al., 1999)**

In an effort to improve detection of renal artery stenosis by Doppler US. Angiotensin converting enzyme (ACE) inhibiting drug like Captopril was added to the examination as with renal Scintigraphy .In tow studies, the use of oral ACE inhibitors improved results of intra-renal Doppler examination in moderate renal artery stenosis (50-70 %). **(97)**

At present, the use of Doppler Us for the diagnosis of renal artery stenosis is still perceived to be dependent on operator skills and experiences (**fig 50**) the technique has not gained widespread acceptance as a robust screening test in general hypertensive population .it may have a role in more selected patient groups or to monitor treatment results in individuals (**fig. 51, 52, 53, 54)**

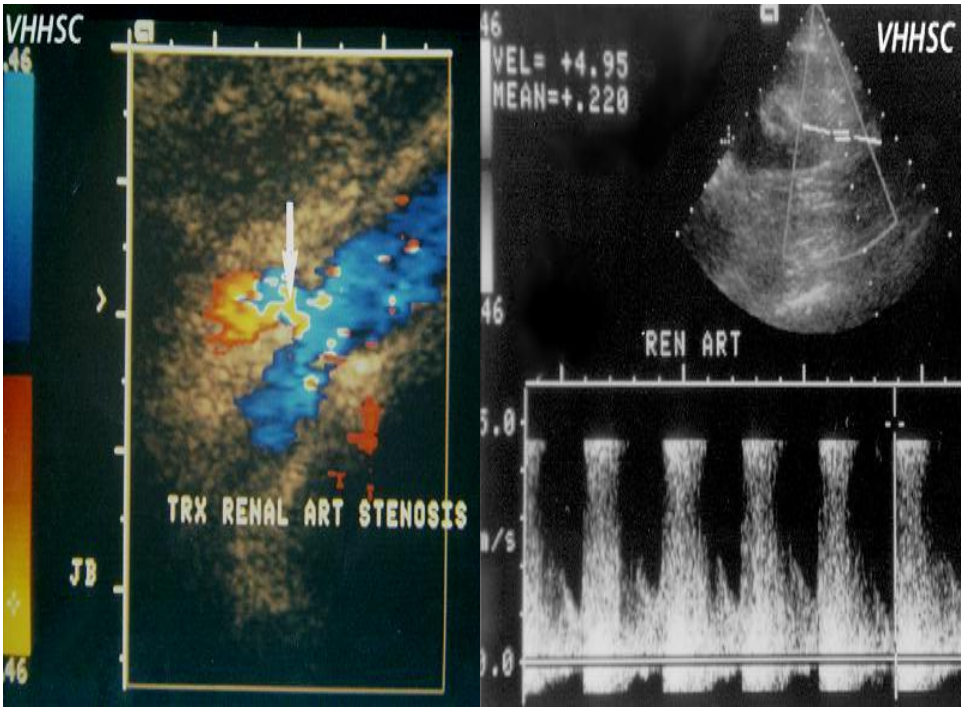

A *B*

*(***Figure 50** - high velocity jet (4.95 m/s) is present proximally in the vessel (**50 A**). Aliasing and turbulent flow are present. CD image of the same stenosis (**50 B**) shows color aliasing (arrows) at the site of the jet. Angiography (**50 c**) reversed diastolic flow in sever acute rejection)

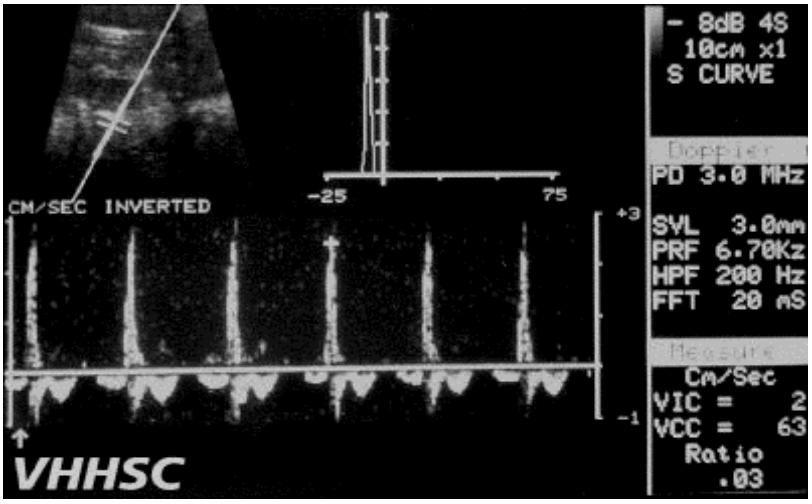

C

(**Figure**: **50 c** reversed diastolic flow in sever acute rejection)

Direct Visualization of the Renal Arteries

The first approach involves direct scanning of the main renal arteries with color or power Doppler US followed by analysis of renal artery velocity with spectral Doppler US (**Fig 51**). An anterior or anterolateral approach usually allows exploration of both renal arteries with an adequate angle of insonation. A coronal approach can be used when bowel gas is present. Owing to various factors such as gas interposition or the anatomy of the left renal artery, a complete examination of both renal arteries can be achieved in only 50%–90% of cases**.(9)**

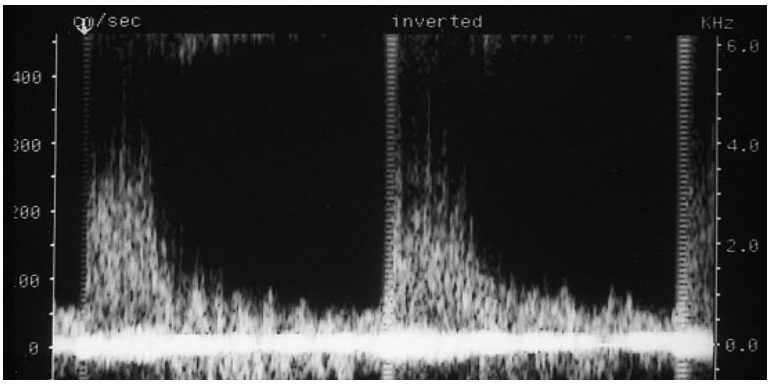

(A)

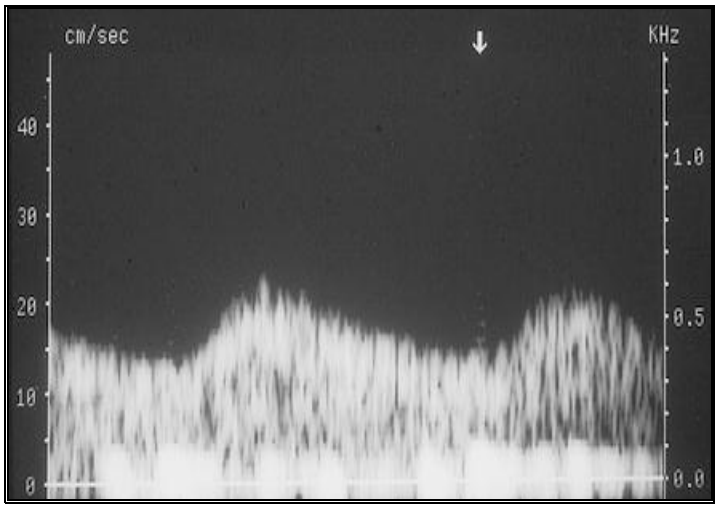

(B)

(Figure 51 – Severe stenosis in a patient with a solitary left kidney who experienced recurring hypertension and renal failure 3 months after stent placement in the left renal artery. (a) Doppler spectrum from the proximal left renal artery shows flow acceleration of close to 300 cm/sec inside the inside the stent. (b) Intrarenal Doppler spectrum shows a waveform with a puls tardus configuration, which indirect severe homodynamic repercussions). **(Quoted from Aitchison et al: 1999)**

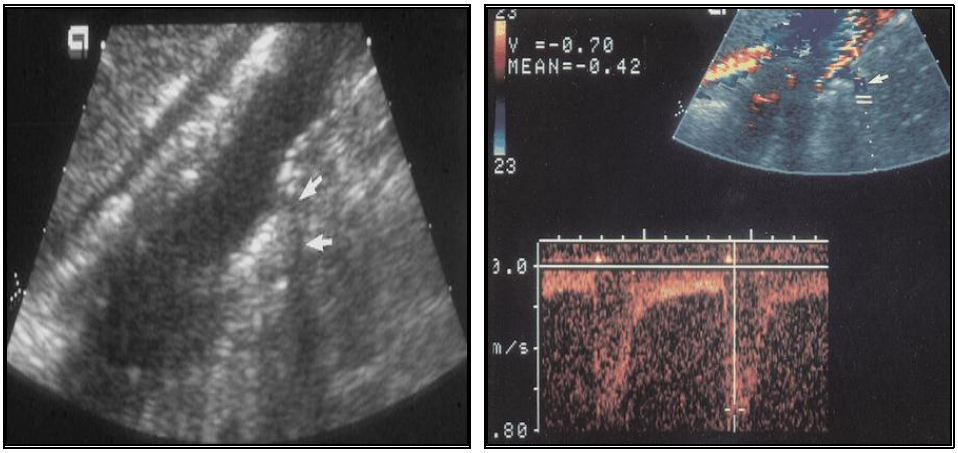

(A) **(B)**

(Figure 52 – Signal enhancement with a contrast agent. (a) Gray-scale US scan of the abdominal aorta obtained with a right coronal approach shows

he left renal artery (arrows). However, results of duplex US were non diagnostic. (b) Color Doppler US scan obtained after injection of a contrast agent shows strong signal inside the aorta and left renal artery **(arrow). The enhanced signal allowed evaluation of the left renal artery** with pulsed Doppler US).

Criteria used to diagnose significant proximal stenosis of a renal artery:

Four criteria are used to diagnose significant proximal stenosis or occlusion of a renal artery: **(a)** An increase in peak systolic velocity in the renal artery (in the literature, the threshold for significant RAS is 100–200 cm/sec); (**b)** a renal-to-aortic ratio of peak systolic velocity greater than 3.5; **(c)** turbulent flow in the post stenotic area; and **(d)** visualization of the renal artery without detectable Doppler signal, a finding that indicates occlusion.

Accessory renal arteries and bowel gas interposition are the main limiting factors in direct scanning of the renal arteries. Therefore, recent studies have demonstrated mixed results, with sensitivities of 0%–93% for detection of RAS. **(98)**

Analysis of Intra-renal Doppler Waveforms

The segmental renal arteries are evaluated by means of a trans lumbar approach. Therefore, technical failure occurs in only 0%–2% of kidneys studied. The different segments of the kidneys must be scanned systematically to detect a stenosis of a segmental or accessory renal artery (**Fig 53**). A dampened appearance (pulsus tardus) of an intrarenal Doppler waveform indicates stenosis. (**Fig 51**) **(99)**

The presence of an early systolic peak can be interpreted as a sign of normality; however, the absence of an early systolic peak does not necessarily indicate stenosis. **(100)**

Detection of significant RAS can be based on a pattern recognition approach (**Fig 54**).

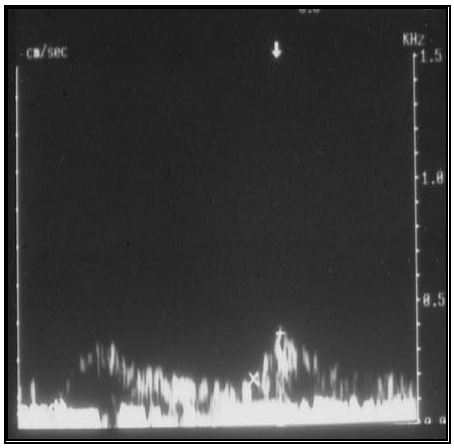

A

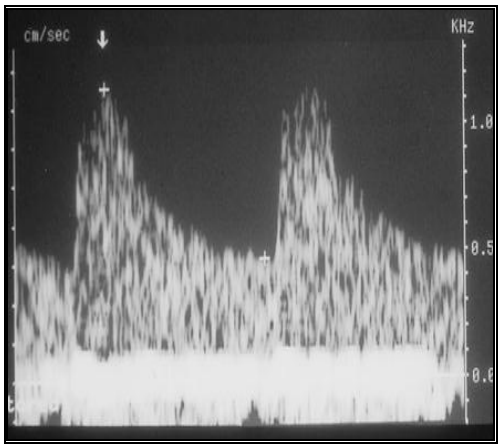

B

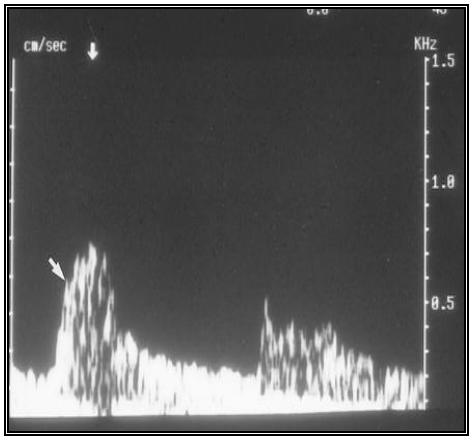

C

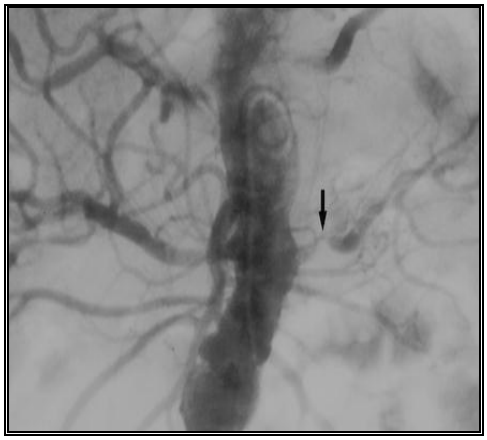

D

E

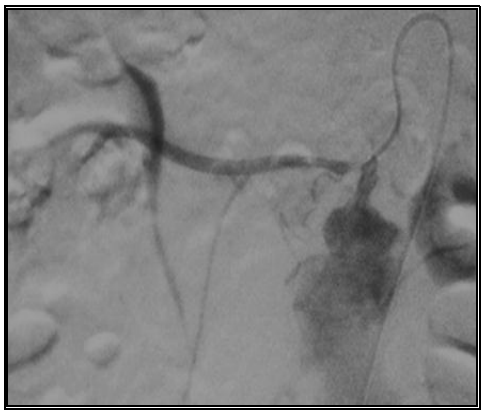

F

(Figure 53 - Stenosis of an accessory renal artery in a patient with recent acceleration of hypertension. **(a)** Doppler spectrum from the left kidney shows a waveform with a pulsus tardus configuration, which is consistent with severe RAS. **(b)** Doppler spectrum from the upper right kidney shows a normal waveform. **(c)** Doppler spectrum from the lower pole of the right kidney shows a waveform with a delayed systolic upstroke (arrow), which suggests stenosis of an accessory or branch renal artery. **(d)** Abdominal aortogram shows severe stenosis of the left renal artery (arrow). The origins of the right main and accessory renal arteries are not adequately visualized. **(e)** Selective arteriogram of the main right renal artery shows no stenosis. **(f)** Arteriogram of an accessory artery to the right lower pole shows ostial stenosis)

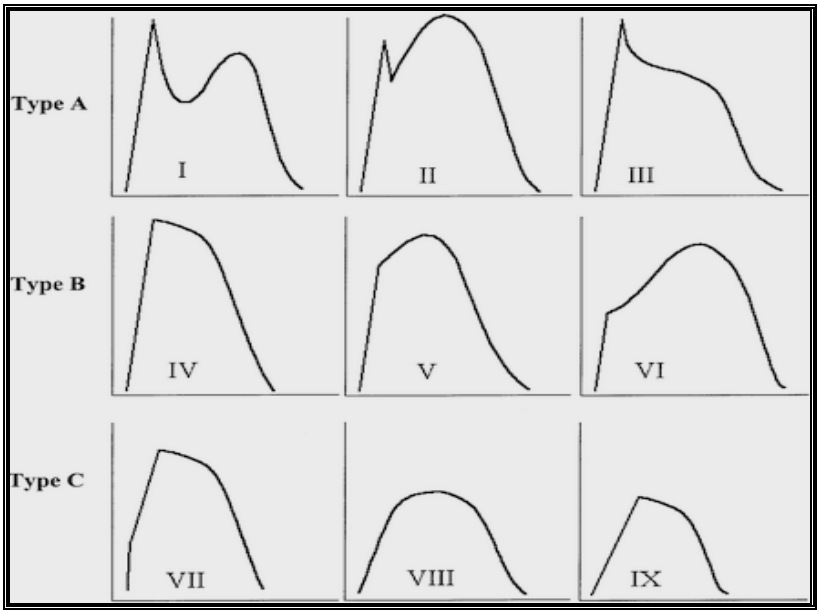

(Figure 54 – Doppler waveform patterns. Types **A** and **B** represent normal Doppler spectra. In type A, a peak is present at the end of the early rise. In type B, no peak is present but the rise remains straight. Note that waveform VI is considered normal despite the high compliance peak; this particular type is most commonly seen in young patients. Type C represents abnormal spectra with varying degrees of a slowed early rise).

In an effort to improve detection of renal artery stenosis by Doppler US, angiotensin converting enzyme (ACE) inhibiting drug like Captopril was added to the examination as with renal scintigraphy. In two studies, the use of oral ACE inhibitor improved results of intra-renal Doppler examination in moderate renal artery stenosis (50-70 %). At present, the use of Doppler US for the diagnosis of renal artery stenosis is still perceived to be dependent on operator skills and experiences the technique has not gained a widespread acceptance as a robust screening test in general hypertensive population. It may have a role in more- selected. **(97)**

Magnetic resonance angiography (MRA)

Three-dimensional (3D) gadolinium-enhanced magnetic resonance (MR) angiography has become very popular in the few years since its inception. A technique that combines speed, superb contrast, and relative simplicity, 3D gadolinium-enhanced MR angiography has been applied to virtually all regions of the body from the extremities to the brain. The ability to cover large regions of interest within a single breath hold makes this technique particularly well suited for abdominal imaging, in which respiratory motion had previously been a major source of artifact. **(101)**

MRA can replace conventional angiography in providing a road map for vascular reconstructive treatment, especially involving the head, neck and extremities. If the MRA is not considered satisfactory due to flow or metal artifacts a conventional but a directed angiogram can be performed due to reassess the vascular segments that were not adequately visualized.**(1)**

Three-dimensional (3D) gadolinium-enhanced magnetic resonance (MR) angiography is a versatile technique that

combines speed, superb contrast, and relative simplicity. It has a wide range of applications, particularly in the abdomen and pelvis, where superb images of the abdominal aorta and renal arteries are routinely obtained. Aneurysms, atherosclerotic lesions, and occlusions of the major mesenteric arteries are also well depicted. In addition, 3D gadolinium-enhanced MR angiography is ideal for noninvasive evaluation of the systemic and mesenteric veins and can be used to demonstrate parenchymal lesions in the liver, pancreas, kidneys, and other organs. It is also useful in staging genitourinary neoplasms: Parenchymal lesions, venous extension, and adenopathy are all clearly depicted. Three-dimensional gadolinium-enhanced MR angiography can be useful in the preoperative evaluation of potential transplant donors and recipients and in the evaluation of vascular complications following transplantation. Delayed 3D acquisitions of the kidneys, ureters, and bladder can be performed routinely to generate gadolinium-enhanced urograms and demonstrate obstruction, delayed function, filling defects, and masses. A variety of methods for increasing the speed and improving the resolution of 3D acquisition are currently under investigation. These include novel imaging and reformatting techniques and the use of intravascular contrast agents with much longer vascular half-lives. **(101)**

(**Figure 55** - In this 3D coronal gadolinium-enhanced MRA, the kidneys and renal arteries appear normal, and there is no aortic aneurysm)

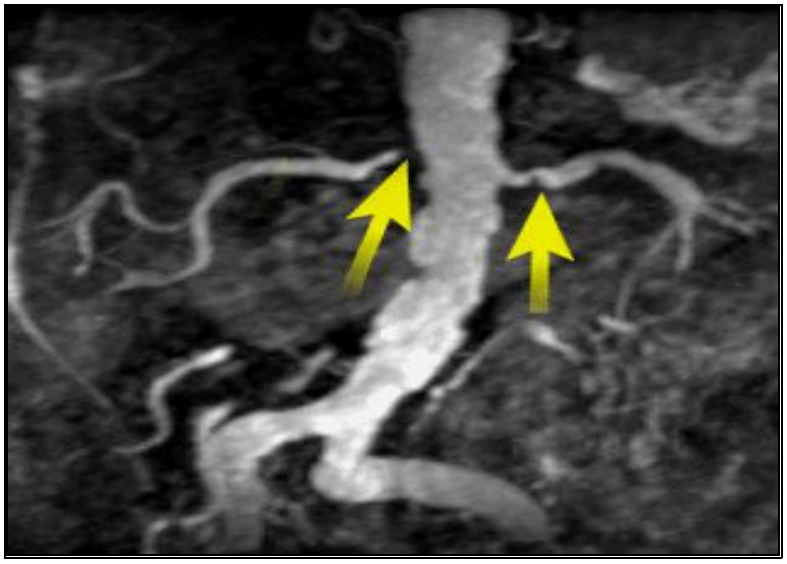

(**Figure 56** - In a patient with severe atherosclerosis, arrows indicate bilateral renal artery stenosis)

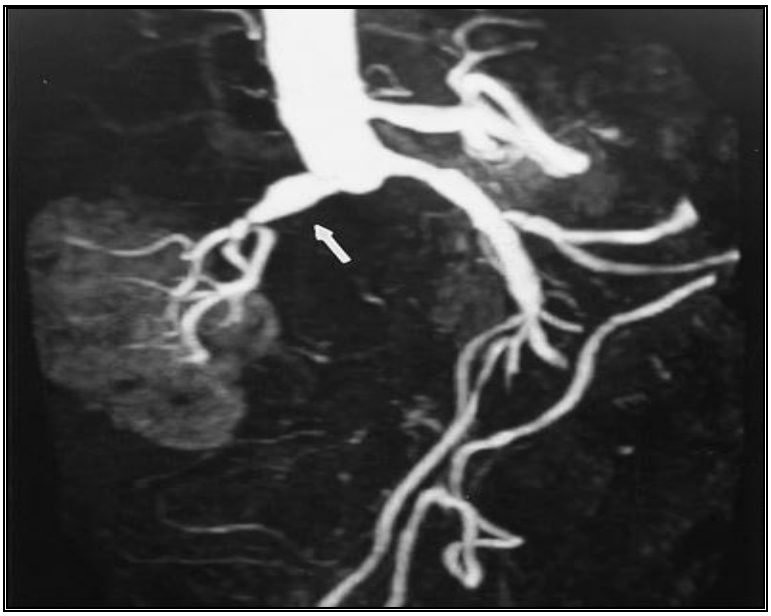

(**Figure 57** - Oblique MIP images from an arterial-phase gadolinium-enhanced MR angiographic examination reveals occlusion of the abdominal aorta below the right renal artery origin. The left renal artery is not visualized, nor is the inferior mesenteric artery. Note the fusiform aneurysm of the proximal right renal artery (arrow)

Limitations and Alternative Techniques

Three-dimensional gadolinium-enhanced MR angiography is not without limitations. Many patients are not candidates for MR angiography because of pacemakers, aneurysm clips, or claustro-phobia. Others may not be capable of performing breath holds sufficient to obtain a diagnostic angiogram. Metallic clips, stents, and embolization coils can cause considerable artifact and obscure important structures. Even when the study is optimal, the resolution of gadolinium-enhanced MR angiography is relatively low compared with that of conventional angiography, and visualization of small peripheral arteries is very limited. Gadolinium-enhanced MR angiography, although less expensive than conventional angiography, is still an expensive examination.

Noninvasive alternatives to gadolinium-enhanced MR angiography include US and CT angiography. US is inexpensive and portable and can be attempted in all patients. Velocity and flow can be measured, providing additional physiologic information not available with other techniques. However, US is often limited by inconsistent visualization of vessels deep in the abdomen in large patients and in patients with extensive bowel gas. One recent study comparing color Doppler US with 3D gadolinium-enhanced MR angiography in visualizing renal arteries and detecting renal artery stenosis found that gadolinium-enhanced MR angiography was superior in detecting accessory renal arteries and had better sensitivity and negative predictive value in depicting renal artery stenosis **(102).**

CT angiography is another attractive alternative to conventional angiography and 3D gadolinium-enhanced MR angiography. Resolution is generally higher than that achieved with gadolinium-enhanced MR angiography, and the speed and quality of studies will improve with widespread availability of multi-detector technology. Although CT angiography can be performed in many patients who are not candidates for gadolinium-enhanced MR angiography, a significant percentage of patients have contraindications for CT angiography, including compromised renal function and contrast material allergy. Very few direct comparisons of 3D gadolinium-enhanced MR angiography and CT angiography have been made. One recent study evaluated both techniques in screening living renal donors and found that the ability to demonstrate accessory vessels was similar; with inter observer intra-modality variation as important as variation related to modality **(103).**

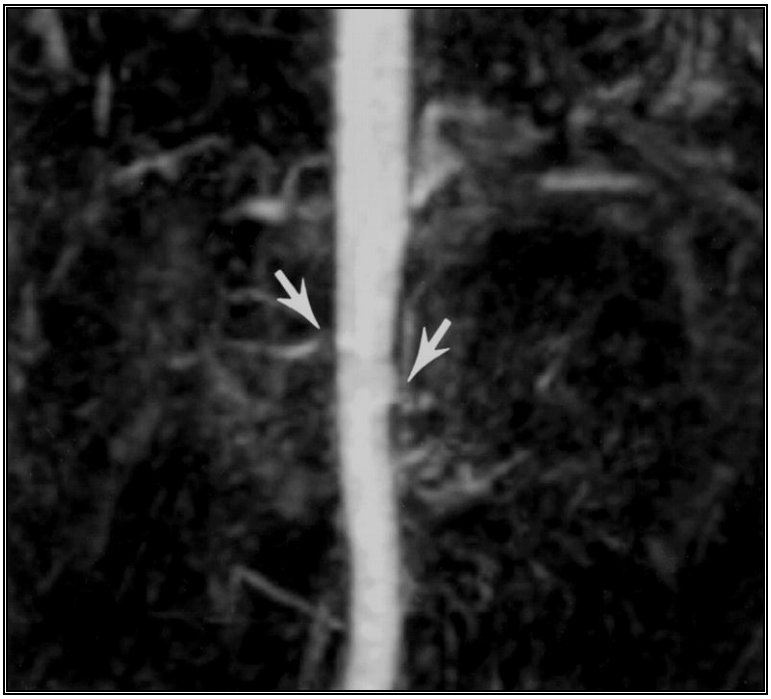

(Figure 58 – Bilateral renal artery stenosis in a 65-year-old woman. Coronal gadolinium-enhanced MR angiogram shows (arrows) bilateral renal artery stenosis)

Spiral CT ANGIOGRAPHY

Helical CT angiography, especially the, combination of transverse sections and maximum intensity-projection reconstructions (**MIP**) can reveal artery fibromuscular dysplasia. However, because some lesions may not be shown, arteriography with pressure measurements remains the only technique that can assess the physiologic significance of the dysplasia. **(104)**

The advantage of helical CT angiography over conventional angiography is that the former is non-invasive, requiring only an Antecubital or forearm venous access, it is performed as an outpatient procedure, and the subject is ambulatory immediately after the procedure, with no loss of working time. This is in contrast to the invasive angiography where 6-8 hours of absolute bed rest is mandatory. **(104)**

The disadvantage of CT angiography compared to invasive angiography is the larger volume of contrast used with the former, two to three more and hence the potential increased risk of nephrotoxicity. However, contrast-induced renal failure is only rarely encountered in individuals with normally functioning kidneys. (**105)**

This potential disadvantage can be avoided if gadolinium enhanced MRA is used. (**106)**

Advantage of CT angiography over MRA is that inadequate breath - holding, causes less sever degradation of image quality, and CT angiography is easier to perform by most technicians in the routine clinical services. The disadvantage of helical CT angiography in comparison to MRA is the use of ionizing radiation and large volume of iodinated contrast material with the form. However, the cost of MRA is significantly higher than CT angiography or conventional angiography. **(104)**

A B

(Figure 59 – Normal renal arteries in a 44-year-old man. **(A)** Anterior volume-rendered image from CT data shows prepolar branching of the left renal artery (arrow). (B) Sagittal angioscopic volume-rendered image from CT data provides a view from "inside" the aorta and clearly depicts the renal ostium (arrowhead). This view can be helpful in the evaluation of dissection flaps and renal artery stenosis)

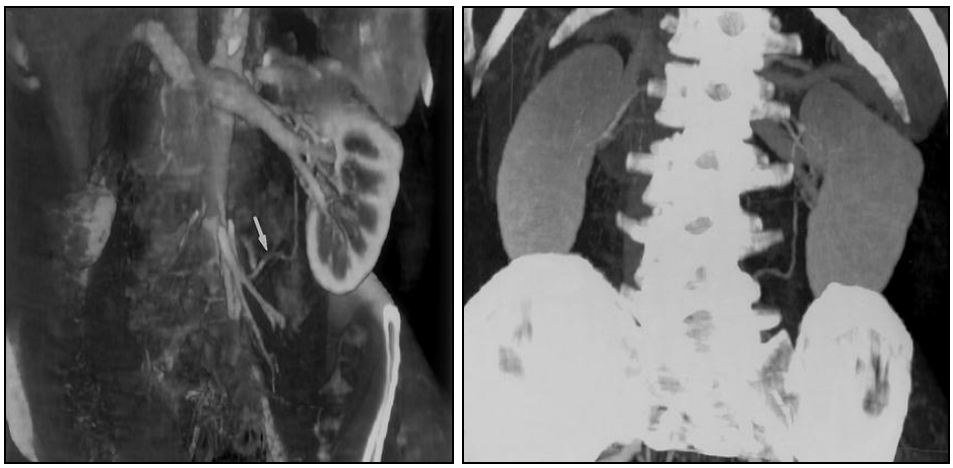

a b

(Figure 60 - Comparison of MIP versus volume-rendered images. **(a)** Anterior volume-rendered image from CT data shows an accessory artery

(arrow) arising from the left iliac artery in a 49-year-old man undergoing a preoperative renal donor evaluation. (b) Anterior MIP image from the same data also reveals the accessory vessel, but its usefulness is limited because overlying bone obscures the aorta and iliac vessels on the anterior view. MIP images can be rotated about an axis to determine depth and better appreciate vascular relationships, but volume-rendered images are probably less cumbersome and easier to interpret in cases with crossing vessels and overlapping anatomy, as in this case).

(Figure 61 – Normal renal arteries in a 39-year-old woman with longstanding hypertension. Axial MIP image, obtained to evaluate for renal artery stenosis, clearly shows the renal arteries (arrows), which are normal and demonstrate no evidence of stenosis).

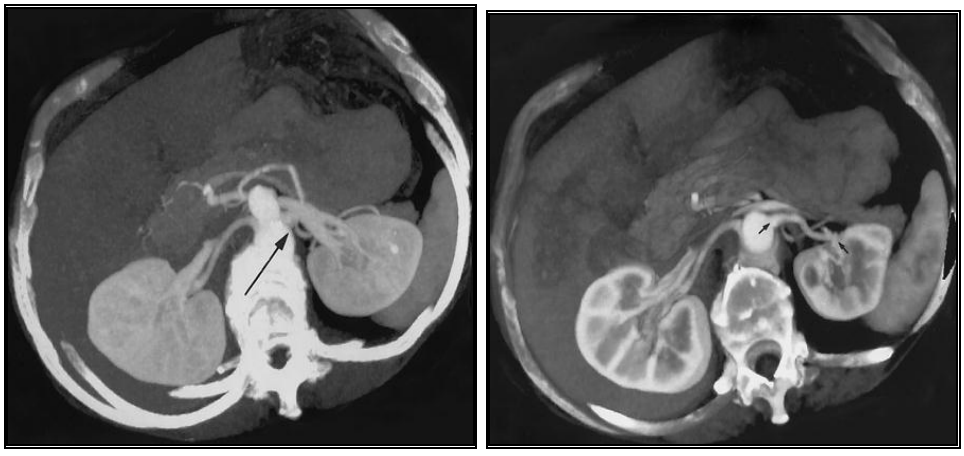

a b

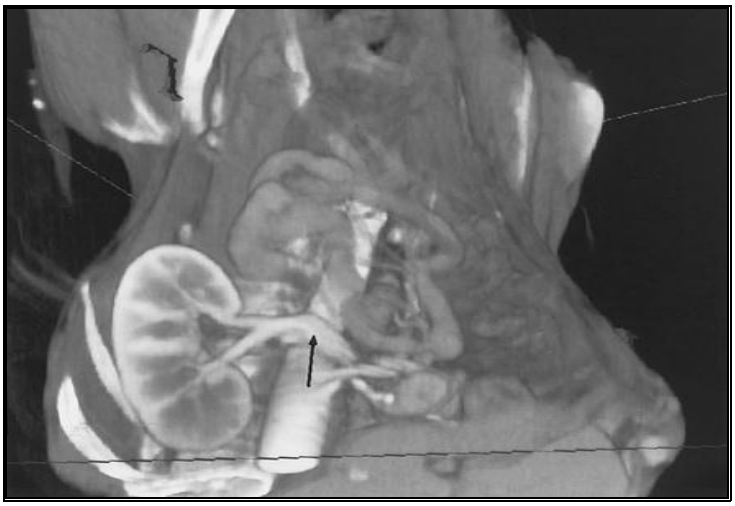

C

(Figure 62 - (a, b, c) Comparison of MIP versus volume-rendered images. **(a)** Axial MIP image of a 62-year-old woman undergoing a preoperative renal donor evaluation shows a confusing tangle of vessels in the left renal hilum (arrow). MIP images, because they only select the voxel with highest attenuation along a line extended from the viewer's eye, do not allow overlapping vessels to be differentiated. **(b, c)** Axial **(b)** and anterior oblique **(c)** volume-rendered images use the entire CT data set and enable easy differentiation of arteries (arrows in b) from veins (arrow in **c**).

(Figure 63 - Normal renal veins. Anterior volume-rendered image of a patient undergoing a preoperative renal donor evaluation demonstrates a single left renal vein (arrow) and two renal veins (arrowheads).

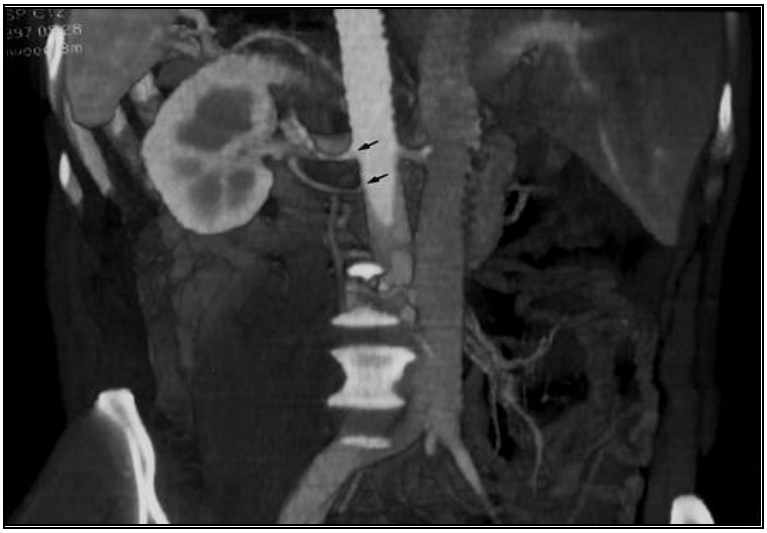

(Figure 64 - Accessory renal arteries in a 58-year-old woman scheduled for donor nephrectomy. Posterior volume-rendered image shows two renal arteries (arrows) supplying the left kidney. The inferior artery was not appreciated on initial axial source images).

(Figure 65 – Prehilar branching of a renal artery in a 62-year-old man undergoing a preoperative renal donor evaluation. Anterior volume-rendered image demonstrates complex, tortuous prehilar branching of the right renal artery (arrowheads).

(Figure 66 - Potential pitfall in assessing an accessory renal artery. Anterior volume-rendered image of a 27-year-old woman obtained before donor nephrectomy shows the superior branch of the inferior mesenteric artery (arrows), which courses toward the left kidney. This vessel can often mimic the appearance of an accessory renal artery on the anterior view. Unlike a true accessory renal artery, however, the mesenteric vessel will not course into the renal hilum).

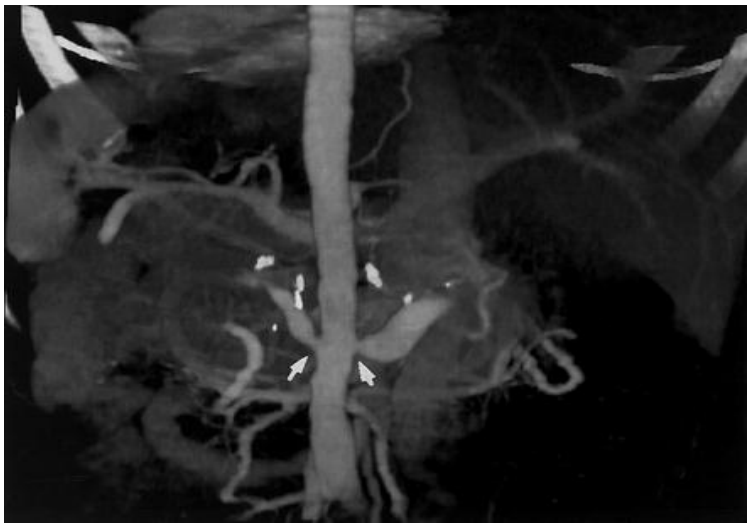

(Figure 67 - Bilateral renal artery stenosis in a 22-year-old woman with Takaysu's arteritis. Anterior volume-rendered image demonstrates

bilateral moderate stenosis (arrows) with marked poststenotic dilatation. The patient also had stenosis of the superior mesenteric artery and had developed an extensive collateral network of the inferior mesenteric artery seen on another view (not shown).

a

b

(Figure 68 – Suspected renal artery stenosis in an elderly patient with hypertension. **(a)** Axial MIP image from a CT angiographic study performed to assess the presence of renal artery stenosis demonstrates extensive calcification near the left renal orifice (arrowhead). However, the calcified plaque obscures the underlying lumen and does not permit appropriate quantification of possible underlying stenosis. **(b)** Axial volume-rendered image, produced after an interactive clip plane has been used to orient the image through the vessel lumen, reveals no evidence of significant stenosis (arrowhead).**(Quoted from Bruce et al., 2001)**

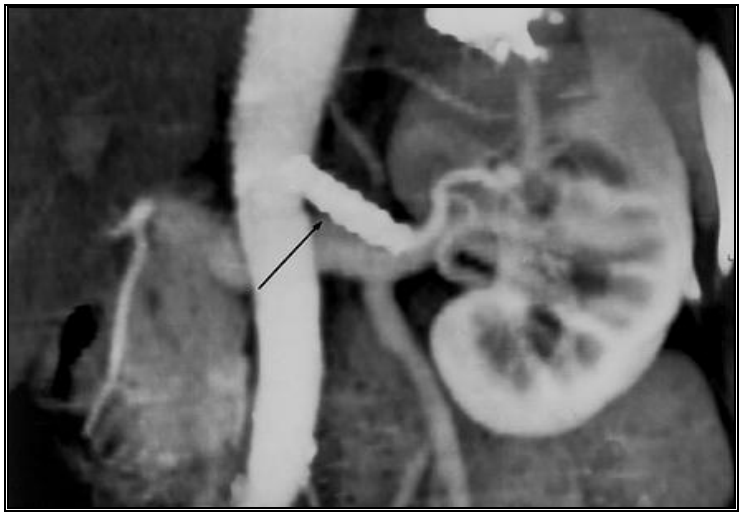

(Figure 69 - Follow-up after placement of an endovascular stent for renal artery stenosis in a 54-year-old man with fibromuscular dysplasia. Anterior volume-rendered image shows flow within the left renal artery stent (arrow). The kidney demonstrates a prompt nephrogram).

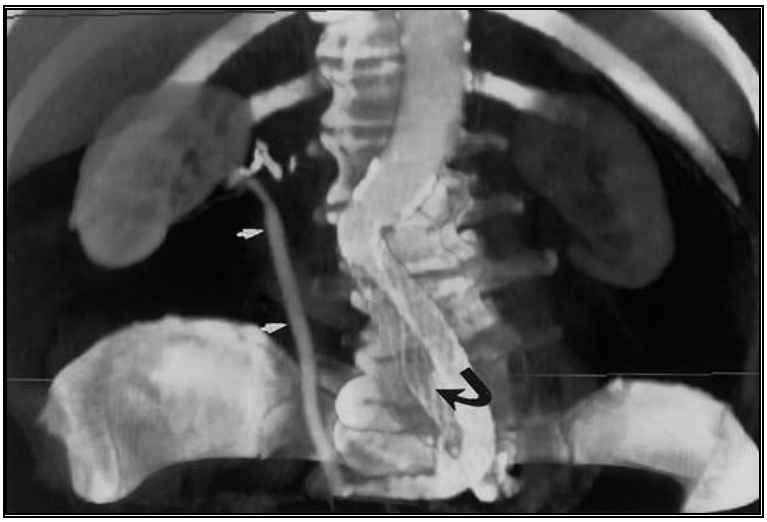

(Figure 70 - Follow-up after placement of an endovascular aortic stent in an 84-year-old man with a history of multiple vascular surgeries including placement of a right iliorenal graft. Anterior volume-rendered image demonstrates that the graft to the right renal artery is patent (white arrows). The right kidney functions well. The aortic graft is clearly seen and is partially thrombosed (black arrow)

(Figure 71– Follow-up study to evaluate for renal artery stenosis to the renal transplant in a 43-year-old man. Anterior oblique volume-rendered image shows the renal artery (arrows), which is normal and has no evidence of stenosis).

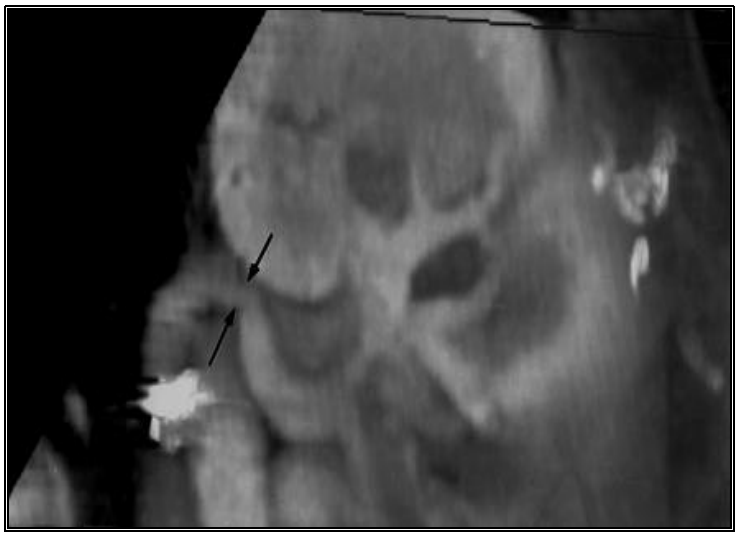

(Figure 72 - Postoperative stenosis in a 42-year-old man who had undergone renal transplantation in the left iliac fossa. Anterior oblique volume-rendered image shows moderate stenosis in the middle segment of the transplanted artery (arrows). This finding was confirmed at angiography).

IV Digital subtraction angiography

The widely available technique of contrast angiography remains the gold standard for diagnosing RAS. Hemodynamic assessment of the lesion may be performed at the same time, and a pressure gradient >20 mm Hg may identify individuals suitable for revascularization. **(107)**

However, there is a risk of worsening renal function related to the contrast agent. In individuals with marked renal insufficiency, either carbon dioxide or gadolinium may be used for digital subtraction aortography in lieu of an iodinated contrast agent. **(107)**

This technique remains the criterion standard for the confirmation and identification of renal artery occlusion in persons with intrinsic renal artery (IRD).Specialists can perform renal arteriography by conventional aortography. (**108)**

Conventional aortography produces excellent radiographic images of the renal artery, but requires an arterial puncture, carries the risk of cholesterol emboli, and uses moderate amount of contrast material with the risk of contrast-induced acute tubular necrosis (ATN).low osmolar contrast material can limit the risk of this complication.**(108)**

Intravenous subtraction angiography is sensitive for identifying stenosis of the main renal artery but does not demonstrate accessory or branch renal arteries sufficiently, however, this technique avoids the use of a high volume of contrast and the risk of artery puncture and atherosclerotic emboli. **(73**)

Intra –arterial digital subtraction angiography has a high diagnostic compared to conventional angiography and is associated with fewer complications, lower doses of contrast, and smaller catheter size. **(73)**

(**Figure 73** - The following image depicts the arteries that supply the kidneys. This X-ray study is called an "arteriogram" A catheter is placed in the arterial tree and X-ray images are acquired during injection of X-ray contrast)**.**

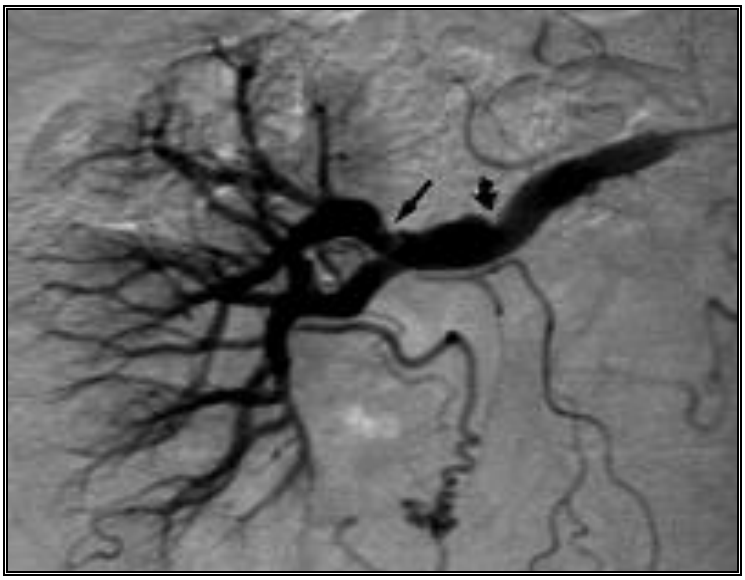

(Figure 74 – Antero-posterior X-ray angiogram obtained in a 73-year-old man reveals a sever stenosis in the right main renal artery).

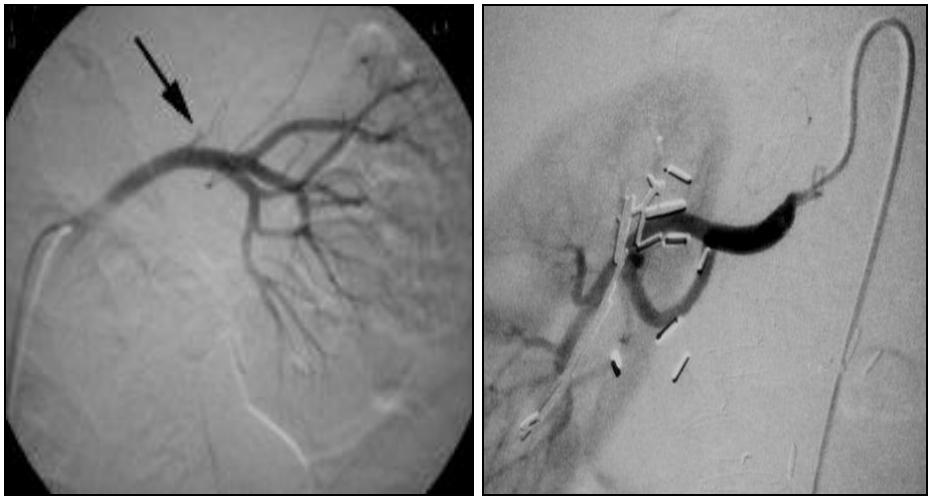

A B

(**Figure75**- In this image (A), the catheter that has been placed into the left renal artery, the catheter that has been placed into the right renal artery **(B)**

(Figure 76 - Coronal MR Angiography shows a sacular aneurysm of the right renal artery (solid arrow) and a fusiform aneurysm of the left renal artery (open arrow).

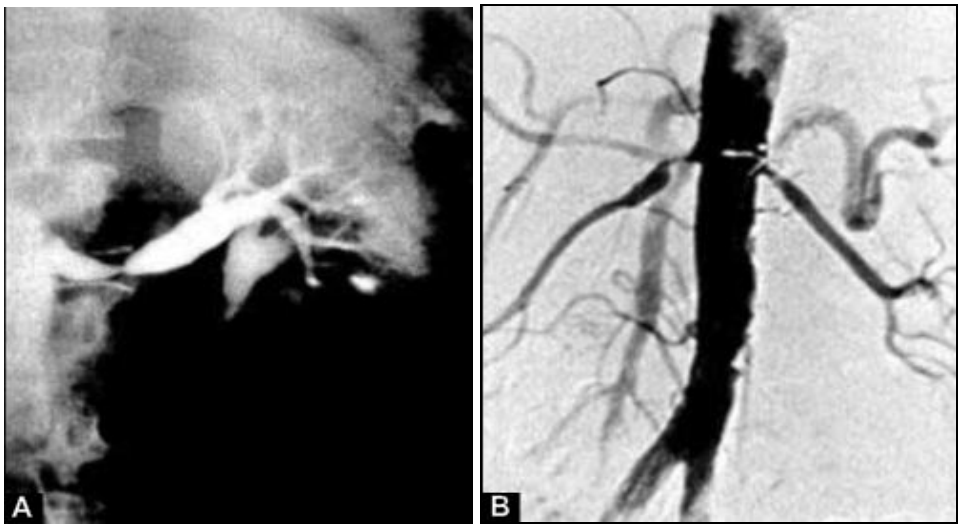

(**Figure 77** - Angiographic examples of atherosclerotic renal artery disease (ASO -RAD). (A) Aortogram demonstrating severe non ostial atherosclerotic renal artery disease of the left main renal artery**.**(B) Intra-arterial digital subtraction aortogram showing severe proximal right renal artery stenosis (ostial lesion) and moderately severe narrowing of the left renal artery due to atherosclerosis)

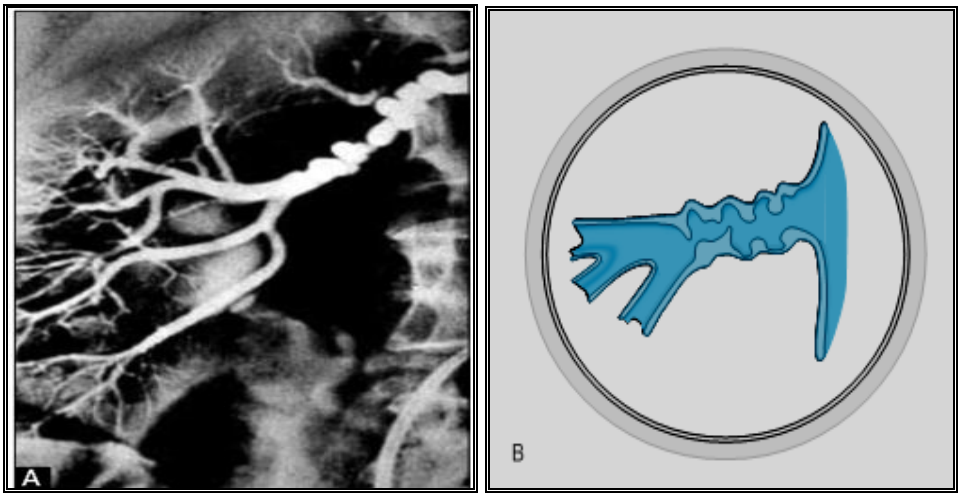

(Figure 78 -Arteriogram and schematic diagrams of medial fibroplasia. (A), Right renal arteriogram demonstrating web like stenosis with interposed segments of dilatation · (large beads) typical of medial fibroplasias.(" **String of beads**") lesion. (B), Schematic diagram of medial fibroplasias).

Table 1-Atherosclerotic Renal artery Disease versus Medial fibroplasia

Men and woman 50- 55 y Total occlusion common Ischemic atrophy common Surgical intervention or angioplasty: Medio cure rate of hypertension	woman 20-40 y Total occlusion rare Ischemic atrophy rare Surgical intervention or angioplasty: Good cure rate of hypertension

Clinical signs suggestive of renal artery stenosis (Table 2)

Young or middle-aged female with severe hypertension and no family history (fibromuscular dysplasia)	**Recurrent flash pulmonary edema** Chronic renal insufficiency with mild proteinuria
Uncontrolled hypertension despite at least three antihypertensive agents in adequate doses (regimen includes a diuretic)	**>1.5 cm difference in renal sizes** Severe hypertensive retinopathy
Worsening blood pressure control in a compliant, long-standing hypertensive patient	**Hypertension with hypokalemia** (secondary hyperaldosteronism due to elevated renin)
Acute renal failure or **creatinine elevation** with angiotensin-converting enzyme	**Bruit over the abdominal aorta** (lateralizing bruit over the renal arteries is more specific.

a b c

(Figure 79 – RAS in a 12-year-old girl with a rising serum creatinine level and hypertension. **(a)** Digital subtraction angiogram shows stenosis of the proximal main renal artery (arrow). Note the superior pole artery anastomosed end-to-side to the external iliac artery. PTA was performed with a 6-mm balloon. **(b)** Spot view of the anastomosis obtained during PTA shows a guide wire that was passed across the stenosis using an ipsilateral approach. Note the "waist" at the stenosis (arrow). **(c)** Post- angioplasty angiogram shows a patent renal artery without residual stenosis).

(**Figure 80** - Angiogram obtained after further expansion of the stent with a 6-mm balloon shows good results. The pressure gradient decreased to 15 mm Hg).

Algorithm for the detection and treatment of renal artery stenosis.

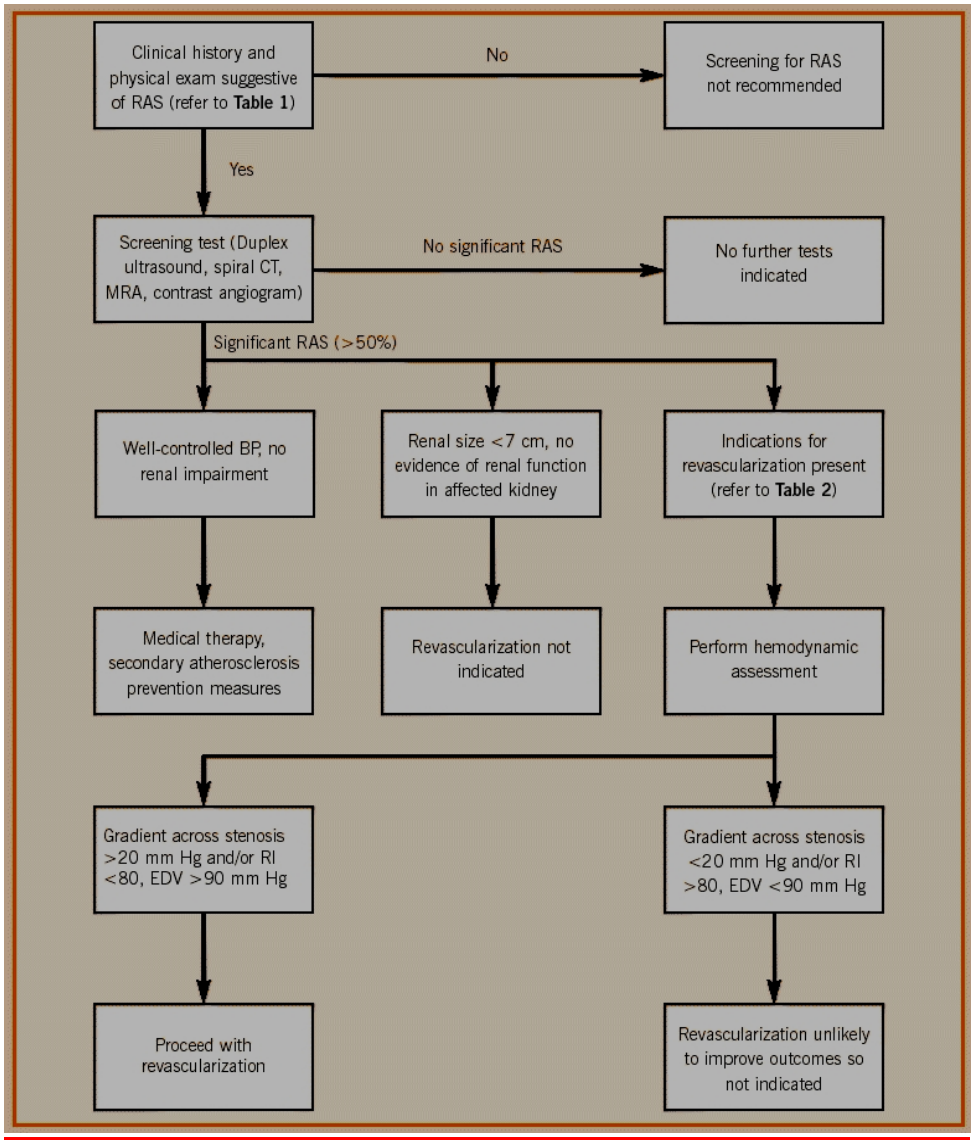

Table 3- Algorithm for the detection and treatment of renal artery stenosis. BP: blood pressure; CT: computed tomography; EDV: end-diastolic velocity; MRA: magnetic resonance angiography; RAS: renal artery stenosis; RI: renal artery resistance index (Adapted with permission from the American College of Cardiology Rev 2003).

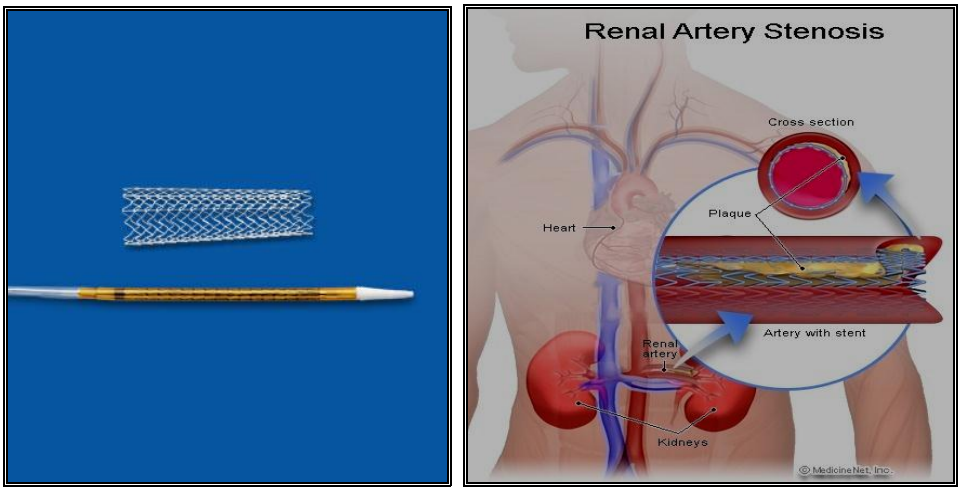

(**Figure 81**- This particular stent is approximately 3 cm in length)

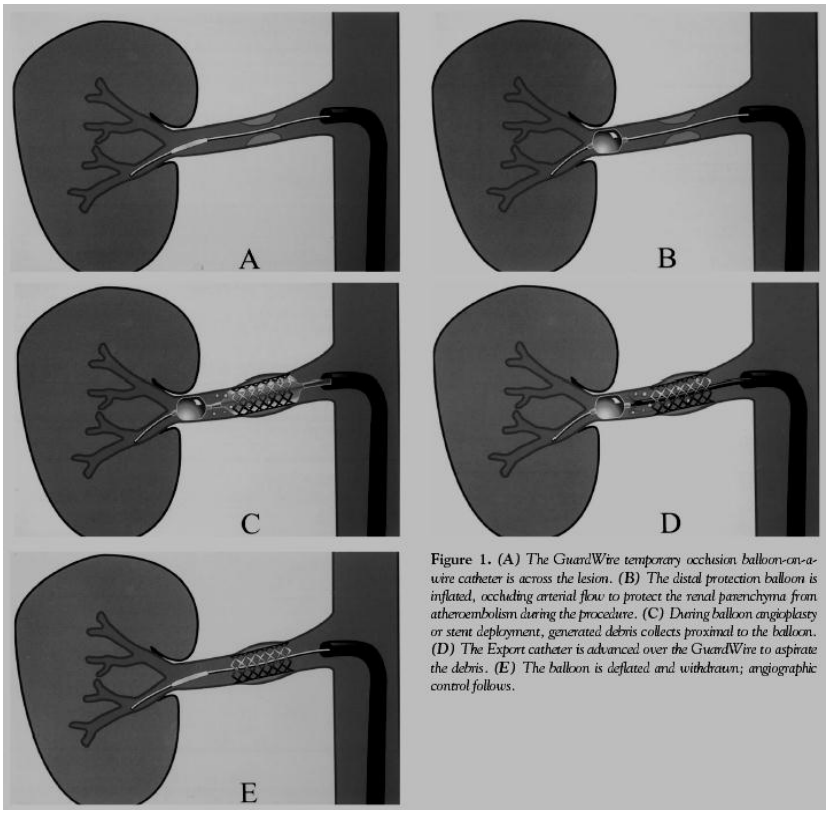

(**Figure 82** - To evaluate the feasibility and safety of renal artery angioplasty)

Renal scintigraphy:

Renal scintigraphy has been reported to be sensitive for detection of renovascular hypertension, but some of its limitations (e.g., in the setting of bilateral renal artery failure) should be considered**. (51)**

ACE Inhibitor Scintigraphy

It has been demonstrated that a kidney with RVH may exhibit impaired function during ACE inhibition. This phenomenon is observed mainly in patients with bilateral RAS or with arterial stenosis in a solitary kidney; it is believed to be caused by disruption of the auto-regulation system of the glomerular filtration rate (GFR), which becomes dependent on angiotensin II under conditions of low perfusion. Although a decline in the GFR can be induced by ACE inhibition in the affected kidney of patients with unilateral RAS, the contralateral kidney preserves the overall renal function.

In patients with unilateral RAS, a unilateral change in renal function induced by ACE inhibition can be revealed with scintigraphy, in these patients, ACE inhibitor scintigraphy induces significant changes. (**109)**

In the time, activity curves of the affected kidney in comparison with baseline scintigraphy. Such changes are not observed in patients with non significant RAS or normal renal arteries. ACE inhibitor scintigraphy is performed 1 hour after an oral dose of 25 mg of captopril or 15 minutes after an intravenous dose of 0.04 mg/kg of enalapril maleate. ACE inhibitor therapy should be stopped 2–5 days prior to the study according to the half-life. (**51**)

and adequate hydration must be ensured. Blood pressure should be monitored during the test. Baseline and ACE inhibitor scintigraphy are performed after intravenous injection of technetium-99m mercaptoacetyltriglycine (**MAG3**), iodine-131 orthoiodohippurate (**OIH**), or Tc-99m diethylene triamine penta acetic acid (**DTPA**). Sequential images and scintigraphic curves are obtained for 30 minutes after injection of the radiopharmaceutical. Time-activity curves are generated from the renal cortex and pelvis. Renal uptake is measured at 1–2minute intervals after injection. **(51)**

Tc-99m MAG3 and I-131 OIH are excreted by means of tubular secretion, and Tc-99m DTPA is excreted by means of glomerular filtration. In patients with RAS, ACE inhibitors induce renal retention of the radiopharmaceutical due to decreased urinary output secondary to reduced **GFR**. Scintigraphic abnormalities provoked by ACE inhibitors can be reversed with balloon dilation **(51).**

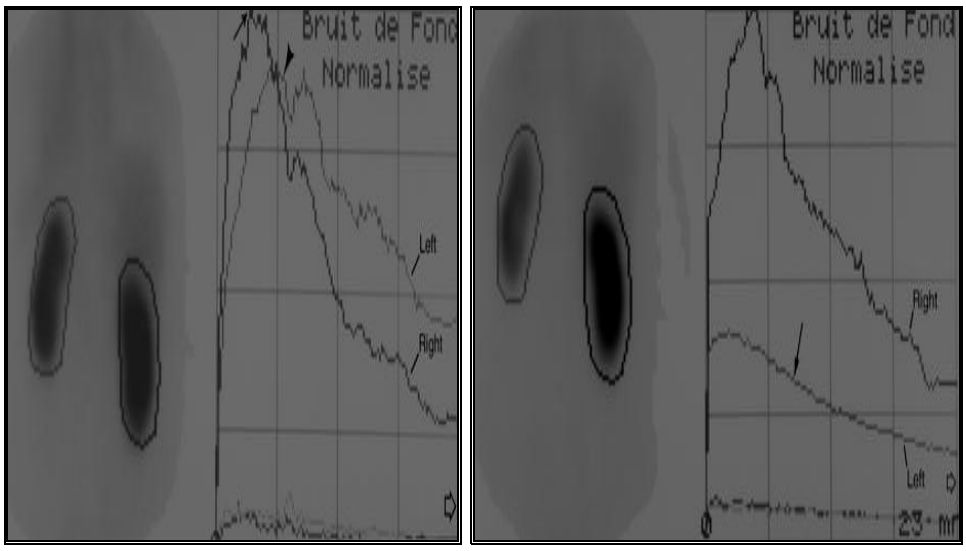

a b

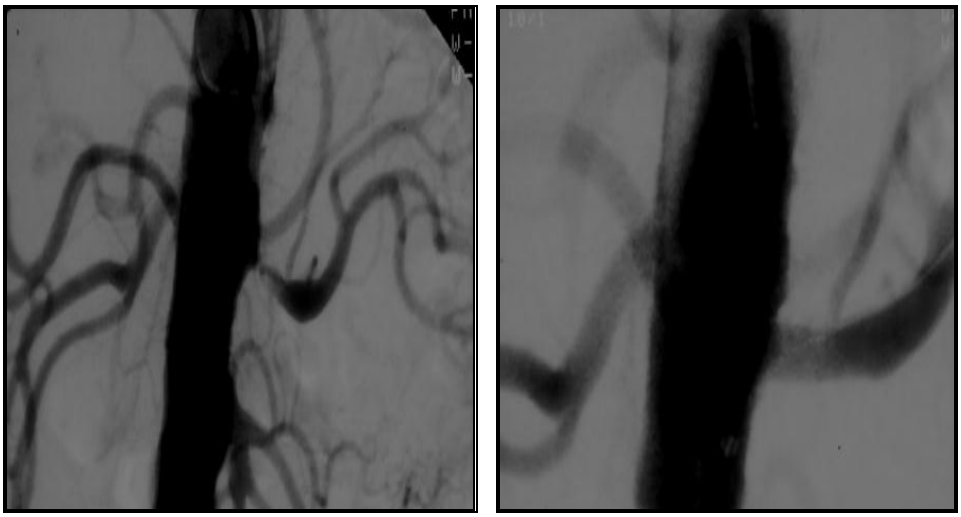

C d

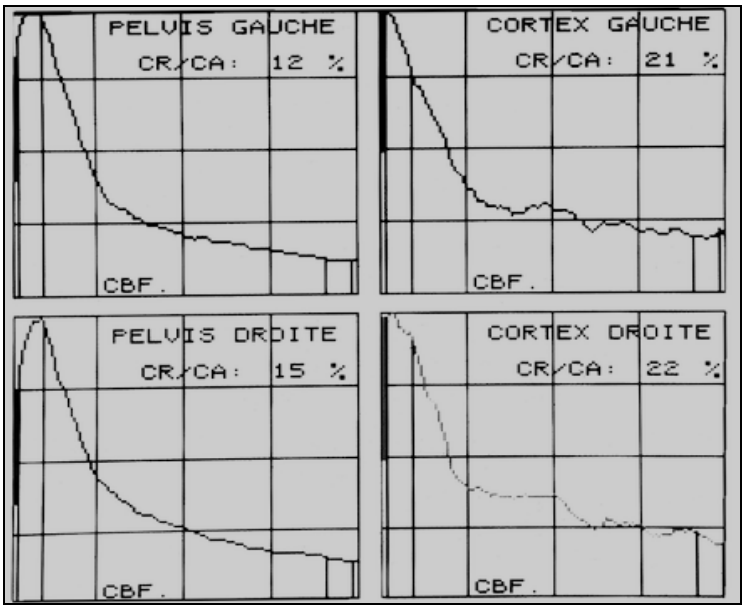

e

(Figure 83 - Renovascular disease in a 60-year-old patient. **(a)** Baseline scintigram (posterior view) obtained with Tc-99m MAG3 shows mild and nonspecific abnormalities, with decreased amplitude and delayed peaking of the left renal curve (arrowhead) relative to the right renal curve (solid arrow). The time reference (open arrow) is 30 minutes. **(b)** Scintigram (posterior view) obtained after administration of captopril shows diminished uptake in the left kidney, with an abnormal curve (solid arrow)

suggesting left-sided renovascular disease. The time reference (open arrow) is 30 minutes. **(c)** Aortogram shows a severe stenosis of the left renal artery. **(d)** Angiogram obtained after angioplasty and stent placement shows wide patency of the left renal artery. **(e)** Scintigraphic curves (top left, left renal collecting system; top right, left renal cortex; bottom left, right renal collecting system; bottom right, right renal cortex) obtained after correction of RAS show normalization of the captopril scintigraphic curve for the left kidney (top curves). The curves were obtained over 30 minutes. **CA** = cortical peak activity (between 1 and 3 minutes), **CBF** = curve with background correction, **CR** = cortical residual activity (between 20 and 23 minutes).

In selected high-risk populations, ACE inhibitor scintigraphy can be very accurate. Its sensitivity for detection of RAS 70% or greater in diameter varies between 51% and 96% (mean, 82%)

Its positive predictive value for detection of RAS associated with clinical improvement in hypertension after revascularization varies between 51% and 100% (mean, 85%). However, ACE inhibitor scintigraphy is much less sensitive and specific in unselected patients. Bilateral RAS, impaired renal function, urinary Obstruction and chronic intake of ACE inhibitors are other factors that lower the sensitivity of ACE inhibitor scintigraphy (**Fig 84**). The latter factor is the reason for withholding **ACE** inhibitors for 2–5 days (depending on the half-life) before the study. When performed under the right conditions, **ACE** inhibitor scintigraphy is a useful tool. Moreover, careful analysis of the scintigram may allow detection of stenotic accessory arteries. (**110)**

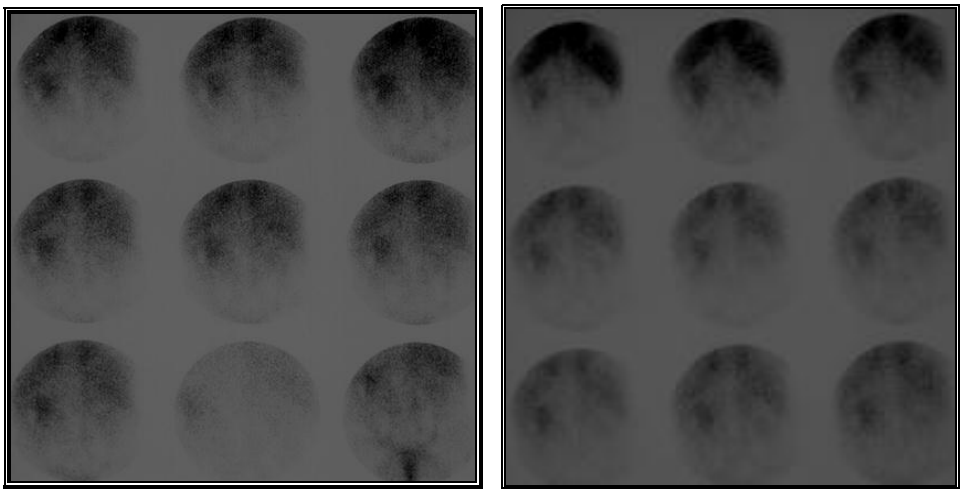

A B

(**Figure 84** - Indeterminate scintigraphic results in a 70-year-old patient with renal insufficiency. Baseline (A) and captopril (B) Tc-99m DTPA scintigrams (sequential images obtained at 2-minute intervals from top left to bottom right) show poor demonstration of both kidneys. No conclusion could be drawn about the possibility of renovascular disease).

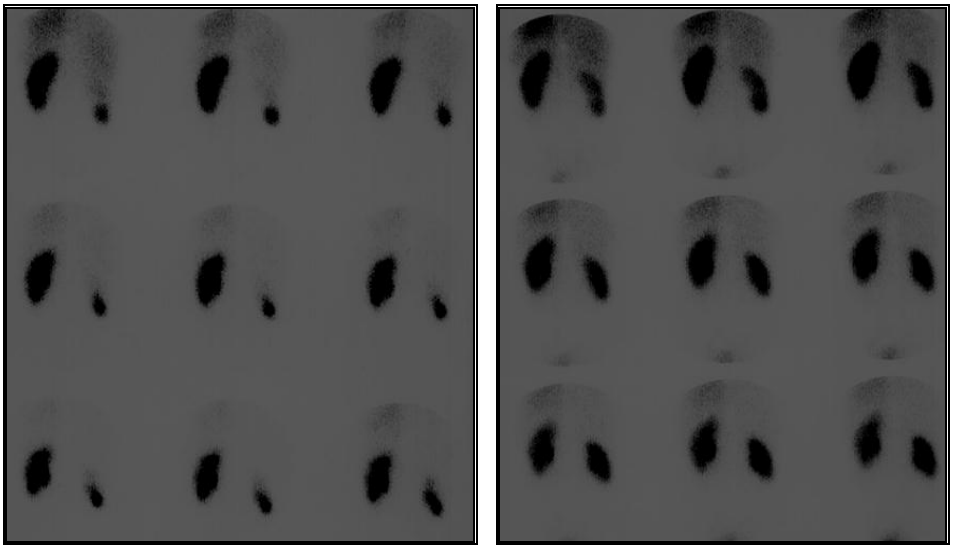

a b

(**Figure 85** - Stenotic accessory artery in a 55-year-old patient with hypertension. **(a)** Baseline Tc-99m DTPA scintigram (sequential posterior views obtained at 2-minute intervals from top left to bottom right) show

slight retention of the radiopharmaceutical in the left renal pelvis. **(b)** Captopril scintigrams show markedly decreased uptake in the upper half of the right kidney, a finding consistent with renovascular disease of a polar artery).

ACE inhibitor scintigrams should be interpreted as consistent with a low, intermediate, or high probability of renovascular disease. The most specific diagnostic criterion for RVH at scintigraphy is an ACE inhibitor–induced change on the scintigram. **(51)**

The general interpretive criteria are as follows:

1. A normal ACE inhibitor scintigram indicates a low probability (<10%) of RVH.

2. A small, poorly functioning kidney (<30% uptake with a time to maximum activity [**Tmax**] ≤2 minutes) that shows no change on the ACE inhibitor scintigram and bilateral symmetric abnormalities such as cortical retention of tubular agents indicate an intermediate probability of RVH.

3. Criteria associated with a high probability of RVH include worsening of the scintigraphic curve, reduction in the relative uptake, prolongation of the renal and parenchymal transit time, increase in the 20-minute/peak uptake ratio, and prolongation of **Tmax.**

Specific interpretive criteria for Tc-99m MAG3 and I-131 OIH scintigrams are as follows:

Unilateral parenchymal retention after ACE inhibition is the most important criterion for Tc-99m MAG3 and I-131 OIH scintigraphy and represents a high probability (>90%) of RVH.

Parenchymal retention can be demonstrated as a change in the 20-minute/peak uptake ratio of 0.15 or greater, a significantly prolonged transit time, or a change in the scintigraphic grade (**Fig 88**). Parenchymal retention can also be demonstrated as a delay in excretion of the tracer into the renal pelvis of greater than 2 minutes after administration of ACE inhibitors or an increase in the **Tmax** of at least 2 minutes or 40%. A greater than10% change in the relative uptake of Tc-99m MAG3 or I-131 OIH after ACE inhibition is uncommon but represents a high probability of RVH. **(51)**

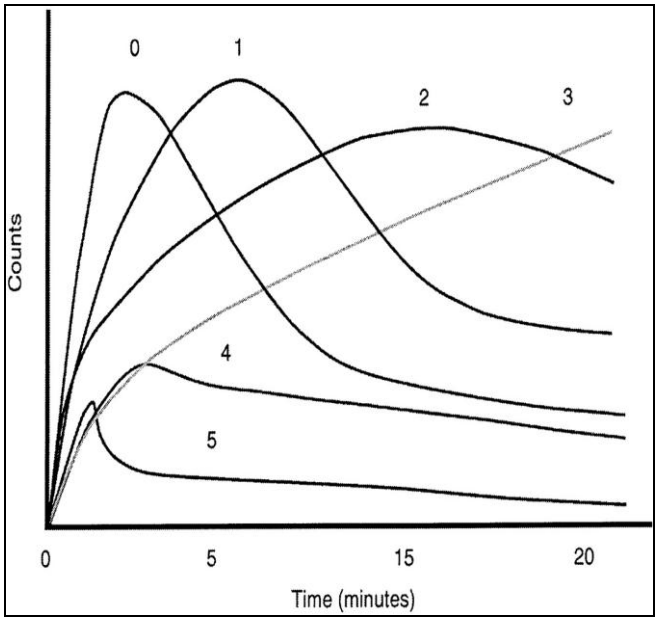

(Figure 86 – Patterns of scintigraphic curves. 0 = normal, 1 = minor abnormalities but with T max greater than 5 minutes and (for Tc-99m MAG3 and I-131 OIH scintigrams) 20-minute/peak uptake ratio greater than 0.3, 2 = marked delayed excretion rate with preserved washout phase, 3 = delayed excretion rate without washout phase (accumulation curve), 4 = renal failure pattern with measurable kidney uptake, 5 = renal failure pattern without measurable kidney uptake (blood background-type curve).

DISCUSSION

The presence of anatomic renal artery stenosis (RAS) does not necessarily establish that the hypertension or renal failure is caused by the RAS is common whereas renovascular hypertension occurs in only 1% to 5% of all patients with hypertension **(111).**

Fibromuscular dysplasia or atherosclerosis most commonly causes RAS. The former predominates in young women, and the latter is encountered most often in individuals over the age of 55. Approximately 90% of all renovascular lesions are secondary to atherosclerosis. The predominant clinical manifestation of fibromuscular dysplasia is hypertension. The hypertension can frequently be cured or significantly improved with Percutaneous Transluminal Angioplasty or surgery. The predominant clinical manifestation of atherosclerosis RAS and recurrent episodes of congestive heart failure (CHF) and flash pulmonary edema. **(3)**

Atherosclerotic RAS most often occurs at the ostium or the proximal 2-cm of the renal artery. Percutaneous or surgical revascularization can lead to improvement or stabilization in renal function and improvement in CHF if the patients are selected carefully patients with renal artery stenosis can often progress to end-stage renal disease if left untreated. **(39)**

An ideal screening test must have adequate sensitivity and specificity to identify patients with significant disease, avoiding costly and invasive diagnostic studies when patients are unlikely to benefit from treatment. The ideal imaging procedure should; (1) identify the main renal arteries and accessory or polar vessels, (ii) localize the site of stenosis or disease, (iii)provide evidence for the hemodynamic significance of the lesion, and (iv) identify associated pathology (i.e., abdominal

aortic aneurysm, renal mass, etc.)That may have an impact on the treatment of the renal artery disease**(112).**

DOPPLER ULTRASONOGRAPHY

Is ideally suited for imaging kidneys. The renal cortex, medulla, and collecting system have different acoustic properties, and pathological changes are easily discernible and correlate well the histological findings. Furthermore, kidneys are easily visualized and show a limited spectrum of anatomic

Variation and pathological changes. This, coupled with the safety, simplicity, and low cost, has made sonography an invaluable tool in nephrology.

When there is a discrepancy in kidney size of 2.0 cm or greater, the ultrasonographer should search carefully for the presence of renal artery stenosis or an occluded renal artery.

Examination of the renal artery is very difficult by gray-scale sonography and is greatly enhanced by Doppler and color Doppler sonography, which show high velocity and turbulence at the stenotic site. **(113)**

However this requires visualization of the entire renal artery (and sometimes multiple arteries) which, even in expert hands, is frequently not possible. This has led to the use of spectral analysis of intrarenal tracing as an indirect indication of renal artery stenosis. Duplex ultrasonography may also be useful in helping to predict those patients who will demonstrate an improvement in blood pressure control or renal function after renal artery angioplasty and stenting. (Radermacher, 2001)Renal artery duplex is an excellent test for the follow up of RAS after Percutaneous therapy or surgical bypass **(112).**

When compared duplex ultrasonography with angiography, duplex ultrasonography has a sensitivity and specificity estimated at 84% to 98% and 62% to 99%, respectively, when used to diagnose renal artery stenosis**(114).**

The Renal Aortic Ratio (RAR), the ratio of the PSV in the renal arteries to the PSV in the aorta, is used to classify the degree of stenosis. 0% to 59% stenosis, 60% to 99% stenosis, and total occlusion (**Table 4**). When the aortic velocity is less than 40 cm\sec or greater than 100cm\sec, the RAR is not accurate representation of the degree of stenosis. In these instances, if the PSV is greater than 200 cm\sec and turbulence is present on color flow, the stenosis would be classified as 60% to 99%.

Table 4 -Classification of Renal Artery Stenosis

Degree of stenosis	Ultrasonographic Criteria
0% to 59%	RAR<3.5 and renal artery PSV<200 cm/sec
60 % 99%	RAR >3.5 or renal artery PSV >200 cm/sec and flow disturbance
Occluded	Absence of arterial flow and low amplitude signal
	RAR= renal aortic ratio,**PSV**=peak systolic velocity

If the end diastolic velocity (EDV) was >150 cm/s, then the degree of stenosis was likely to be >80%. It may be useful to

measure the resistive index during the renal artery duplex examination. A Doppler waveform is obtained from the parenchyma of the kidney.**(115)**

A recent study used Doppler ultrasonography to predict the outcome of therapy in patients with RAS. Ninety-seven percent of patients with resistance index >80 demonstrated no improvement in blood pressure, and 80% had no improvement in renal function. The authors suggest that the increased resistive index identify structural abnormalities in the small vessels of the kidney. Such small-vessel disease has been seen with long-standing hypertension associated with nephrosclerosis or glomerulosclerosis. If this study is confirmed, it could provide a method for predicting which patients would improve after percutaneous intervention or surgical revascularization. **(116)**

The RAR and PSV in the main renal arteries are used to determine the degree of stenosis present. Nazzal and co-workers 1997 compared angiographic findings with the use of AI and AT in 114 patients. An AI below 3.78 kHz/sec/MHZ is associated with an 89% and 92% sensitivity and specificity, respectively, for predicting stenosis of 50% or greater. The AT had a sensitivity of 63% and a specificity of 98%. The RI is calculated as the PSV-WDV/PSV and is a measure of the resistance within the renal circulation. An elevated RI may present in renal parenchymal disease, and the RI may be influenced by some antihypertensive drugs and age. It is not useful for predicting the degree of renal artery stenosis. In the authors' noninvasive vascular laboratory the RAS and PSV in the main renal arteries are used to determine the degree of stenosis present. Parameters such as the AT and AI may provide corroborative evidence but often are not used to make the diagnosis of renal artery stenosis. **(114)**

Gadolinium-enhanced MR angiography (MRA) versus color Doppler ultrasound (CDU) in evaluation of RAS has been discussed in a study by F.De Cobelli; et al, 2000. They found that MAR shows better sensitivity and similar specificity than ultrasound in evaluation of stenosis. They also found the MRA is superior to CDU in accessory artery detection. The duplex study identified 3 of 13 accessory arteries, whereas MR angiography demonstrated 12 of 13 accessory vessels.

The sensitivity of identifying accessory renal arteries is approximately 67%. If there is a high index of suspicion for renal artery stenosis and the duplex examination fails to reveal a significant stenosis the clinician may suspect an accessory vessel as the culprit. Because polar arteries are a major consideration in the renal transplant donor, and because ultrasonography does not provide good visualization of other associated structures, it is not an optimal examination for preoperative planning for transplant donors or in renal cancer **(117)**

Unlike MRA angiography (which may be affected by artifact or scatter produced by the stent), ultrasound transmission through the stent is not a problem. **(18)**

Frequently Duplex ultrasonography has some technical limitations approximately 4% to 13% of examinations may be inadequate owing to excess gas or large body habitués. **(114)**

Hint about the value of micro bubbles in increasing accuracy of u/s for detection of RAS, the first and still most important application of micro bubbles is in echocardiography to ‘opacity’ the cardiac chambers, similar considerations apply to Doppler of deep abdominal vessels; ultrasound has long been used as a screening Test for renal artery stenosis in the evaluation of hypertension and of progressive renal failure in arteriopaths but is subject to Because of technical difficulties.

With the use of micro bubbles, successful examinations are the rule so that the study can be completed more quickly and more invasive procedures such as angiography can be avoided. For the large vessel approach, signals from arteries or veins are collected as the bolus transits and this can give information on the overall function of the organ. This has been tried for native and transplant kidneys using spectral Doppler and it promises to improve the diagnosis of renal artery stenosis and, in transplant, to distinguish between rejection and acute tubular necrosis.

Although excellent sensitivities and specificities have been reported, the use of Doppler scanning to screen for renal artery stenosis is controversial and probably only feasible in select centers with specific expertise in this area. **(118)**

MR angiography

Now provide renal artery imaging that compares well with the quality and accuracy of angiography. In fact, as the technology of MR angiography for the evaluation of renal artery disease completely. Factors such as the patients body habits or the degree of renal impairment can help to determine which screening test should be used; however, institutional experience and expertise are perhaps the most important factors determining which of the noninvasive imaging studies should be ordered **(119).**

During, the past decade. MRA has evolved from an experimental technique into the modality of choice for the noninvasive evaluation of renovascular disease. The recent widespread application of MRA for these indications has been driven primarily by the advent of 3D contrast-enhanced MRA. Which provides a fast, reliable technique for imaging large vascular and generates images, after post processing, similar in appearance to digital subtraction angiography. The cross-sectional volumetric nature of contrast-enhanced MRA affords some advantages over conventional catheter angiography **(119).**

MRA is unique among noninvasive imaging modalities in that it offers a comprehensive evaluation of anatomy of renal artery. The availability and reliability of MRA extend renal artery screening to a wider spectrum of patients. Current applications of renal MRA range from detection of renal artery stenosis to evaluation for renal transplant donors. Angiography should be reserved for patients in whom the diagnoses have been made and there are indications to proceed with PTA and stent implantation. **(120)**

Among individuals with chronic renal insufficiency for whom the risk of a dye load may be prohibitive, 3D-MRA, a minimally invasive technique with a high degree of sensitivity and specificity in the diagnosis of RAS, is rapidly becoming the diagnostic tool of choice. **(120)**

Because TOF and PC imaging rely on flow, both techniques are prone to artifacts related to distributions and variations in blood flow (eg, pulsatile flow and turbulent flow) turbulent flow is particularly problematic because it result in intravoxel phase dispersion and regions with complex geometries, which unfortunately are typically the regions of clinical interest. Intravoxel dephasing is a known limitation of TOF and PC MRA, which results in the overestimation of the severity of a stenosis or even in the erroneous appearance of a stenosis or occlusion. These pitfalls of the TOF and PC imaging have contributed to the general lack of enthusiasm for their routine clinical use for imaging of the RAS **(121).**

Contrast-enhanced MR angiography provides a superior quality study when compared with non-contrast studies since its introduction, arterial phase gadolinium-enhanced studies rabidly have become the accepted standerd for MR angiography because of significant improvements and enhancement in vascular imaging. The imaging time is shortened substantially; 20 to 40 second. The shorter time eliminates some artifact created by gross patient movement. Signal strength is increased,

providing better visualization of distal small caliber vessels. Unlike in flow-based techniques (time-of-flight, phase contrast), areas of slow flow or turbulence may be better visualized. The signal defends only on gadolinium concentration in the vessel. Flow-related artifacts are almost entirely avoided. The technique is quick, fairly easy to perform, and provides high-resolution three-dimensional arterial images sets. As a result, Gd-enhanced three-dimensional MRA can be tailord for most efficient high spatial resolution imaging (ie, parallel to the length of the vessel). **(122)**

Gadolinium also may enhance the ability to identify accessory vessels, which without contrast, may have signal degradation. Hahn and co-workers compared three-dimensional phase contrast MR angiography (un-enhanced) with gadolinium-enhanced three dimensional MR angiography. The unenhanced study identified zero of eight accessory vessels, whereas the gadolinium-enhanced study identified five of eight accessory vessels.**(123)**

MRA compares favorably with the gold standerd for morphological evaluation of RAS, renal angiography, especially for high grade stenosis.

Bakker et al (1998) studied patients with suspected RAS and found 99% sensitivity for 50% or greater RAS and 92% specificity.

Mittal et al. (2001) similarity showed a high degree of sensitivity (96%) and specificity (96%) in the diagnosis of RAS.

Masunaga et al (2001) compared MRA with conventional angiographgy and found 100% sensitivity and specificity in detecting greater than 50% stenosis.

Thorton and co-workers (1999) compared breath-hold MR angiography with conventional DSA. They demonstrated 100% sensitivity and 98% specificity for detecting greater than 50% stenosis. Overall, MR angiography revealed 85 of 87 renal arteries, 20 of 20 stenosis, and 5 of 5 occlusions. The two arteries not identified were accessory vessels.

Accuracy of gadolinium-enhanced MRA in detecting renal artery stenosis in comparison with arterial DSA has been discussed by, Bereg, et al, 2002, they made comparison study between gadolinium-enhanced MRA and DSA. They found that gadolinium-enhanced MRA is more accurate than DSA for the detection of main RAS. **(124)**

The vessel visibility found in 3D-Gd-MRA for the vessel ostium was significantly higher than in DSA, whereas no significant differences were present for the proximal and distal part. For the hilar vessel segments, four of the seven readers most commonly could not identify the vessel at all in 3D-Gd-MRA, whereas maximum vessel visibility was still reported in DSA for this particular segment. This difference became more prominent for the intra renal vessels. For both hilar and intra renal vessel segments, significant differences in visibility between DSA and 3D-Gd-MRA were found in favor of DSA **(125).**

Conversely, DSA has various pitfalls as well. As a two-dimensional technique limited to a few projections, overlaying structures such as torturous vessels or calcified plaques can mask the presence of renal artery stenosis. Eccentric stenosis, which often occurs in atherosclerotic disease, can be falsely graded when viewed only en face rather than in various projection as on 3D-Gd-MRA.In addition, the position of the catheter in the aorta is crucial for optimum enhancement of the arteries of interest. Accessory renal arteries that arise usually high or low from the aorta might not be displayed on an injection from a standard catheter position. Distal renal artery

stenosis often requires selective catheterization for accurate grading,which,however,increase the frequency of complications from atherosclerotic emboli **(125).**

Angiography is invasive and costly when compared with other imaging modalities. Potential disadvantages associated with angiography include access site complications, such as hematoma, pseudoaneurysm, and arterial venous fistula, and acute renal failure from contrast-induced nephrotoxicity or atheromatous embolization to the kidneys, bowel, or lower extremities. Angiography is a poor screening test for renal artery stenosis but an excellent confirmatory test once it has been decided that intervention **(126).**

Two limitations of 3D-Gd-MRA remain, such as obese patients who do not fit into the MRA system and patients with implanted electronid devices such as cardiac pacemakers. At most centers, the cost of performing MR angiography exceeds that of duplex ultrasonography.

Gadolinium-enhanced three-dimensional MRA has been shown to be very accurate (sensitivity 91% to 100% specificity 89% to 100%) for the detection of greater than 50% diameter stenosis of the main renal artery **(70).**

CT angiography

It is to be mentioned that CT angiography and renal scintigraphy still has a role in evaluation of RAS has sensitivity and specificity for detecting RAS of 59% to 96% and 82% to 99% respectively, when compared with angiography the potential difficulties with this procedure is that protocol parameters for table speed, time delay to image acquisition, and scan volume may vary between institution if time delay is insufficient, or if an inadequate volume of contrast is infused, the opacification of vessels may be inadequate. This effect could be interrupted erroneously as a stenosis or occlusion. CT

angiography is not ideal screening test for patients with renal disease.**(94)**

Renal Scintigraphy

Radionuclide imaging techniques are a noninvasive and safe way of evaluating renal blood flow. However, the renal flow scan has unacceptably high false positive and false negative rates. The renal scintigraphy was once the noninvasive diagnostic test of choice for patients with RAS, it is now relegated to a secondary screening modality because the quality of the images of duplex ultrasound and MRA are so good, and it does not give good anatomic and spatial, non specific for etiology, Renal scintigraphy has a reported sensitivity for renovascular diseases equal 88% **(89).**

Summary and Conclusion

It is estimated that approximately l millions persons in United States have potentially correctable vascular hypertension. Additionally, a significant percentage of those patients with potentially correctable hypertension are at risk for progressive renal insufficiency in addition to their hypertension. The potential etiologies for this condition included atherosclerosis, fibromuscular dysplasia, and neurofibromatosis and Takaysu's arteritis. In a middle-aged patient with evidence of atherosclerotic disease elsewhere, atherosclerosis is considered the most likely etiology. Over the past decades, **DSA** has become a well-established modality for the visualization of blood vessels in the human body. This technique remain; the criterion standard for the confirmation if and identification of renal artery occlusion in persons with I intrinsic renal disease (**IRD**), Continued improvements in imaging technology have changed many of the traditional diagnostic algorithms for evaluating renal artery disease. Newer imaging modalities offer more accurate, specific, and early diagnosis but can be time consuming and Costly less invasive modalities, such as ultrasound, computed tomography, and magnetic resonance imaging have widespread applications in practice. The risks of radiation exposure, contrast toxicity, and sedation or versus the potential benefits, of obtaining precise diagnostic information always bet considered before selecting any imaging procedure.

Renal magnetic resonance (MR) angiography allows accurate evaluation of patients suspected to have renal artery stenosis the risks associated with nephrotoxic contrast agents, ionizing radiation, or arterial catheterization. With the availability of simpler, safer, less expensive, but still accurate contrast materia1-enhanced MR. Arteriography, screening for renal artery stenosis can be expanded to a broader spectrum of patients.

Computed tomography (CT) is also promising but is limited by the risks associated with iodinated contrast material and ionizing radiation. **Ultrasonography** (US) has been considered promising because it is noninvasive and inexpensive and provides how information from which homodynamic effects can be inferred. However; the use of US a screening tool for renal artery stenosis has been limited by the need for experienced operators, a variable failure rate, and controversy over the usefulness of the flow information.

Color Doppler US has some limitations; the accessory vessel detection is low. Moreover, the sensitivity and the negative predictive value, acceptable, is significantly lower than those for MR angiography. Improved US technology, such as the use of US contrasts agents may have a role to play in the future.**Renal scintigraphy** with angiotensin converting enzyme inhibitors is a sensitive and specific way to screen patients with suspected renovascular hypertension.

In conclusion

The main challenge is not to detect all cases of RAS 50% or greater in diameter but to identify stenosis that will benefit from revascularization. Another major issue is avoidance of unnecessary diagnostic angiography, especially in patients with renal failure. The proposed screening should begin with a functional investigation such as Doppler US or scintigraphy. In a center with good expertise with Doppler US, the cost-effectiveness of this technique is probably superior to that of scintigraphy. MR angiography, with its higher cost and lesser availability, should be reserved for patients with indeterminate functional imaging results, patients with normal functional imaging results but high clinical suspicion of RVH, and patients with abnormal functional imaging results who have a contraindication to conventional angiography, such as renal failure or a history of allergy to iodinated contrast material.

REFERENCES

1. Berkow R, Fletcher AJ: The Merck Manual, Merck Research Laboratories, and 429- 430:1992

2. Zierler RE, Bergelin Ro, Isaacson JA, et al: Natural history of atherosclerotic renal artery stenosis: a prospective study with duplex · ultrasonography. J Vasc Surg; 19:250-258. 1994

3. Decobelli F, Mellon R, Sailori M, et al: Renal artery stenosis value of Screening with three-dimensional phases contrast MR angiography with phase array multicoil. Radiology.201:697-703, 1996

4. Hunt JC, Sheps SG, Harrison EG, et al: Functional characteristics of renovascular hypertension: a reasoned approach to diagnosis and management. Arch Intern Med 1974; 133:988-1999

5. Safian RD, Textor SC: Renal- artery stenosis. N Engl J Med 344:-422, 2001

6. Bruce S Spinnowitz, Jonna Rodriguez MR, et al: angiography of renal artery Stenosis; value of the combination of three dimensional time phase-contrast MR angiography sequence .AJR J Rontgenol 167(2): 489-494, 1996

7. Dorros G, Jaff M, Matlniak L, et al: Four-year follow-up of Palmaz-Schatz stent revascularization as treatment for atherosclerotic renal artery stenosis. Circulation; 98:642-647. 1998

8. Krijnen P, van Jaarsveld BC, steyerberg EW,et al: and Man in Veld AJ, Schalel amp MA Jabbema JD: A clinical prediction-rule for renal artery stenosis Ann intern Med 129: 705-711, 1998.

9. Berland LL, Kuslin DB, Routh WD, et al: Keller FS. Renal artery stenosis: prospective evaluation of diagnosis with color duplex US compared with angiography. Radiology; 174:421-423. 1990

10. Miralles M, Cairols M, Cotillas J, et al: Gimenez A, Santiso A. Value of Doppler parameters in the diagnosis of renal arte stenosis. J Vasc Surg; 23:428-435. 1996

11. Journal of the American society of Nephrology volume 13 Number 11 November2002 copy ight@2002 American society of Nephrology.

12. Beregi JP, Elkohen M, Deklunder G, et al;helical CT angiography compared with angiography in the detection of renal artery stenosis. AJR Am j Roentgenol 167:4%-501, 1996.

13. Earls JP, Rofsky NM, DeCorato DR, et al: Breath-hold single dose Gd-enhanced three-dimensional MR aortography: usefulness of a timing examination and MR power injector.Radio1ogy; 201:705-10. 1996

14- Van Jaarsveld BC, Pieterman H, Van Dijk LC ,et al:alzvan Seijen AJ, Krinjen P Derkx FH, Man intVeld AJ, Schaleltamp MA: Inter-observer variability in the angiographic assessment of renal artery stenosis 17: 1731-l736,l999

15. Wasser MN, Wesenberg J, van der Hulst, et al: Homodynamic significance of renal artery stenosis digital subtraction versus systolically gated through dimentional phase-contrast MR angiography. 1997

16. Dawson, Westenberg J,Aslmk Ragayan, et al: digital subtraction I Angiography, clinical radiology, 39, 5,474-477, 1998

17. Taylor A, Nally J, Au rell M, et al: Consensus report on ACE inhibitor renography for detecting of renovascular hypertension. Nuclear Med; 37:1876- 82. I996

18. Taylor AT, Fletcher IW, Nally JR JV, et al: Procedure guidelines for diagnosis of renovascular hypertension. J Nucl Med; 39:1297-l302, 1998

19. Snell Richard S: clinical anatomy: 8th edition 13-135:453-4l55, 2007

20. Resnick M1, Pounds DM, Boyce WH, et al: Surgical anatomy of the human kidney and its applications. Urology 17:367, 1981.

21. Gray H, Pick TPB Howden R: Gray's Anatomy, New York, Bounty Books, 556-557, 985-994. 1984

22. Lasts anatomy: Regional and applied, 8 edition, 70-71,Churrchill Livingstone book company, U.K. 1991.

23. Sampaio FJ, Aragao AH; Anatomical relationship between the intrarenal arteries and the kidney collecting system. J Urol, 1413:679, 1990.

24. Tanagho EA: Anatomy of the lower urinary tract. InWalsh PC, Retik AB, and STOMEY TA, et al (Eds):Campbell's Urology. Philadelphia, WB Saunders, pp 40-69,1992.

25.Wilman AH, Riederer SJ, King BF, Dobbins .JP, Rossman PJ. EhmanRL:f1uoroscopically triggered contrast-enhancedthree -dimensional MR angiography with elliptical centric view order: Application to the renal arteries.Radiology 205; 137 146, 1997.

26. Henry Gray: Anatomy of the Human Body.1211-1222, Mosbey puplisher 1996

27. Walsh P, Rofsky NM,Krinsky GA, et al: Asymmetric siognal intensity of renal artery stenosis follow administration of gadopentetate dimeglumine J; 20:812-814; 1996

28. Ashcraft KW: pediatric Urology,W.B.Ssaunder,77-6-86:1999

29. Berkow R, Fletcher AJ: The Merck Manual, Merck Research Laboratories, 429-430; l992.

30. Rubin GD, VVa1ker PJ, Dake MD, et al: Three-dimensional spiral computed tomographic angiography; an alternative imaging modality for the abdominal aorta and itsbranches. J Vase Surg 18656-665, 1993

31. Safian RD, Textor, or SC. Renal artery stenosis Engl J Med: 344:431- 42. 2001.

32. SOS, TA, Pickering, T.G, Sinderman, and K: Percutaneous transluininal renal angioplasty in Reno vascular hypertension due toatheroma or fibromuscular dysplasia. N. Engl.j.Med .309:274 1983.

33. Textor SC, Wilcox C Ischemic nephropathy/azotemic renovascular disease. Sem Nephrol, 20489-502. 2000;

34. Lee VS, Rofsky NM, Krinsky GA, et al: Single dose breath-hold gadolinium-enhanced three-dimensional MR angiographyofthe renal arteries., 211:69-78., Radiology 1999 .

35. Walsh P, Rofsky NM, Krinsky GA,et al: Weinreb,Asymmetric signal intensity of the renal collecting system as a sign of unilateral renal, artery stenosis follow administration of gadopentetate dimeglumine.J.Assist Tomogr; 20:812-814; 1996.

36. Anderson JR: Muri's textbook of pathology. London. Edward Arnold (publisher). 14, 1:14-3 6.1995

37. Desanctis Rw, Doroghazi RM, Austin WG, et al: Aortic dissection, N .Engl.J.Med.:317:1060.1987

38. Hall S:Takayasu arteritis.A study of 32 North American patient.Medicin, 1985:64:89.

39. Schreiber MJ, Pohl MA, Novick AC: The natural history of atherosclerotic and fibrous renal artery disease. Urol Clin NAm, 11; 383-92. 1984.

40. Fry WJ Ernest CB, Stanley JC: Renovascular hypertensionin the pediatric patient. Arch. Surg 198·3:107,692-698.1983

51. Taylor Jr AT, Fletcher JW, Nally Jr JV, Blaufox MD, DubovskyEV, Fine EJ, et al.; Procedure guideline fordiagnosis of renovascular hypertension. Society ol`Nue1earMedicine Nucl Med, 39;1297-302 1998

52. Nada NC: History of echocardiographic contrast agents clin cardiol,20:17-11;1997.

53. Burns physical principles of Doppler and spectral A: analysis of JCU; 15:567-590; 1995

54. Olin JW: Role of duplex ultrasonography in screening for significant renal artery disease. Urol Clin North Am.; 0 21:215-26; 1994.

55. Barnes RW,Bone GE and Reinterson J: Non invasive US carotid angiography : prospective validation by contrastangiography.surgery 1979;80382. 1979

56. Francesco De Cobelli, , Massimo Venturini, , Angelo Vanzulli, , Sandro Sironi, , Marco Salvioni, , Enzo Angeli,

Renal Arterial Stenosis: Prospective Comparison of` Color Doppler US and Breath-hold, Three-dimensional, Dynamic Gadolinium-enhanced. MR. Angiography Radiology. 214:373-380, 2000.

57. Krebs CA, Giyanni VZ, Eisenberg RL,et al: Ultrasound atlas of1 J vascular diseases. Appelton and Lange.; 184-187. 1999

58. Hahn U, Miller S, Nagele T, et al: Renal MR angiography at 1.0 T: three-dimensional (3D) phase-contrast techniques versus gadolinium-enhanced 3D fast low-angle shot breath-hold imaging. AJR; 172:1501-1508.1999

59. Duda SH, Schick F, Teufl F, et al. Phase-contrast MR angiography for detection of arteriosclerotic renal artery stenosis. Acta Radiol; 38:287-291. 1997

60. Rosner MH: Renovascular hypertension: can we identify apopulation at high risk,South Med J, 94:1058-1064; 2001.

61. Nazzal M·MS, Hoballah JJ, Miller EV, et al: Renal hilar Doppler analysis is of value in the management of patients with renovascular disease. Am J Surg 174:164-168, 1997.

62. Melany ML, Grant EG, Duerinckx AJ, Watts TM, Levine0 BS: Ability of a phase shift US contrast agent to improve imaging of` the main renal arteries, Radiology; 205:147-152; 1997.

63. Missouris CG, Allen:CM, Balen FG, Buckenham T, LeesWR, MacGregor GA: Non-invasive screening for renal artery5 stenosis with ultrasound contrast enhancement J Hypertens, 14.519-524;1996

64. Porter TR, Li S, Kilzer K: Smaller intravenous perfluorocarbon-containing micro bubbles produce greater myocardial contrast with intermittent harmonic imaging and better delineation of risk area during acute myocardial ischemia J Am Soc Echocardiogr, 10:792-797; 1997.

65. Helenon O, El Rody F, Correas JM, Melki P, Chauveau D,Chretien Y, Moreau IF: Color Doppler US of

renovascular disease in native kidneys. Radiographics, 15:833-54; l995

66. Souza de Oliveira IR, Widman A, Molnar LJ, JT,Praxedes_JN, Cerri GG: Colour Doppler ultrasound: a new index improves the diagnosis of renal artery stenosisUltrasound Med Biol, 26:41-47; 2000.

67. Claudon M, Plouin PF, Baxter GM, Rohban T, Devos DM: Renal arteries in patients at risk of renal arterial stenosis; multicenter evaluation of the echo-enhancer Renal Artery Study Group Radiology, 214:739-746; 2000.

68. Teixeira, Odila UN, Luiz A Bortolotto and Helio Bernardes Silva. The contrast-enhanced Doppler ultrasound with perfluorocarhon exposed sonicated albumin does not improve the diagnosis of renal artery stenosis compared with angiography. Journal of Negative Results inBiomedicine, .11861477-5751-3-3; 2004.

69. Keller PJ, Saloner D, Potchen EJ, Siebert JE, and Haacke E.M: Time of flight imaging in Magnetic Resonance Angiography, concepts and applications, St. Louis, Mosby ,:146-159. 1993

70. Schoenberg SO, Bock M, Knopp MV, et al: Renal arteries: optimization of three-dimensional gadolinium-enhanced MR angiography with bolus-timing-independent last multiphase acquisition in a single breath hold. Radiology,21 1:667-79. 1999.

71. Maki JH, Prince MR, Londy FJ, et al: The effects of time varying intravascular signal intensity and k-space acquisition order on three-dimensional MR angiography image quality. J Magn Reson1maging, 6; 642-51. 1996.

72. Marks B, Mitchell DG, Simelaro JP,**et al:** Breath-holding in healthy and pulmonary-compromised populations: effects of hyperventilation and oxygen inspiration. JMRI; 7:595-597; 1997.

73. Gilfeather M., Yoon HC, Siege1man ES, et al:Renal artery stenosis: evaluation, With conventional angiography

versus gadolinium-enhanced MR angiography. Radiology; 210:367-9 372; 1999.

74. Prince MR, Yucel EK, Kaufman JA, et al: Dynamic gadolinium-enhanced three-dimensional abdominal MR arteriography. J Magn Reson Imaging; 3; 877-81+1998.

75. Schoenberg SO, Knopp MV, Londy F et al: Morphologic and functional magnetic resonance imaging of the renal artery stenosis: a multi-reader tri-center study. J Am Soc Nephrol; 13: 158-169; 2002

76. Schoenberg SO, Knopp MV, Bock M et al: Renal artery stenosis; grading of homodynamic changes with cine phase-contrast MR blood flow measurements. Radiology; 11:203: 45-53; l997.

77. Maki JH, Chenevert TL, Prince MR: Contrast-enhanced MRangiography. Abdomen imaging; .23:469-484; 1998.

78. Weiger M, Pruessmann KP, Kassner A et al: Cont enhanced 3D MRA using SENSE. J Magn Reson d -Imaging; 12: 671-677; 2000.

79. Wedeen VJ,Meluli RA,Edelman RR Kassner A,et al. contrast- enhanced 3D MRA using SENSE.J Magn Reson imaging;12:671-7.2000

80. Ruehm SG, Goye Barkhausen J et a1: Rapid magnetic resonance angiography for detection of atherosclerosis.Lancet; 357: 1086-1091; 2001.

81. Levy Bl, Duriez M, Samuel JL. Coronary micro vasculature alteration in hypertensive rats. Effect of treatment with adiuretic and an ACE inhibitor. Am J Hypertens; 14: 7-13;2001.

82. Dietrich O, Nikolou K, Wintersperger B et al: Integrated parallel acquisition techniques (iPAT): applications for fast and cardiovascular MR imaging. Electromedia; 70: 133-145; 2002

83. Schoenberg SO, Bock M, Kallinowski F, Just A. Correlation of homodynamic impact and morphologic degree of renal artery stenosis in a canine model. J Am Soc Nephrol;0 11:2190-2198; 2000.

84. Aumann S, Schoenberg SO, Just A, et al: Quantification of renal perfusion using an intravascular contrast agent (part 1): results in a canine model. Magn Resonance Med 2003; 49:276–287

85. Buckley DL, Shurrab AE, Jones AP,et al: Kilgallon JE, MamtoraI H, Kalra PA. Quantitative assessment of renal function using dynamic Gd-DTPA-enhanced MRI. Proceeding of the Tenth Scientific Meeting ·and Exhibition. International Society ofMagnetic Resonance in Medicine: .811; 2002.

86. FOX, S. H, Tanenbaum, L. N., Ackelsberg, S., He, H. D,Hsieh, J., Hu, and H.: Future directions in CT technology.Neuro imaging clinics of North America; 8:497-513; 1998.

87. Brink JA, Davros WJ, Zeman RK, Costello P (edn):Helical Spiral CT. a practical approach. New York, McGrawHill, l-26; l995.

88. Foo TK, saranathan M, Prince MR, et al: automated detection of bolus arrivaland initiation of data acquisition in fast, three-dimensional gadolinium-enhanced MR angiography. Radio1ogy; 203:275-80, 1997

89. Kaplan-Parloveie S, Nadja C: Captopril renography and duplex Doppler sonography in the diagnosis of renovascular hypertension. Nephrol Dial Transplant l3:3l3-317, 1998.

90. Kopka L, Vosshenrich R, Rodenwaldt J, et al: Differences in injection rates on contrast-enhanced breath-hold three-dimensional MR angiography. AJR AmJ Rontgenol170:345-8. 1998.

91. Kuszyk BS, Fishman EK. Technical aspects of CTangiography, Semin Ultrasound MR; 19:383-393; 1998.

92. Chapman S, Nakielny R: A guide to radiological S procedures. Baillire Tindal1, 201-241; 1997.

93. Uday D. Patil, Ashok Ragavan, Nadaraj, Keshava M , Ravi Shankar, Bahar Bastani and Sudarshan H. Ballal, PJ; Renal artery stenosis: CT angiography-comparison of real-time volume rendering and intensity projectiona1algorithms Nephrol Dial Transplant, 16:1900-1904;2001

94. Prigent A. and Nally JV, the diagnosis of renovascular hypertension: the role of captopril renal scintigraphy and related issues. Eur J Nucl Med; 20:625-644; 1998.

95. Aitkison F, Page A: Diagnostic imaging of renal arterystenosis. J Hum Hypertension; l999:l3:595-603.

96.Boos M, Seheffler K, Haselhorst R, et al. Arterial first pass gadolinium-CM dynamics as a function of several intravenous saline flush and Gd volumes. . J Magn Reson Imaging l3:568-76,**2001.**

97 . **Rimmer J, Gennari FJ.** Atherosclerotic renovascular disease and progressive renal failure. Ann InternMed, 118:712-9. 1993.

98. Handa N, Komada T. Efficacy of echo-Doppler for the valuation of renovascular disease. Ultrasound Med Biol; 14:1-5.1998

99. Patriquin H, Lafortune M, Jéquier JC, et al: Stenosis of the renal artery: assessment of slowed systole in the down stream circulation with Doppler sonography. Radiology 1992; 184:479-485.

100. Halpern EJ, Needleman L, Nack TL, East SA. Renal artery stenosis: should we study the main renal artery or segmental vessels. Radiology 1995; 195:799-804

101. Prince MR,Gadolinium-enhanced MR aortography. Radiology 1994; 191:155-164.

102. Bakker J, Beek FJ, Beutler JJ, et al. Renal artery stenosis and accessory renal arteries: accuracy of detection and visualization with gadolinium-enhanced breath-hold MR angiography. Radiology 1998; 207:497-504

103 . Halpern EJ, Mitchell DG, Wechsler RJ, et al: Preoperative evaluation of living renal donors: comparison of CT angiography and MR angiography. Radiology 2000; 216:434-439

104. Bruce A. Urban, Lloyd E. Ratner, and Elliot K. Fishman; Three-dimensional Volume rendered CT Angiography of the Renal Arteries and Veins: Normal

Anatomy, Variants, and Clinical Applications l Radiographics. 2l:373-386; 2001.

105. Barrett BJ. And Halpern EJ, Contrast nephrotoxicity. J Am s Soc Nephrol; 5: 125-137; 1994.

106. Siegel man ES, Gilgeather M, Holland GA,et al: Breath-ho1dultrafast three-dimens1onal gadolinium enhanced MRangiography of Reno vascular system. AM Rontgenol; 168·p 1035-1040; 1997.

107. Gross CM, Kramer J, Weingartner O. et al: Determination of renal arterial stenosis severity: comparison of pressure gradient and vessel diameter. Radiology. 2001; 220: 751–64].

108. Tegtmeyer CJ, Peter B. Sachs Renal Angioplasty,lIn:Abram's Angiography, Little Brown, RA: 294-325; 1999.

109. Mittai BR, Kumar P, Arora P, et al: Role of captopril renography in the diagnosis of renovascular hypertension. Am J Kidney Dis 1996; 28:209-213

110. Prigent A. The diagnosis of renovascular hypertension: the role of captopril renal scintigraphy and related issues. Eur J Nucl Med 1993; 20:625-644.

111. Harding MB,Smith LR, Hammerstein SI, et al: Renal artery stenosis; prevalence and associated risk factors in patients undergoing routine cardiac catheterization.

112. Carman T, Olin JW, Czum J Noninvasive imaging of renal arteries. Urol Clin N am: 28:815-26. 2001

113. Platt JF; Doppler ultrasound of the kidney. Semin Ultrasound CT MR 18:22-32, 1997.

114. Malatino LS, Polizzi G, Garozzo M, et al: Diagnosis of renovascular disease by extra- and intrarenal Doppler parameters. Angiology 49:707-721, 1998.

115. Isaacson J, Neumyer MM: Direct and indirect renal arterial duplex and Doppler color flow evaluations. Journal o Vascular Technology 19(5-6): 309-316, 1995

116. Radermacher J, Chavan A, Bleek J, et al: Use of Doppler ultrasonography to predict the outcome of therapy for renal artery stenosis. N Engl J Med 344:410-7. 2001

117. Miralles M, Santiso A, Gimenez A, et al: Renal duplex scanning; Correlation with angiography and isotopic renography., Eur J Vasc Surg 7:188-194, 1993

118. Helenon O, Meki P, Correas J-M, Boyer J-c, Moreau J-F Renovascular diseases: Doppler ultrasound. 18:136-146, 1997.

119. Leung DA, Hoffman U, Pfammatter T, et al: Magnetic resonance angiography versus duplex sonography for L diagnosing renovascular disease. Hypertension 3:726-731, 1999

120 . Pedersen EB: New tools in diagnosing renal artery stenosis. Kidney 1nt 57:2657-2677, 2000

121. Kaufman JA, McCarter D, Geller SC, et al: Two-dimensional time-flight MR angiography of the lower extremities: artifacts and pitfalls. AJR Am J Rontgenol: 171:129-35. 1998

122. Saloner D: Determinants of image appearance in contrast-enhanced magnetic resonance angiography; A review lnvest Radiol 33:4188-4195, 1998

123. Hahn U, Miller S, Ngele T, et al; Renal MR angiography at 1.0 T: Three-dimensional (3D) phase- contrast techniques versus gadolinium-enhanced 3D fast low angle .et.1 short breath-hold imaging. AJR Am J Roentge172: 11508, 1999

124. Joseph P. Hornak, Ph.D. Copyright J.P. Hornak .AllRights Reserved. 1996-2002

125. Paul JF, Cherrak I, Jaulent MC, Chatellier G, Plouin PF, Degoulet P, Gaux JC: Interobserver variability in the interpretation of renal digital subtraction angiography. Am J Rontgenol 173: 12854288, 1999

126. Teresa L. Carman MD Jeffrey Olin DO Julianna Czum MD Urologic Clinics of North AmericaVo1ume 28 Number 4 Department of Vascular Medieine.2001

varicose